

Non-adiabatic Dynamics using the Generators of the $\mathfrak{su}(N)$ Lie Algebra

Duncan Bossion,^{1, a)} Sutirtha N. Chowdhury,^{1, 2} and Pengfei Huo^{1, 3, b)}

¹⁾Department of Chemistry, University of Rochester, 120 Trustee Road, Rochester, New York 14627, USA

²⁾Department of Chemistry, Duke University, 3236 French Science Center, 124 Science Drive, Durham, North Carolina 27708, USA

³⁾The Institute of Optics, Hajim School of Engineering, University of Rochester, Rochester, New York 14627, USA

(Dated: 6 April 2022)

We present the rigorous theoretical framework of the generalized spin mapping representation for non-adiabatic dynamics. This formalism is based on the generators of the $\mathfrak{su}(N)$ Lie algebra to represent N discrete electronic states, thus preserving the size of the original Hilbert space in the state representation. We use the generalized spin coherent states representation and the Stratonovich-Weyl transform to describe these electronic spin-mapping variables in the continuous variables space. Wigner representation is used to describe the nuclear degrees of freedom. Using the above representations, we derived an exact expression of the time-correlation function as well as the exact quantum Liouvillian. Making the linearization approximation, this exact Liouvillian is reduced to the Liouvillian of the recently proposed spin-Linearized Semi-Classical (spin-LSC) dynamics. These expressions lead to a self-consistent trajectory-based method to simulate non-adiabatic dynamics, which is based entirely on the generalized spin mapping formalism to treat the electronic states without the necessity of converting back to the cartesian mapping variables of the bosonic DOF (which are commonly referred to as the Meyer-Miller-Stock-Thoss mapping variables). The accuracy of this approach is tested with several challenging non-adiabatic model systems.

I. INTRODUCTION

Studying non-adiabatic dynamics in quantum systems, particularly in condensed phase, is a central challenge for modern theoretical chemistry.¹ In order to avoid an exponential numerical scaling with the number of degrees of freedom (DOFs) of the system, different approximate methods have been developed. Trajectory-based quantum-classical methods are among the most successful ones as they scale linearly with the number of DOFs and allow for a simple numerical propagation scheme. One of the most popular trajectory based approach is the surface-hopping method,^{2–6} where an ensemble of classical trajectories hop among electronic states upon non-adiabatic transitions, mimicking the wavepacket branching dynamics. In a separate direction, mapping variables are used to represent quantum transitions among discrete electronic states as classical-like motion of the continuous phase space variables,^{7,8} thus treating all the DOFs on an equal footing.

To this end, the Meyer-Miller-Stock-Thoss (MMST) mapping formalism is proposed,^{8–10} which maps a N -level system onto N singly excited harmonic oscillators, and thus can be viewed as a generalization of the Schwinger's bosonization approach. The mapping variables of the MMST formalism are conjugate position and momentum of each mapping oscillator. This method, despite its great success and broad applications,^{11–19} has known flaws.^{20,21} This is because the MMST representa-

Major problems:

- 1) Too many equations identical to or highly similar to those of previous papers by other scholars, especially Ref. 29 and Ref. 52. Much of the content repeated the works in Ref. 29, Ref. 52, Ref. 55 and Ref. 56., some without citation.
- 2) In various places, the authors failed to mention the important contributions by others, as if they came up with the ideas. For instance, the original form of mapping kernel with generalized coherent states of SU(N) group had long been proposed by Tilma and Nemoto in J. Phys. A: Math. Theor. 45, 015302 (2012), dating back to 2012. However, there is no citation in the proper corresponding place around the mapping kernel eq (26) in this manuscript. Moreover, some statements about the continuous region of the phase space parameter in Section III-B and Section III-D were directly plagiarized from Refs. 55, 56 and Acc. Chem. Res. 54, 23, 4215 -4228 (2021).
- 3) There is a serious mistake in this manuscript. The EOMs eqs (98), (99), (101), (105) on Stratonovich phase space are incompatible with the generalized coherent states eq (17), as the derivations of eqs (B2-B3) mismatch these coherent states. Since the EOMs with the starting point eq (17) are incorrect, we seriously query the fidelity of original data of the numerical tests for three-electronic-state systems.

^{a)}Electronic mail: dbossion@ur.rochester.edu

^{b)}Electronic mail: pengfei.huo@rochester.edu

Non-adiabatic Dynamics using the Generators of the $\mathfrak{su}(N)$ Lie Algebra

Duncan Bossion,^{1, a)} Sutirtha N. Chowdhury,^{1, 2} and Pengfei Huo^{1, 3, b)}

¹⁾Department of Chemistry, University of Rochester, 120 Trustee Road, Rochester, New York 14627, USA

²⁾Department of Chemistry, Duke University, 3236 French Science Center, 124 Science Drive, Durham, North Carolina 27708, USA

³⁾The Institute of Optics, Hajim School of Engineering, University of Rochester, Rochester, New York 14627, USA

(Dated: 6 April 2022)

We present the rigorous theoretical framework of the generalized spin mapping representation for non-adiabatic dynamics. This formalism is based on the generators of the $\mathfrak{su}(N)$ Lie algebra to represent N discrete electronic states, thus preserving the size of the original Hilbert space in the state representation. We use the generalized spin coherent states representation and the Stratonovich-Weyl transform to describe these electronic spin-mapping variables in the continuous variables space. Wigner representation is used to describe the nuclear degrees of freedom. Using the above representations, we derived an exact expression of the time-correlation function as well as the exact quantum Liouvillian. Making the linearization approximation, this exact Liouvillian is reduced to the Liouvillian of the recently proposed spin-Linearized Semi-Classical (spin-LSC) dynamics. These expressions lead to a self-consistent trajectory-based method to simulate non-adiabatic dynamics, which is based entirely on the generalized spin mapping formalism to treat the electronic states without the necessity of converting back to the cartesian mapping variables of the bosonic DOF (which are commonly referred to as the Meyer-Miller-Stock-Thoss mapping variables). The accuracy of this approach is tested with several challenging non-adiabatic model systems.

tion has a larger size of Hilbert space (that contains other states outside the singly excited manifold of the mapping oscillators) than the original electronic subspace, and it requires a projection back to the singly excited mapping subspace to obtain accurate results.^{20–22} As a consequence, the identity operator is not preserved through the MMST mapping and there is an ambiguity of how to evaluate it.²² Related to the problem of the non-conserving identity, the non-adiabatic dynamics is sensitive to the separation between the state-dependent and the state-independent Hamiltonian.^{21,23}

One of the most natural ways to map a quantum system is to respect its original symmetry, which is described by the $\mathfrak{su}(N)$ symmetry group for a N -level system. For $N = 2$, it is well-known that the quantum dynamics of two electronic states can be mapped as the spin precession around a magnetic field (represented by the Hamiltonian) described by the motion of the Bloch vector on the Bloch sphere, due to the $\mathfrak{su}(2)$ symmetry shared by both problems. Recently, Runeson and Richardson used this spin mapping approach to map a two-level system on a single spin- $\frac{1}{2}$ DOF.²⁴ One can in principle generalize this idea by mapping a N -level system with the generators of the $\mathfrak{su}(N)$ Lie Algebra. The corresponding quantum equations of motion (EOMs) were first introduced by Hioe and Eberly,²⁵ and can be viewed as the generalization of the spin precession to N -dimensions with a $\mathfrak{su}(N)$ symmetry. Meyer, McCurdy, and Miller also used a similar idea to map two-state or three-state systems with spin- $\frac{1}{2}$ and spin-1 operators, although the matrices of the spin-1 operators^{7,26,27} (which are not necessarily traceless) are different than the $\mathfrak{su}(N)$ generators (which are traceless). Note that the $\mathfrak{su}(N)$ mapping formalism is different than the recent spin-mapping formalism in-

troduced by Cotton and Miller,²⁸ which maps N states onto N spin- $\frac{1}{2}$ particles (hence having the symmetry of a $\bigotimes_N \mathfrak{su}(2)$ system).

Recently, Runeson and Richardson²⁹ used the generators of the $\mathfrak{su}(N)$ Lie Algebra to perform the mapping non-adiabatic dynamics in a N -state system. In particular, the Stratonovich-Weyl transform³⁰ is used to convert generalized spin operators (generators) into continuous variables, resulting in a classical-like Hamiltonian that depends on $N^2 - 1$ expectation values of the spin operators under the generalized spin coherent states.^{31,32} The spin coherent states are further expressed as a linear expansion of the diabatic electronic states, and the real and imaginary parts of the expansion coefficients are further defined as the conjugate position and momentum variables (which are $2N$),²⁹ leading to the equivalence between the generalized spin-based mapping Hamiltonian and the MMST mapping Hamiltonian. Using the connection between these two Hamiltonians, one can find the particular choice of zero-point energy parameter as well as the sampling procedure of the initial conditions in the MMST formalism, which guarantee a total population equal to one. This is a reasonable choice for constructing an algorithm for approximate quantum dynamics, as it avoids deriving the EOMs in the spin coherent state variables, which is highly non-trivial.

In this work, we provide the rigorous theoretical derivation of mapping non-adiabatic dynamics using the generators of the $\mathfrak{su}(N)$ Lie Algebra. In Sec. II, we introduce the generators of the $\mathfrak{su}(N)$ Lie algebra which are used as the basis to map the vibronic Hamiltonian, and derive the analytic expression of the structure constants of the $\mathfrak{su}(N)$ Lie algebra. In Sec. III we give a description of the Stratonovich-Weyl transform for N electronic states and the spin coherent states. We also derive properties of this transformation, and the transformation that connects the $\mathfrak{su}(N)$ mapping Hamiltonian and the MMST mapping Hamiltonian. In Sec. IV, we present a mixed Wigner/Stratonovich-Weyl representation that performs Wigner transform on the nuclear DOFs and Stratonovich-Weyl transform on the electronic DOFs, and derive the exact expressions of the time-correlation function (TCF). In Sec. V, we derive the exact quantum Liouvillian expression under the mixed Wigner/Stratonovich-Weyl representation, as well as the approximate form of the Liouvillian under the linearization approximation. The corresponding EOMs are rigorously derived, in three equivalent forms with (1) the spin coherent state expectation values, (2) the Bloch sphere angles, and (3) the MMST phase space variables. The TCF and the EOMs under the linearized approximation are used as a trajectory-based non-adiabatic method in the mixed Wigner/Stratonovich-Weyl formalism. We perform numerical simulations to demonstrate the accuracy of this method by simulating non-adiabatic population dynamics of challenging model systems.

II. GENERATORS OF THE $\mathfrak{su}(N)$ LIE ALGEBRA

In this section, we show how to use the generators of the $\mathfrak{su}(N)$ Lie algebra^{7,25,29} to represent a Hamiltonian operator. We are interested in the quantum dynamics of a system with N electronic states coupled to nuclear DOFs as follows

$$\begin{aligned}\hat{H} &= [\hat{T}_R + U_0(\hat{R})]\hat{\mathcal{I}} + \hat{V}_e(\hat{R}) \\ &= [\hat{T}_R + U_0(\hat{R})]\hat{\mathcal{I}} + \sum_{n,m} V_{nm}(\hat{R})|n\rangle\langle m|,\end{aligned}\quad (1)$$

where \hat{T}_R is the nuclear kinetic energy, $U_0(\hat{R})$ represents the state-independent part of the potential, and $\hat{V}_e(\hat{R})$ is the state-dependent part of the potential. Further, \hat{R} represents a nuclear DOF, $\{|n\rangle\}$ represents a set of diabatic electronic states, and $V_{nm}(\hat{R}) = \langle n|\hat{V}_e(\hat{R})|m\rangle$ is the matrix element of $\hat{V}_e(\hat{R})$ in this diabatic representation. The identity operator $\hat{\mathcal{I}} = \sum_{n=1}^N |n\rangle\langle n|$ represents the identity in the electronic Hilbert space. Below we discuss how to represent the same Hamiltonian with the generators of the $\mathfrak{su}(N)$ Lie algebra.

The $\mathfrak{su}(N)$ Lie algebra and its corresponding Lie groups are widely used in fundamental physics, particularly in the Standard Model of particle physics.^{33–35} For example, the $\mathfrak{su}(2)$ Lie algebra is used to describe the spin- $\frac{1}{2}$ system. The generators of $\mathfrak{su}(2)$ are the spin operators $\hat{\mathcal{S}}_j = \frac{\hbar}{2}\sigma_j$ with the Pauli matrices defined as follows

$$\sigma_1 = \begin{pmatrix} 0 & 1 \\ 1 & 0 \end{pmatrix}, \quad \sigma_2 = \begin{pmatrix} 0 & -i \\ i & 0 \end{pmatrix}, \quad \sigma_3 = \begin{pmatrix} 1 & 0 \\ 0 & -1 \end{pmatrix}.$$

The generators of the $\mathfrak{su}(3)$ Lie algebra are $\hat{\mathcal{S}}_j = \frac{\hbar}{2}\lambda_j$, where λ_j are the well-known Gell-Mann λ -matrices³⁶ defined as follows

$$\begin{aligned}\lambda_1 &= \begin{pmatrix} 0 & 1 & 0 \\ 1 & 0 & 0 \\ 0 & 0 & 0 \end{pmatrix}, \quad \lambda_2 = \begin{pmatrix} 0 & -i & 0 \\ i & 0 & 0 \\ 0 & 0 & 0 \end{pmatrix}, \quad \lambda_3 = \begin{pmatrix} 1 & 0 & 0 \\ 0 & -1 & 0 \\ 0 & 0 & 0 \end{pmatrix}, \\ \lambda_4 &= \begin{pmatrix} 0 & 0 & 1 \\ 0 & 0 & 0 \\ 1 & 0 & 0 \end{pmatrix}, \quad \lambda_5 = \begin{pmatrix} 0 & 0 & -i \\ 0 & 0 & 0 \\ -i & 0 & 0 \end{pmatrix}, \quad \lambda_6 = \begin{pmatrix} 0 & 0 & 0 \\ 0 & 0 & 1 \\ 0 & 1 & 0 \end{pmatrix}, \\ \lambda_7 &= \begin{pmatrix} 0 & 0 & 0 \\ 0 & 0 & -i \\ 0 & i & 0 \end{pmatrix}, \quad \lambda_8 = \frac{1}{\sqrt{3}} \begin{pmatrix} 1 & 0 & 0 \\ 0 & 1 & 0 \\ 0 & 0 & -2 \end{pmatrix}.\end{aligned}$$

They are widely used in quantum chromodynamics as an approximate symmetry of the strong interaction between quarks and gluons.³⁶ The generators of an algebra can be obtained in different ways, but the most commonly used ones in physics are based on a generalization of the Pauli matrices of $\mathfrak{su}(2)$ and of the Gell-Mann matrices³⁶ of $\mathfrak{su}(3)$, which are what we used in this work. This specific way of expressing the generators is commonly referred to as the Generalized Gell-Mann matrix (GGM) basis. Thus, the mapping formalism in this work can be

referred to as the generalized spin mapping, the $\mathfrak{su}(N)$ mapping, or GGM mapping. We will not distinguish the above three in the paper when we mention this mapping formalism.

We express the generators of the $\mathfrak{su}(N)$ Lie algebra (which can be viewed as the generalized spin operators) in the GGM basis, and we denote them as $\hat{\mathcal{S}}_i$ with $i \in [1, N^2 - 1]$. There are $N(N - 1)/2$ symmetric matrices

$$\hat{\mathcal{S}}_{\alpha_{nm}} = \frac{\hbar}{2}(|m\rangle\langle n| + |n\rangle\langle m|), \quad (2)$$

$N(N - 1)/2$ anti-symmetric matrices,

$$\hat{\mathcal{S}}_{\beta_{nm}} = -i\frac{\hbar}{2}(|m\rangle\langle n| - |n\rangle\langle m|), \quad (3)$$

and $N - 1$ diagonal matrices,

$$\hat{\mathcal{S}}_{\gamma_n} = \frac{\hbar}{\sqrt{2n(n-1)}}\left(\sum_{l=1}^{n-1}|l\rangle\langle l| + (1-n)|n\rangle\langle n|\right), \quad (4)$$

where we introduced the indices α_{nm} related to the symmetric matrices, β_{nm} related to the anti-symmetric matrices, and γ_n related to the diagonal matrices as follows

$$\alpha_{nm} = n^2 + 2(m - n) - 1, \quad (5a)$$

$$\beta_{nm} = n^2 + 2(m - n), \quad (5b)$$

$$\gamma_n = n^2 - 1. \quad (5c)$$

Note that in the above definitions, $1 \leq m < n \leq N$ and $2 \leq n \leq N$, and the generators are ordered according to the conventional ordering of the GGM matrices.^{35,37} Another commonly used notation³⁷ is Λ , where $\hat{\mathcal{S}}_i = \frac{\hbar}{2}\hat{\Lambda}_i$.

These generators are orthonormal to each other as

$$\text{Tr}_e[\hat{\mathcal{S}}_i \hat{\mathcal{S}}_j] = \frac{\hbar^2}{2}\delta_{ij}. \quad (6)$$

Their commutation and anti-commutation relations define the Lie algebra as follows

$$[\hat{\mathcal{S}}_i, \hat{\mathcal{S}}_j] = i\hbar \sum_{k=1}^{N^2-1} f_{ijk} \hat{\mathcal{S}}_k, \quad (7a)$$

$$\{\hat{\mathcal{S}}_i, \hat{\mathcal{S}}_j\}_+ = \frac{\hbar^2}{N}\delta_{ij}\hat{\mathcal{I}} + \hbar \sum_{k=1}^{N^2-1} d_{ijk} \hat{\mathcal{S}}_k, \quad (7b)$$

where $\{\hat{\mathcal{S}}_i, \hat{\mathcal{S}}_j\}_+$ represents the anti-commutator between $\hat{\mathcal{S}}_i$ and $\hat{\mathcal{S}}_j$, the indices $i, j, k \in \{\alpha_{nm}, \beta_{nm}, \gamma_n\}$, and f_{ijk} and d_{ijk} are the totally anti-symmetric and totally symmetric structure constants, respectively. Using Eqs. 7a-7b, one can obtain the following well-known expressions for these structure constants

$$f_{ijk} = -i\frac{2}{\hbar^3} \text{Tr}[[\hat{\mathcal{S}}_i, \hat{\mathcal{S}}_j]\hat{\mathcal{S}}_k], \quad (8a)$$

$$d_{ijk} = \frac{2}{\hbar^3} \text{Tr}[\{\hat{\mathcal{S}}_i, \hat{\mathcal{S}}_j\}_+ \hat{\mathcal{S}}_k]. \quad (8b)$$

Despite the extensive usage and the crucial role these structure constants play in modern physics, there is no analytic expression (closed formulas) of f_{ijk} and d_{ijk} . Here, we derive these analytic formulas for these structure constants in Appendix A, with their analytic expressions listed in Eq. A5 for f_{ijk} and in Eq. A14 for d_{ijk} .

With the generators of $\mathfrak{su}(N)$, as well as the relation between $|n\rangle\langle m|$ and the GMM matrices³⁷ $\hat{\mathcal{S}}_k$, one can represent the Hamiltonian in Eq. 1 as follows^{25,29}

$$\hat{H} = \mathcal{H}_0(\hat{R}) \cdot \hat{\mathcal{I}} + \frac{1}{\hbar} \sum_{k=1}^{N^2-1} \mathcal{H}_k(\hat{R}) \cdot \hat{\mathcal{S}}_k, \quad (9)$$

where the elements $\mathcal{H}_0(\hat{R})$ and $\mathcal{H}_k(\hat{R})$ are expressed as

$$\mathcal{H}_0(\hat{R}) = \frac{1}{N} \text{Tr}_e[\hat{H} \cdot \hat{\mathcal{I}}] = \hat{T}_R + U_0(\hat{R}) + \frac{1}{N} \sum_{n=1}^N V_{nn}(\hat{R}), \quad (10a)$$

$$\mathcal{H}_k(\hat{R}) = \frac{2}{\hbar} \text{Tr}_e[\hat{H} \cdot \hat{\mathcal{S}}_k] = \frac{2}{\hbar} \text{Tr}_e[\hat{V}_e(\hat{R}) \cdot \hat{\mathcal{S}}_k]. \quad (10b)$$

Here, we explicitly indicate the trace over the electronic DOFs by using Tr_e . Note that Eq. 10 has an explicit separation of the trace and traceless parts of the potential, due to the traceless generators in Eqs. 2-4 where $\text{Tr}_e[\hat{\mathcal{S}}_i] = 0$. Enforcing this separation in the MMST mapping formalism can significantly improve the stability and accuracy of the dynamics.^{21,23,38} In the $\mathfrak{su}(N)$ mapping formalism, this is intrinsically achieved.

Using the generators defined in Eqs. 2-4, we can explicitly write these terms as

$$\mathcal{H}_{\alpha_{nm}}(\hat{R}) = V_{mn}(\hat{R}) + V_{nm}(\hat{R}), \quad (11a)$$

$$\mathcal{H}_{\beta_{nm}}(\hat{R}) = i(V_{mn}(\hat{R}) - V_{nm}(\hat{R})), \quad (11b)$$

$$\mathcal{H}_{\gamma_n}(\hat{R}) = \sum_{l=1}^{n-1} \sqrt{\frac{2}{n(n-1)}} V_{ll}(\hat{R}) - \sqrt{\frac{2(n-1)}{n}} V_{nn}(\hat{R}), \quad (11c)$$

with $1 \leq m < n \leq N$ and $2 \leq n \leq N$ as previously introduced.

In the special case where the system does not have any nuclear (or other) DOF, we can write down the exact quantum Liouville equation for this closed system as

$$i\hbar \frac{\partial \hat{\rho}}{\partial t} = [\hat{H}, \hat{\rho}], \quad (12)$$

where the commutator is taken within the electronic subspace. Using the $\mathfrak{su}(N)$ representation for the density operator

$$\hat{\rho} = \frac{1}{N} \hat{\mathcal{I}} + \frac{1}{\hbar} \sum_{k=1}^{N^2-1} \mathcal{S}_k \cdot \hat{\mathcal{S}}_k, \quad (13)$$

where $\mathcal{S}_k = \frac{2}{\hbar} \text{Tr}[\hat{\rho} \hat{\mathcal{S}}_k]$, as well as the corresponding expression for $\hat{H} = \mathcal{H}_0 \cdot \hat{\mathcal{I}} + \frac{1}{\hbar} \sum_{k=1}^{N^2-1} \mathcal{H}_k \cdot \hat{\mathcal{S}}_k$, the quantum

Liouville equation is equivalently expressed as²⁵

$$\frac{d}{dt} \mathcal{S}_i = \frac{1}{\hbar} \sum_{j,k=1}^{N^2-1} f_{ijk} \mathcal{H}_j \mathcal{S}_k, \quad (14)$$

which can be viewed as the generalization of the spin precession to N dimensions, discovered by Hioe and Eberly.²⁵ This relation was suggested as the time development of the N -level coherence vector. In the following sections, we will generalize this formalism and develop the corresponding theory when the Hamiltonian explicitly contains nuclear DOFs.

III. STRATONOVICH-WEYL TRANSFORM OF THE $\mathfrak{su}(N)$ GENERATORS AND THE MAPPING FORMALISM

The *Stratonovich-Weyl* (SW) transform³⁰ can be used to evaluate the quantum electronic trace of an operator. Here, we present the properties of this transformation for a general N -level system.

A. Spin coherent states

For a spin (or equivalently, a two-level system), one can use the following spin coherent states

$$|\mathbf{u}\rangle = \cos \frac{\theta}{2} e^{-i\varphi/2} |1\rangle + \sin \frac{\theta}{2} e^{i\varphi/2} |2\rangle \quad (15)$$

as a basis to describe the quantum dynamics,^{24,38} where θ and φ are the angles defining the Bloch vector, with the radius of the Bloch sphere being fixed. The spin coherent states can be generalized for a N -level system as follows^{32,39,40}

$$|\Omega\rangle = \sum_{n=1}^N |n\rangle \langle n| \Omega \rangle = \sum_{n=1}^N c_n |n\rangle, \quad (16)$$

where the expansion coefficients are

$$\langle n| \Omega \rangle = \begin{cases} \cos \frac{\theta_1}{2} e^{-i\varphi_1} & n = 1, \\ \cos \frac{\theta_n}{2} e^{-i\varphi_n} \prod_{l=1}^{n-1} \sin \frac{\theta_l}{2} e^{i\varphi_l} & 1 < n < N, \\ \prod_{l=1}^{N-1} \sin \frac{\theta_l}{2} e^{i\varphi_l} & n = N. \end{cases} \quad (17)$$

with $\{\theta_n\} \in [0, \pi]$ and $\{\varphi_n\} \in [0, 2\pi]$. The expansion coefficients can be derived from the usual recursive expression²⁹ given in Eq. B1. Note that the definition of the spin-coherent states used here is different than those used in the previous generalized spin mapping formalism²⁹ as we symmetrically split the phase $e^{i\varphi_n}$ between $|n\rangle$ and $|n+1\rangle$ states, which allows to conveniently transform all of these coefficients into the phase space mapping variables later (see Eq. 44). This is necessary in order to introduce both real and imaginary part of the expansion coefficient c_n (for all n) as the phase space mapping variables, which will be discussed in Sec. III D.

The coherent states eq (17) defined here are completely incompatible with the following derivations eqs (B2) and (B3).

$$\begin{aligned} \hbar \Omega_{\alpha nm} &\equiv \langle \Omega | \hat{\mathcal{S}}_{\alpha nm} | \Omega \rangle \\ &= \hbar \left(\cos \frac{\theta_m}{2} \prod_{j=1}^{m-1} e^{-i\varphi_j} \sin \frac{\theta_j}{2} \cos \frac{(1-\delta_{nN})\theta_n}{2} \prod_{k=1}^{n-1} e^{i\varphi_k} \right. \\ &\quad \times \sin \frac{\theta_k}{2} + \cos \frac{\theta_m}{2} \prod_{j=1}^{m-1} e^{i\varphi_j} \sin \frac{\theta_j}{2} \cos \frac{(1-\delta_{nN})\theta_n}{2} \\ &\quad \times \left. \prod_{k=1}^{n-1} e^{-i\varphi_k} \sin \frac{\theta_k}{2} \right) \\ &= \hbar \prod_{j=1}^{m-1} \sin^2 \frac{\theta_j}{2} \cos \frac{\theta_m}{2} \prod_{k=m}^{n-1} \sin \frac{\theta_k}{2} \cos \frac{(1-\delta_{nN})\theta_n}{2} \\ &\quad \times \cos \left(\sum_{l=m}^{n-1} \varphi_l \right), \end{aligned} \quad (B2)$$

$$\begin{aligned} \hbar \Omega_{\beta nm} &\equiv \langle \Omega | \hat{\mathcal{S}}_{\beta nm} | \Omega \rangle \\ &= \hbar \prod_{j=1}^{m-1} \sin^2 \frac{\theta_j}{2} \cos \frac{\theta_m}{2} \prod_{k=m}^{n-1} \sin \frac{\theta_k}{2} \cos \frac{(1-\delta_{nN})\theta_n}{2} \\ &\quad \times \sin \left(\sum_{l=m}^{n-1} \varphi_l \right), \end{aligned} \quad (B3)$$

It is easy to verify that to derive eqs (B2) and (B3), the correct coherent states are the ones shown directly below, not (17)!

$$\langle n | \Omega \rangle = \begin{cases} \cos \frac{\theta_1}{2} & n = 1, \\ \cos \frac{\theta_n}{2} \prod_{l=1}^{n-1} \sin \frac{\theta_l}{2} e^{i\varphi_l} & 1 < n < N, \\ \prod_{l=1}^{N-1} \sin \frac{\theta_l}{2} e^{i\varphi_l} & n = N. \end{cases}$$

Serious mistake had Huo and coworkers made here. Since there is a long passage stating the pros of using eq (17) as the definition of coherent states, this is never a typo but a mistake with no doubt!

The spin coherent states $|\Omega\rangle$ are normalized such that $\langle\Omega|\Omega\rangle = 1$. Further, we can define a resolution of identity

$$\hat{\mathcal{I}} = \int d\Omega |\Omega\rangle\langle\Omega|, \quad (18)$$

where the differential phase-space volume element $d\Omega$ is

$$d\Omega = \frac{N!}{(2\pi)^{N-1}} \prod_{n=1}^{N-1} K_n(\theta_n) d\theta_n d\varphi_n, \quad (19)$$

where

$$K_n(\theta_n) = \cos \frac{\theta_n}{2} \left(\sin \frac{\theta_n}{2} \right)^{2(N-n)-1}. \quad (20)$$

For the two-level special case, it reduces to $K(\theta) = \frac{1}{2} \sin \theta$. Our definition of $K_n(\theta_n)$ in Eq. 20 is different than the one used in the previous literature.^{29,39,40} We find that this new expression of $d\Omega$ guarantees the identity relation of Eq. 18 and a correct distribution for each angle θ_n , whereas the previous expression (*e.g.* Eq. D4 in Ref. 29 or Eq. 4.29 in Ref. 40) does not. The proof of the current differential phase-space volume element definition is given in Appendix C.

B. Basic Properties of the Stratonovich-Weyl Transform

To evaluate any operator $\hat{A}(\hat{R})$ under a SW transformation, one starts by decomposing it on the GGM basis (Eqs 2-4) as follows

$$\hat{A}(\hat{R}) = \mathcal{A}_0(\hat{R}) \cdot \hat{\mathcal{I}} + \frac{1}{\hbar} \sum_{k=1}^{N^2-1} \mathcal{A}_k(\hat{R}) \cdot \hat{\mathcal{S}}_k, \quad (21)$$

where $\mathcal{A}_0(\hat{R}) = \frac{1}{N} \text{Tr}_e[\hat{A}(\hat{R})\hat{\mathcal{I}}] = \frac{1}{N} \sum_{n=1}^N A_{nn}(\hat{R})$ with $A_{nm}(\hat{R}) = \langle n|\hat{A}(\hat{R})|m\rangle$ and $\mathcal{A}_k(\hat{R}) = \frac{2}{\hbar} \text{Tr}_e[\hat{A}(\hat{R})\hat{\mathcal{S}}_k]$. Here, we explicitly consider a system (with the Hamiltonian in Eq. 1) that contains both electronic and nuclear DOFs. Similar to the expressions in Eq. 11, we can write down each component of \mathcal{A}_i as follows

$$\mathcal{A}_{\alpha_{mn}}(\hat{R}) = A_{mn}(\hat{R}) + A_{nm}(\hat{R}), \quad (22a)$$

$$\mathcal{A}_{\beta_{nm}}(\hat{R}) = i(A_{mn}(\hat{R}) - A_{nm}(\hat{R})), \quad (22b)$$

$$\mathcal{A}_{\gamma_n}(\hat{R}) = \sum_{l=1}^{n-1} \sqrt{\frac{2}{n(n-1)}} A_{ll}(\hat{R}) - \sqrt{\frac{2(n-1)}{n}} A_{nn}(\hat{R}), \quad (22c)$$

with $1 \leq m < n \leq N$ and $2 \leq n \leq N$ as previously introduced (under Eq. 4). To keep our notation concise, we will write \hat{A} instead of $\hat{A}(\hat{R})$ for the following equations, because the SW transform is performed only on the *electronic* DOFs and does not involve the nuclear DOFs.

The SW transform of an operator \hat{A} is defined as

$$[\hat{A}]_s(\Omega) = \text{Tr}_e[\hat{A} \cdot \hat{w}_s]. \quad (23)$$

This form of integral measure, though not normalized, had long been proposed by Nemoto [J. Phys. A Math. Gen. 33, 3493-3506 (2000)]:

$$d\mu_n = \cos \theta \sin^{2n-3}(\theta) \cos(\xi_1) \sin^{2n-5}(\xi_1) \cdots \cos(\xi_{n-2}) \sin(\xi_{n-2}) d\theta d\xi_1 \cdots d\xi_{n-2} d\varphi_1 \cdots d\varphi_{n-1}.$$

though different symbols are used and each angle is divided by two in this manuscript. This original result early in 2000 had not been properly cited here.

Comment: This is a copy of a formula before eq

(18) in Ref. 29. There is no citation.

In particular for the W-representation, we have $[\hat{\mathcal{I}}]_W(\Omega) = 1$ and $[\hat{S}_i]_W(\Omega) = \sqrt{N+1}\langle\Omega|\hat{S}_i|\Omega\rangle$ so that for a general operator $\hat{A} = A_0\hat{\mathcal{I}} + \sum_{i=1}^{N^2-1} A_i\hat{S}_i$, we get

$$A_W(u) = A_0 + \sqrt{N+1} \sum_{i=1}^{N^2-1} A_i \langle \Omega | \hat{S}_i | \Omega \rangle. \quad (18)$$

Comment: This is a copy of a statement in Ref. 29., without citation.

$$\hat{w}_W(\Omega) = \frac{1}{N} \hat{\mathcal{I}} + 2\sqrt{N+1} \sum_{i=1}^{N^2-1} \langle \Omega | \hat{S}_i | \Omega \rangle \hat{S}_i, \quad (17c)$$

giving the SW-representations $[\hat{A}]_s(\Omega) = \text{tr}[\hat{A}\hat{w}_s(\Omega)]$ for $s \in \{Q, P, W\}$. The readers can easily convince themselves that, with

Here, the generalized SW kernel \hat{w}_s is expressed as^{41–43}

$$\begin{aligned}\hat{w}_s(\Omega) &= \frac{1}{N} \hat{\mathcal{I}} + r_s \cdot \frac{2}{\hbar^2} \sum_{k=1}^{N^2-1} \langle \Omega | \hat{\mathcal{S}}_k | \Omega \rangle \hat{\mathcal{S}}_k \\ &= \frac{1}{N} \hat{\mathcal{I}} + r_s \cdot \frac{2}{\hbar} \sum_{k=1}^{N^2-1} \Omega_k \cdot \hat{\mathcal{S}}_k,\end{aligned}\quad (24)$$

where r_s is a constant related to the radius of the Bloch sphere^{44–46} in the $\mathfrak{su}(N)$ Lie algebra and $|\Omega\rangle$ are the generalized spin-coherent states defined previously. To simplify our notation, we rewrite the expectation value of the spin operator (in Eq. 24) as

$$\hbar\Omega_k \equiv \langle \Omega | \hat{\mathcal{S}}_k | \Omega \rangle, \quad (25)$$

where $\hbar\Omega$ is equivalent to the Bloch vector and its components' detailed expressions can be found in Eqs. B2-B4. In terms of the spin coherent states, we can also express the kernel as

$$\hat{w}_s(\Omega) = \frac{1 - r_s}{N} \hat{\mathcal{I}} + r_s |\Omega\rangle \langle \Omega|. \quad (26)$$

The kernel defines an identity

$$\hat{\mathcal{I}} = \int d\Omega \hat{w}_s, \quad (27)$$

that is proven in Eq. C23. Further, it is straightforward to show that

$$[\hat{\mathcal{S}}_k]_s(\Omega) = \text{Tr}_e [\hat{\mathcal{S}}_k \cdot \hat{w}_s] = \hbar r_s \Omega_k, \quad (28a)$$

$$[\hat{\mathcal{I}}]_s(\Omega) = \text{Tr}_e [\hat{\mathcal{I}} \cdot \hat{w}_s] = 1, \quad (28b)$$

by using the properties of the generators given in Eq. 7. The property in Eq. 28b means that the SW transform preserves the identity in the electronic Hilbert subspace, contrarily to the Wigner transform^{47,48} of the identity operator in the MMST formalism^{22,49} and hence, does not introduce any ambiguity of the identity expression.⁵⁰

Thus, Eq. 23 performs a mapping of an operator in the electronic subspace onto a phase space of continuous variables Ω as follows

$$\hat{A} \rightarrow [\hat{A}]_s(\Omega). \quad (29)$$

This is the basic idea of the generalized spin-mapping variables proposed by Runeson and Richardson in Ref. 24 and Ref. 29. Using the expression of \hat{w}_s (Eq. 24), $[\hat{A}(\hat{R})]_s$ in Eq. 23 becomes

$$[\hat{A}(\hat{R})]_s(\Omega) = \mathcal{A}_0(\hat{R}) + r_s \sum_{k=1}^{N^2-1} \mathcal{A}_k(\hat{R}) \cdot \Omega_k. \quad (30)$$

One of the important properties of the SW transform is that it can be used to compute a quantum mechanical trace in the continuous space as follows

$$\begin{aligned}\int d\Omega [\hat{A}]_s(\Omega) &= \int d\Omega \text{Tr}_e [\hat{A} \cdot \hat{w}_s] = \text{Tr}_e \left[\int d\Omega \hat{w}_s \cdot \hat{A} \right] \\ &= \text{Tr}_e [\hat{A}],\end{aligned}\quad (31)$$

Comment: A copy of Appendix F in Ref. 29 without citation.

where we used the short-hand notation $\varrho_s = R_s^2/2$ and $S_i(\Omega) = \frac{1}{\hbar} \langle \Omega | \hat{S}_i | \Omega \rangle$. Explicitly, we have $\varrho_Q = 1$, $\varrho_W = \sqrt{N+1}$ and $\varrho_P = N+1$ so that $\varrho_s \varrho_s = N+1$. Note that $A_s(\Omega) = A_0 + \varrho_s \sum_i A_i S_i(\Omega)$.

This structure, involving out product of generalized coherent states, had already been indicated by Tilma and Nemoto in J. Phys. A Math. Theor. 45, 015302 (2012). In their work, eq (3.13) reads,

$$\begin{aligned}F_{N,1}^{+1}(\theta, \phi) &= |(\theta, \phi)_N^1\rangle \langle (\theta, \phi)_N^1| \\ &= \frac{1}{N} \mathbb{1}_N + \frac{1}{2} \sum_{k=1}^{N^2-1} \langle (\theta, \phi)_N^1 | \Lambda_{N,1}(k) | (\theta, \phi)_N^1 \rangle \Lambda_{N,1}(k).\end{aligned}\quad (3.13)$$

where the out product is utilized, and then generalized to kernels with other choices of parameter as eq (4.7),

$$\begin{aligned}F_{N,1}^{s'}(\theta, \phi) &= \frac{\Omega(s')}{\Omega(s)} \tilde{F}_{N,1}^s(\theta, \phi) + \frac{1}{N} \mathbb{1}_N, \\ &= \frac{\Omega(s')}{\Omega(s)} \left(F_{N,1}^s(\theta, \phi) - \frac{1}{N} \mathbb{1}_N \right) + \frac{1}{N} \mathbb{1}_N, \\ &= \frac{\Omega(s')}{\Omega(s)} F_{N,1}^s(\theta, \phi) + \left(1 - \frac{\Omega(s')}{\Omega(s)} \right) \frac{1}{N} \mathbb{1}_N.\end{aligned}\quad (4.7)$$

Though the specific choice of generalized coherent states used by Tilma and Nemoto, and that by Huo and coworkers are different, the structure of mapping kernel has been already proposed by Tilma and Nemoto, and is not cited here.

Comment: Comparison to the text before eq (18) in Ref. 29. There is no citation.

In particular for the W-representation, we have $[\hat{\mathcal{I}}]_W(\Omega) = 1$ and $[\hat{S}_i]_W(\Omega) = \sqrt{N+1} \langle \Omega | \hat{S}_i | \Omega \rangle$ so that for a general operator

Comment: Comparison to eq (18) in Ref. 29. There is no citation.

$$A_W(u) = A_0 + \sqrt{N+1} \sum_{i=1}^{N^2-1} A_i \langle \Omega | \hat{S}_i | \Omega \rangle. \quad (18)$$

Comment: Comparison to eqs (14-15) in Ref. 29. There is no citation.

$$\text{tr}[\hat{A}\hat{B}] = \int d\mathbf{u} A_Q(\mathbf{u})B_P(\mathbf{u}) = \int d\mathbf{u} A_P(\mathbf{u})B_Q(\mathbf{u}). \quad (14)$$

$$\text{tr}[\hat{A}\hat{B}] = \int d\mathbf{u} A_W(\mathbf{u})B_W(\mathbf{u}). \quad (15)$$

where we have used the identity given in Eq. 27.

For two operators $\hat{A}(\hat{R})$ and $\hat{B}(\hat{R})$, one cannot compute the trace of a product of operators $\text{Tr}_e[\hat{A}\hat{B}]$ as $\int d\mathbf{u}[\hat{A}]_s[\hat{B}]_s(\Omega)$ for a given value of r_s , because generally $[\hat{A}\hat{B}]_s(\Omega) \neq [\hat{A}]_s[\hat{B}]_s(\Omega)$. It is required to use two matching values of the radius, r_s and $r_{\bar{s}}$, with complementing indices s and \bar{s} which will be defined in Eq. 36. It can be shown that the SW transform has the following property

$$\text{Tr}_e[\hat{A}\hat{B}] = \int d\Omega [\hat{A}\hat{B}]_s(\Omega) = \int d\Omega [\hat{A}]_s(\Omega)[\hat{B}]_{\bar{s}}(\Omega), \quad (32)$$

where $[\hat{B}]_{\bar{s}}(\Omega)$ is SW transformed through Eq. 30 using $r_{\bar{s}}$. The proof is given in Supplemental Material.

The sum of the squares of the generators (the so-called Casimir operator of $\mathfrak{su}(N)$) can be expressed with the identity operator as follows²⁹

$$\sum_{k=1}^{N^2-1} \hat{S}_k^2 = \hbar^2 \frac{N^2 - 1}{2N} \hat{\mathcal{I}}, \quad (33)$$

where the proof can be found in Appendix A of Ref. 29. Performing the SW transform on both sides of the above identity leads to the squared spin magnitude as follows

$$\sum_{k=1}^{N^2-1} [\hat{S}_k]_s [\hat{S}_k]_{\bar{s}} = \hbar^2 r_s r_{\bar{s}} \sum_{k=1}^{N^2-1} \Omega_k^2 = \hbar^2 \frac{N^2 - 1}{2N}, \quad (34)$$

which is a conserved quantity. Using the fact²⁹ that $\sum_{k=1}^{N^2-1} \Omega_k^2 = \frac{N-1}{2N}$ (see the proof in Appendix E of Ref. 29) together with the identity in Eq. 34, we have

$$r_s r_{\bar{s}} = N + 1. \quad (35)$$

The commonly used values²⁹ for r_s and $r_{\bar{s}}$ are

$$r_s = r_{\bar{s}} = \sqrt{N + 1}, \quad (\text{for } s = \bar{s} = W), \quad (36a)$$

$$r_s = 1, \quad r_{\bar{s}} = N + 1, \quad (\text{for } s = Q, \quad \bar{s} = P), \quad (36b)$$

$$r_s = N + 1, \quad r_{\bar{s}} = 1, \quad (\text{for } s = P, \quad \bar{s} = Q). \quad (36c)$$

Note that these parameters are not restricted to the above special cases, and in principle, can take any value in the range of $r_s \in (0, \infty)$.

Using the complementing $r_{\bar{s}}$, one can define the inverse SW transform⁵¹ as follows

$$\hat{A} = \int d\Omega \hat{w}_s(\Omega) [\hat{A}]_{\bar{s}}(\Omega), \quad (37)$$

where $[\hat{A}]_{\bar{s}}(\Omega)$ is defined in Eq. 30 $r_{\bar{s}}$. A simple proof of Eq. 37 is given in the Supplemental Material.

It is also useful to derive the expression of the SW transform of the product of two electronic operators $[\hat{A}\hat{B}]_s$ in order to compute commutation and anti-commutation relations. To proceed, we use the detailed

Comment: Repeating eq (19) in Ref. 29 without citation.

$$\begin{aligned} \sum_{i=1}^{N^2-1} [\hat{S}_i]_W(\Omega)^2 &= \sum_i [\hat{S}_i]_Q(\Omega)[\hat{S}_i]_P(\Omega) \\ &= (N+1) \sum_i \langle \Omega | \hat{S}_i | \Omega \rangle^2 = \frac{N^2 - 1}{2N}, \end{aligned} \quad (19)$$

$$\sum_{n=1}^F \left[\frac{(x^{(n)})^2 + (p^{(n)})^2}{2} - \gamma \right] = 1 \quad (6)$$

the mapping Hamiltonian eq 4 is equal to the conventional Meyer–Miller Hamiltonian eq 3. This was first proposed in ref 41 for general F -state systems. The simplest way is to use the full constraint electronic space that eq 6 defines, i.e.,

$$S(\mathbf{x}, \mathbf{p}): \delta \left(\sum_{n=1}^F \left[\frac{(x^{(n)})^2 + (p^{(n)})^2}{2} \right] - (1 + F\gamma) \right) \quad (7)$$

for constructing the formulation for physical properties in the mapping approach. The possible value of parameter γ for eq 6 or eq 7 implies $\gamma \in (-\frac{1}{F}, \infty)$.

In J. Phys. Chem. Lett. 12, 2496 (2021)(submitted on January 22, 2021 and published online on March 5, 2021)

$$S(\mathbf{x}, \mathbf{p}): \sum_{n=1}^F \left[\frac{1}{2}((x^{(n)})^2 + (p^{(n)})^2) \right] = 1 + F\gamma \quad (4)$$

Although we use the diabatic representation to reach eq 4, the constraint holds in the adiabatic representation as well. The constraint (eq 4) has already been implied in eqs 43 and 44 of ref 17, and used in ref 15 where $\gamma = 0$ is considered. The physical meaning of eq 4 requires only $\gamma > -1/F$. This confirms that negative values for the ZPE parameter, γ , are possible!

In Acc. Chem. Res. 54, 23, 4215-4228 (2021)(submitted on August 14, 2021 and published online on November 10, 2021)

$$S(\mathbf{x}, \mathbf{p}): \delta \left(\sum_{n=1}^F \frac{(x^{(n)})^2 + (p^{(n)})^2}{2} - (1 + F\gamma) \right) \quad (34)$$

for developing the formulation for evaluation of physical observables. In eq 34, the possible value of parameter γ lies in $(-\frac{1}{F}, \infty)$. The trace of a product of two operators is expressed

The continuous parameter space was first proposed in J. Phys. Chem. Lett. 12, 2496 (2021), which was submitted on January 22, 2021 and published online on March 5, 2021. Huo and coworkers did not cite these contributions above at all! The relationship between CMM and spin mapping had been clearly stated in J. Phys. Chem. Lett. 12, 2496 (2021),

eq 22 offers the only physical value for parameter γ in the region $(-\frac{1}{F}, \infty)$ to make eq 23 hold. We note that the so-called spin mapping model of refs 43 and 44 intrinsically based on the Meyer–Miller mapping Hamiltonian model (especially when $F \geq 3$ electronic states are involved) is only a special case of the exact phase space mapping formulation that we established first in refs 13 and 41 and then in ref 42, i.e., parameter $\gamma = 0, (\sqrt{F+1}-1)/F$, or 1 in our exact phase space mapping formulation corresponds to the Q-version, W-version, or P-version of refs 43 and 44, respectively. Interestingly, the

where we have used the identity given in Eq. 27.

For two operators $\hat{A}(\hat{R})$ and $\hat{B}(\hat{R})$, one cannot compute the trace of a product of operators $\text{Tr}_e[\hat{A}\hat{B}]$ as $\int d\mathbf{u}[\hat{A}]_s[\hat{B}]_s(\Omega)$ for a given value of r_s , because generally $[\hat{A}\hat{B}]_s(\Omega) \neq [\hat{A}]_s[\hat{B}]_s(\Omega)$. It is required to use two matching values of the radius, r_s and $r_{\bar{s}}$, with complementing indices s and \bar{s} which will be defined in Eq. 36. It can be shown that the SW transform has the following property

$$\text{Tr}_e[\hat{A}\hat{B}] = \int d\Omega [\hat{A}\hat{B}]_s(\Omega) = \int d\Omega [\hat{A}]_s(\Omega) [\hat{B}]_{\bar{s}}(\Omega), \quad (32)$$

where $[\hat{B}]_{\bar{s}}(\Omega)$ is SW transformed through Eq. 30 using $r_{\bar{s}}$. The proof is given in Supplemental Material.

The sum of the squares of the generators (the so-called Casimir operator of $\mathfrak{su}(N)$) can be expressed with the identity operator as follows²⁹

$$\sum_{k=1}^{N^2-1} \hat{S}_k^2 = \hbar^2 \frac{N^2-1}{2N} \hat{\mathcal{I}}, \quad (33)$$

where the proof can be found in Appendix A of Ref. 29. Performing the SW transform on both sides of the above identity leads to the squared spin magnitude as follows

$$\sum_{k=1}^{N^2-1} [\hat{S}_k]_s [\hat{S}_k]_{\bar{s}} = \hbar^2 r_s r_{\bar{s}} \sum_{k=1}^{N^2-1} \Omega_k^2 = \hbar^2 \frac{N^2-1}{2N}, \quad (34)$$

which is a conserved quantity. Using the fact²⁹ that $\sum_{k=1}^{N^2-1} \Omega_k^2 = \frac{N-1}{2N}$ (see the proof in Appendix E of Ref. 29) together with the identity in Eq. 34, we have

$$r_s r_{\bar{s}} = N + 1. \quad (35)$$

The commonly used values²⁹ for r_s and $r_{\bar{s}}$ are

$$r_s = r_{\bar{s}} = \sqrt{N+1}, \quad (\text{for } s = \bar{s} = W), \quad (36a)$$

$$r_s = 1, \quad r_{\bar{s}} = N + 1, \quad (\text{for } s = Q, \quad \bar{s} = P), \quad (36b)$$

$$r_s = N + 1, \quad r_{\bar{s}} = 1, \quad (\text{for } s = P, \quad \bar{s} = Q). \quad (36c)$$

Note that these parameters are not restricted to the above special cases, and in principle, can take any value in the range of $r_s \in (0, \infty)$.

Using the complementing $r_{\bar{s}}$, one can define the inverse SW transform⁵¹ as follows

$$\hat{A} = \int d\Omega \hat{w}_s(\Omega) [\hat{A}]_{\bar{s}}(\Omega), \quad (37)$$

where $[\hat{A}]_{\bar{s}}(\Omega)$ is defined in Eq. 30 $r_{\bar{s}}$. A simple proof of Eq. 37 is given in the Supplemental Material.

It is also useful to derive the expression of the SW transform of the product of two electronic operators $[\hat{A}\hat{B}]_s$ in order to compute commutation and anti-commutation relations. To proceed, we use the detailed

where we have used the identity given in Eq. 27.

For two operators $\hat{A}(\hat{R})$ and $\hat{B}(\hat{R})$, one cannot compute the trace of a product of operators $\text{Tr}_e[\hat{A}\hat{B}]$ as $\int d\mathbf{u}[\hat{A}]_s[\hat{B}]_{\bar{s}}(\Omega)$ for a given value of r_s , because generally $[\hat{A}\hat{B}]_s(\Omega) \neq [\hat{A}]_s[\hat{B}]_{\bar{s}}(\Omega)$. It is required to use two matching values of the radius, r_s and $r_{\bar{s}}$, with complementing indices s and \bar{s} which will be defined in Eq. 36. It can be shown that the SW transform has the following property

$$\text{Tr}_e[\hat{A}\hat{B}] = \int d\Omega [\hat{A}\hat{B}]_s(\Omega) = \int d\Omega [\hat{A}]_s(\Omega)[\hat{B}]_{\bar{s}}(\Omega), \quad (32)$$

where $[\hat{B}]_{\bar{s}}(\Omega)$ is SW transformed through Eq. 30 using $r_{\bar{s}}$. The proof is given in Supplemental Material.

The sum of the squares of the generators (the so-called Casimir operator of $\mathfrak{su}(N)$) can be expressed with the identity operator as follows²⁹

$$\sum_{k=1}^{N^2-1} \hat{S}_k^2 = \hbar^2 \frac{N^2 - 1}{2N} \hat{\mathcal{I}}, \quad (33)$$

where the proof can be found in Appendix A of Ref. 29. Performing the SW transform on both sides of the above identity leads to the squared spin magnitude as follows

$$\sum_{k=1}^{N^2-1} [\hat{S}_k]_s [\hat{S}_k]_{\bar{s}} = \hbar^2 r_s r_{\bar{s}} \sum_{k=1}^{N^2-1} \Omega_k^2 = \hbar^2 \frac{N^2 - 1}{2N}, \quad (34)$$

which is a conserved quantity. Using the fact²⁹ that $\sum_{k=1}^{N^2-1} \Omega_k^2 = \frac{N-1}{2N}$ (see the proof in Appendix E of Ref. 29) together with the identity in Eq. 34, we have

$$r_s r_{\bar{s}} = N + 1. \quad (35)$$

The commonly used values²⁹ for r_s and $r_{\bar{s}}$ are

$$r_s = r_{\bar{s}} = \sqrt{N + 1}, \quad (\text{for } s = \bar{s} = W), \quad (36a)$$

$$r_s = 1, \quad r_{\bar{s}} = N + 1, \quad (\text{for } s = Q, \quad \bar{s} = P), \quad (36b)$$

$$r_s = N + 1, \quad r_{\bar{s}} = 1, \quad (\text{for } s = P, \quad \bar{s} = Q). \quad (36c)$$

Note that these parameters are not restricted to the above special cases, and in principle, can take any value in the range of $r_s \in (0, \infty)$.

Using the complementing $r_{\bar{s}}$, one can define the inverse SW transform⁵¹ as follows

$$\hat{A} = \int d\Omega \hat{w}_s(\Omega) [\hat{A}]_{\bar{s}}(\Omega), \quad (37)$$

where $[\hat{A}]_{\bar{s}}(\Omega)$ is defined in Eq. 30 $r_{\bar{s}}$. A simple proof of Eq. 37 is given in the Supplemental Material.

It is also useful to derive the expression of the SW transform of the product of two electronic operators $[\hat{A}\hat{B}]_s$ in order to compute commutation and anti-commutation relations. To proceed, we use the detailed

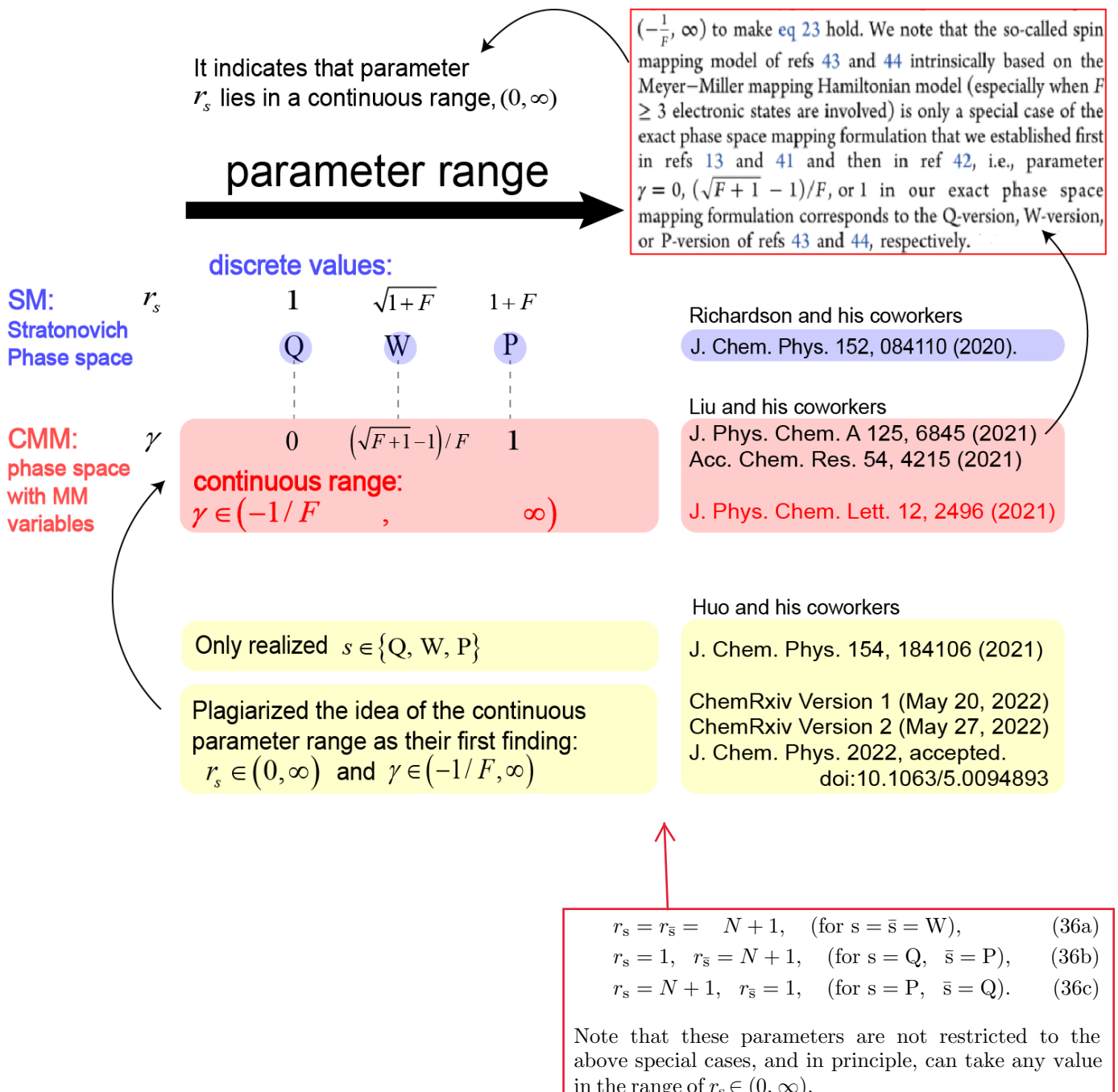
We had pointed out that spin mapping method with P, Q, W versions are only three special cases of CMM in *J. Phys. Chem. A* 125, 6845 -6863, (2021) (submitted on May 19, 2021, released on arXiv on July 7, 2021 and officially published on August 2, 2021):

$(-\frac{1}{F}, \infty)$ to make eq 23 hold. We note that the so-called spin mapping model of refs 43 and 44 intrinsically based on the Meyer–Miller mapping Hamiltonian model (especially when $F \geq 3$ electronic states are involved) is only a special case of the exact phase space mapping formulation that we established first in refs 13 and 41 and then in ref 42, i.e., parameter $\gamma = 0, (\sqrt{F+1} - 1)/F$, or 1 in our exact phase space mapping formulation corresponds to the Q-version, W-version, or P-version of refs 43 and 44, respectively. Interestingly, the

Also in *Acc. Chem. Res.* 54, 23, 4215-4228 (2021) (submitted on August 14, 2021 and published online on November 10, 2021) :

As pointed out in ref 42, it is trivial to show that the Q-version, W-version, or P-version of ref 36 corresponds to parameter $\gamma = 0, (\sqrt{F+1} - 1)/F$, or 1 of the exact phase space mapping formulation that we *first* proposed in refs 1 and 3 and then in ref 4, respectively. It will be interesting to use our general phase space mapping formulation to include or reformulate other approaches that use the Meyer–Miller mapping model.^{21,25,28–30,34,37,41,45,48}





expressions of \hat{A} and \hat{B} in their $\mathfrak{su}(N)$ representation, and express $[\hat{A}\hat{B}]_s$ as follows

$$\begin{aligned} [\hat{A}\hat{B}]_s(\Omega) &= [(\mathcal{A}_0(\hat{R}) \cdot \hat{\mathcal{I}} + \frac{1}{\hbar} \sum_{k=1}^{N^2-1} \mathcal{A}_k(\hat{R}) \cdot \hat{\mathcal{S}}_k) \\ &\quad \times (\mathcal{B}_0(\hat{R}) \cdot \hat{\mathcal{I}} + \frac{1}{\hbar} \sum_{k=1}^{N^2-1} \mathcal{B}_k(\hat{R}) \cdot \hat{\mathcal{S}}_k)]_s \\ &= [\mathcal{A}_0\mathcal{B}_0 \cdot \hat{\mathcal{I}} + \frac{\mathcal{A}_0}{\hbar} \sum_{k=1}^{N^2-1} \mathcal{B}_k \cdot \hat{\mathcal{S}}_k + \frac{\mathcal{B}_0}{\hbar} \sum_{k=1}^{N^2-1} \mathcal{A}_k \cdot \hat{\mathcal{S}}_k \\ &\quad + \frac{1}{\hbar^2} \sum_{j,k=1}^{N^2-1} \mathcal{A}_j \mathcal{B}_k \cdot \hat{\mathcal{S}}_j \hat{\mathcal{S}}_k]_s. \end{aligned} \quad (38)$$

Using the fact that

$$\hat{\mathcal{S}}_j \hat{\mathcal{S}}_k = \frac{1}{2} ([\hat{\mathcal{S}}_j, \hat{\mathcal{S}}_k] + \{\hat{\mathcal{S}}_j, \hat{\mathcal{S}}_k\}_+),$$

together with Eqs. 7 and 28, we can evaluate the SW transform of the product of operators as follows

$$\begin{aligned} [\hat{A}\hat{B}]_s(\Omega) &= \mathcal{A}_0\mathcal{B}_0 + \frac{1}{2N} \sum_{i=1}^{N^2-1} \mathcal{A}_i\mathcal{B}_i \quad (39) \\ &\quad + r_s \sum_{i=1}^{N^2-1} (\Omega_i \mathcal{A}_i \mathcal{B}_0 + \Omega_i \mathcal{A}_0 \mathcal{B}_i) \\ &\quad + \frac{r_s}{2} \sum_{i,j,k=1}^{N^2-1} \Omega_i \mathcal{A}_j \mathcal{B}_k (d_{ijk} + i f_{ijk}), \end{aligned}$$

where $\mathcal{A}_i(\hat{R})$ and $\mathcal{B}_i(\hat{R})$ are expressed in Eq. 22.

C. Mapping Formalism using the Stratonovich-Weyl Transform

Performing the SW transform of the Hamiltonian \hat{H} (Eq. 9) through Eq. 23, we have

$$[\hat{H}(\hat{R})]_s(\Omega) = \mathcal{H}_0(\hat{R}) + r_s \sum_{k=1}^{N^2-1} \mathcal{H}_k(\hat{R}) \cdot \Omega_k. \quad (40)$$

This is the mapping Hamiltonian expression in terms of the expectation values of the generalized spin operators.^{29,52}

In addition, we can also perform the SW transform of electronic projection operators and obtain

$$\begin{aligned} [|n\rangle\langle n|]_s &= \text{Tr}_e[|n\rangle\langle n|\hat{w}_s] \quad (41) \\ &= \frac{1}{N} + r_s \sum_{m=n+1}^N \sqrt{\frac{2}{m(m-1)}} \Omega_{\gamma_m} - r_s \sqrt{\frac{2(n-1)}{n}} \Omega_{\gamma_n}, \end{aligned}$$

with $1 \leq n \leq N$. The complementary expression $[|n\rangle\langle n|]_{\bar{s}}$ can be obtained by replacing r_s in Eq. 41 by $r_{\bar{s}}$.

Note that the first sum in Eq. 41 is null when the condition $m > n$ is not satisfied, *i.e.* when $n = N$, and the last term is null when $n = 1$. The population estimators only depend on the expectation values of the diagonal spin operators $\{\Omega_{\gamma_m}\}$ (see Eq. B4), hence they are independent of the mapping variables $\{\varphi_m\}$ for $i \in [1, N - 1]$. As expected, summing all the state population estimators gives a total population equal to 1, because the SW transformation explicitly preserves the identity in the electronic subspace (see Eq. 28b).

For an off-diagonal electronic operator with $m < n$, the SW transform is

$$[|n\rangle\langle m|]_s = r_s(\Omega_{\alpha_{nm}} - i\Omega_{\beta_{nm}}), \quad (42a)$$

$$[|m\rangle\langle n|]_s = r_s(\Omega_{\alpha_{nm}} + i\Omega_{\beta_{nm}}), \quad (42b)$$

where the detailed expressions of $\Omega_{\alpha_{nm}}$ and $\Omega_{\beta_{nm}}$ are provided in Eq. B2 and Eq. B3, respectively.

D. Connections with the MMST Mapping Formalism

Interestingly, there exists a variable transformation between the expectation values of the spin operators $\{\Omega_{\alpha_{nm}}, \Omega_{\beta_{nm}}, \Omega_{\gamma_n}\}$ and the harmonic oscillator phase space variables $\{q_n, p_n\}$. We express the expectation values of the spin coherent states using complex expansion coefficients $c_n = \langle n|\Omega \rangle$, leading to²⁹

$$\hbar\Omega_k = \langle \Omega | \hat{S}_k | \Omega \rangle = \sum_{n,m} \langle n | \hat{S}_k | m \rangle \cdot c_n^* c_m. \quad (43)$$

One can then define the following transformation^{29,53}

$$c_n = \langle n | \Omega \rangle = \frac{1}{\sqrt{2r_s}}(q_n + ip_n), \quad (44)$$

where $q_n/\sqrt{2r_s}$ is the real part of c_n and $p_n/\sqrt{2r_s}$ is the imaginary part of c_n . This transformation provides the connection between a given pair of q_n and p_n and the angle variables of the generalized spin coherent state $\{\theta_n, \varphi_n\}$ through Eq. 17. Using this transform, Eq. 43 becomes

$$2r_s\Omega_k = \sum_{n,m} \langle n | \hat{S}_k | m \rangle \cdot (q_n - ip_n)(q_m + ip_m). \quad (45)$$

Explicitly using the matrix elements of $\langle n | \hat{S}_k | m \rangle$ (see Eqs. 2-4), Eq. 45 becomes

$$2r_s\Omega_{\alpha_{nm}} = q_n q_m + p_n p_m, \quad (46a)$$

$$2r_s\Omega_{\beta_{nm}} = p_n q_m - q_n p_m, \quad (46b)$$

$$2r_s\Omega_{\gamma_n} = \frac{1}{\sqrt{2n(n-1)}} \left(\sum_{l=1}^{n-1} q_l^2 + p_l^2 - (n-1)(q_n^2 + p_n^2) \right). \quad (46c)$$

Note that this transformation does depend on the choice of r_s , which must match the index in the mapped Hamiltonian evolving the dynamics (see Sec. IV).

Cartesian variables had been carefully discussed before in Appendix B of J. Chem. Phys. 145, 204105 (2016). The authors failed to cite it.

$$c_n(t) = x^{(n)}(t) + ip^{(n)}(t), \quad (B2)$$

Comment: A copy of eq (29) in Ref. 29 without citation.

$$[\hat{S}_i]_W(\Omega) = \sum_{n,m=1}^N \langle n | \hat{S}_i | m \rangle \frac{1}{2}(X_n - iP_n)(X_m + iP_m). \quad (29)$$

For a purely real Hamiltonian (such that in Eq. 11b $\mathcal{H}_{\beta_{nm}} = 0$), using the transform defined in Eq. 46, the spin mapping Hamiltonian $[\hat{H}(\hat{R})]$ in Eq. 40 can be expressed as the well-known MMST mapping Hamiltonian^{7,8,10}

$$\mathcal{H} = \mathcal{H}_0(\hat{R}) + \sum_n \frac{1}{2} [V_{nn}(\hat{R}) - \bar{V}(\hat{R})] (q_n^2 + p_n^2 - \gamma) \quad (47)$$

$$+ \sum_{n < m} V_{nm}(\hat{R}) (q_n q_m + p_n p_m),$$

where $\bar{V}(\hat{R}) = \frac{1}{N} \sum_l V_{ll}(\hat{R})$, $\mathcal{H}_0(\hat{R}) = \frac{\hat{p}^2}{2m} + U_0(\hat{R}) + \bar{V}(\hat{R})$ is the trace part of the potential, which is naturally separated from the traceless part. Further, the parameter γ is expressed as follows

$$\gamma = \frac{2}{N} (r_s - 1), \quad (48)$$

or equivalently, $r_s = 1 + N\gamma/2$. In the MMST mapping formalism, this parameter is viewed as the zero-point energy (ZPE) parameter.^{23,54,55} In the $\mathfrak{su}(N)$ mapping formalism, it is the parameter related to the choice of r_s . Nevertheless, Eq. 48 helps to establish the connection between the boundaries on the SW radius and the boundaries on the γ parameter in the MMST mapping. The constraint of the radius $r_s \in (0, \infty)$ leads to a corresponding constraint for the ZPE parameter, $\gamma \in (-\frac{2}{N}, \infty)$. The negative values of the ZPE parameter has been proposed in the MMST framework,⁵⁵ and simply correspond to $r_s \leq r_Q = 1$.

Using the conjugate variables $\{q_n, p_n\}$ defined in Eq. 44, the SW kernel in Eq. 26 can be equivalently expressed in the diabatic electronic basis

$$\hat{w}_s = \frac{1 - r_s}{N} \hat{\mathcal{I}} + r_s \sum_{a,b} c_a c_b^* |a\rangle \langle b| \quad (49)$$

$$= \frac{1 - r_s}{N} \hat{\mathcal{I}} + \frac{1}{2} \sum_{a,b} (q_a + ip_a)(q_b - ip_b) |a\rangle \langle b|,$$

which is identical to the kernel (expressed in Eq. 7 of Ref. 55) derived in the extended classical mapping model (eCMM),^{55,56} when adding an additional total population constraint in the MMST mapping phase space. Here, the total population constraint is naturally satisfied in the $\mathfrak{su}(N)$ framework and within the SW transform. The reason why the two kernels are identical is because the kernel derived in Ref. 55 is based on all the assumptions and constraints used to derive the SW kernel, with the difference of using the Cartesian coordinates defined in Eq. 44. Hence, the work in Ref. 55 can be viewed as a reformulation of the SW kernel that leads to an equivalent transformation of the quantum phase space into a classical phase space. The mathematical reason behind this equivalence of the kernels for two different formalism could also be explained as follows. Using the additional population constraint and the phase arbitrariness,

Just repeating our contribution without any citation:

In J. Phys. Chem. A 125, 31, 6845-6863 (2021)

(submitted on May 19, 2021, released on arXiv on July 7, 2021 and officially published on August 2, 2021)

$$\sum_{n=1}^F \left[\frac{(x^{(n)})^2 + (p^{(n)})^2}{2} - \gamma \right] = 1 \quad (6)$$

the mapping Hamiltonian eq 4 is equal to the conventional Meyer–Miller Hamiltonian eq 3. This was first proposed in ref 41 for general F -state systems. The simplest way is to use the full constraint electronic space that eq 6 defines, i.e.,

$$\mathcal{S}(\mathbf{x}, \mathbf{p}): \delta \left(\sum_{n=1}^F \left[\frac{(x^{(n)})^2 + (p^{(n)})^2}{2} \right] - (1 + F\gamma) \right) \quad (7)$$

for constructing the formulation for physical properties in the mapping approach. The possible value of parameter γ for eq 6 or eq 7 implies $\gamma \in (-\frac{1}{F}, \infty)$.

In J. Phys. Chem. Lett. 12, 2496 (2021)(submitted on January 22, 2021 and published online on March 5, 2021)

$$\mathcal{S}(\mathbf{x}, \mathbf{p}): \sum_{n=1}^F \left[\frac{1}{2} ((x^{(n)})^2 + (p^{(n)})^2) \right] = 1 + F\gamma \quad (4)$$

Although we use the diabatic representation to reach eq 4, the constraint holds in the adiabatic representation as well. The constraint (eq 4) has already been implied in eqs 43 and 44 of ref 17, and used in ref 15 where $\gamma = 0$ is considered. The physical meaning of eq 4 requires only $\gamma > -1/F$. This confirms that negative values for the ZPE parameter, γ , are possible!

In Acc. Chem. Res. 54, 23, 4215-4228 (2021)(submitted on August 14, 2021 and published online on November 10, 2021)

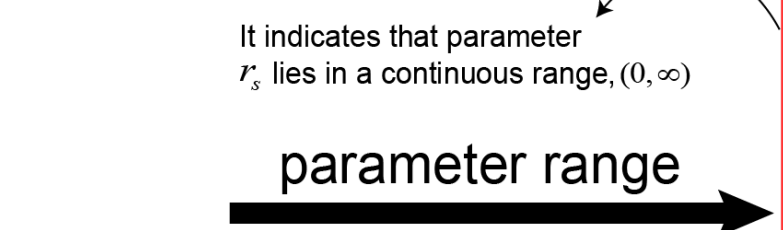
$$\mathcal{S}(\mathbf{x}, \mathbf{p}): \delta \left(\sum_{n=1}^F \frac{(x^{(n)})^2 + (p^{(n)})^2}{2} - (1 + F\gamma) \right) \quad (34)$$

for developing the formulation for evaluation of physical observables. In eq 34, the possible value of parameter γ lies in $(-\frac{1}{F}, \infty)$. The trace of a product of two operators is expressed

The continuous parameter space was first proposed in J. Phys. Chem. Lett. 12, 2496 (2021), which was submitted on January 22, 2021 and published online on March 5, 2021. Huo and coworkers did not cite these contributions above at all!

$$\gamma = \frac{2}{N}(r_s - 1), \quad (48)$$

or equivalently, $r_s = 1 + N\gamma/2$. In the MMST mapping formalism, this parameter is viewed as the zero-point energy (ZPE) parameter.^{23,54,55} In the $\mathfrak{su}(N)$ mapping formalism, it is the parameter related to the choice of r_s . Nevertheless, Eq. 48 helps to establish the connection between the boundaries on the SW radius and the boundaries on the γ parameter in the MMST mapping. The constraint of the radius $r_s \in (0, \infty)$ leads to a corresponding constraint for the ZPE parameter, $\gamma \in (-\frac{2}{N}, \infty)$. The negative values of the ZPE parameter has been proposed in the MMST framework,⁵⁵ and simply correspond to $r_s \leq r_Q = 1$.



SM: Stratonovich Phase space	r_s	1	$\sqrt{1+F}$	$1+F$
CMM: phase space with MM variables	γ	Q	W	P

discrete values:

continuous range:
 $\gamma \in (-1/F, \infty)$

$(-\frac{1}{F}, \infty)$ to make eq 23 hold. We note that the so-called spin mapping model of refs 43 and 44 intrinsically based on the Meyer–Miller mapping Hamiltonian model (especially when $F \geq 3$ electronic states are involved) is only a special case of the exact phase space mapping formulation that we established first in refs 13 and 41 and then in ref 42, i.e., parameter $\gamma = 0, (\sqrt{F+1} - 1)/F$, or 1 in our exact phase space mapping formulation corresponds to the Q-version, W-version, or P-version of refs 43 and 44, respectively.

Richardson and his coworkers
J. Chem. Phys. 152, 084110 (2020).

Liu and his coworkers
J. Phys. Chem. A 125, 6845 (2021)
Acc. Chem. Res. 54, 4215 (2021)
J. Phys. Chem. Lett. 12, 2496 (2021)

Huo and his coworkers
J. Chem. Phys. 154, 184106 (2021)
ChemRxiv Version 1 (May 20, 2022)
ChemRxiv Version 2 (May 27, 2022)
J. Chem. Phys. 2022, accepted.
doi:10.1063/5.0094893

Only realized $s \in \{Q, W, P\}$

Plagiarized the idea of the continuous parameter range as their first finding:
 $r_s \in (0, \infty)$ and $\gamma \in (-1/F, \infty)$

the $2N$ -dimensional MMST phase space of $\{q_n, p_n\}$ is reduced to a complex projective (CP) space, mathematically denoted as $CP(N-1)$.⁵³ For a given algebra, there is an associated group which carries a natural geometrical manifold and the above $CP(N-1)$ space is in fact a subspace of the parameterized manifold of $\mathfrak{su}(N)$.⁵⁷

Using this expression of the kernel, the SW transform of an electronic operator $|n\rangle\langle m|$ (based upon the definition in Eq. 23) is

$$\begin{aligned} [|n\rangle\langle m|]_s &= \frac{1-r_s}{N}\delta_{nm} + \frac{1}{2}(q_m + ip_m)(q_n - ip_n) \quad (50) \\ &= -\frac{\gamma}{2}\delta_{nm} + \frac{1}{2}(q_m + ip_m)(q_n - ip_n). \end{aligned}$$

The same result can be obtained by performing the transform defined in Eq. 46 directly on Eq. 41 and Eq. 42. For the diagonal projection operators ($n = m$), Eq. 50 becomes

$$[|n\rangle\langle n|]_s = \frac{1}{2}(q_n^2 + p_n^2 - \gamma). \quad (51)$$

For the complementary index \bar{s} , the expression $[|n\rangle\langle n|]_{\bar{s}} = \text{Tr}_e[|n\rangle\langle n|\hat{w}_{\bar{s}}]$ is

$$\begin{aligned} [|n\rangle\langle n|]_{\bar{s}} &= \frac{1-r_{\bar{s}}}{N} + \frac{1}{2} \cdot \frac{r_{\bar{s}}}{r_s}(q_n^2 + p_n^2) \quad (52) \\ &= \frac{N+1}{2(1+\frac{N\gamma}{2})^2} \cdot (q_n^2 + p_n^2) - \frac{1-\frac{\gamma}{2}}{1+\frac{N\gamma}{2}}, \end{aligned}$$

where we have used the fact that $r_{\bar{s}}/r_s = (N+1)/r_s^2 = (N+1)/(\frac{N\gamma}{2} + 1)^2$ and $r_{\bar{s}} = (N+1)/(\frac{N\gamma}{2} + 1)$ based on Eq. 48 and Eq. 35. Eq. 51 and 52 are identical to the estimators defined in the Spin-LSC²⁹ and in the eCMM⁵⁵ approaches.

In the $\mathfrak{su}(N)$ mapping formalism, the total population constraint on the $2N$ -dimensional phase space comes naturally from the normalization of the generalized spin coherent state^{53,57} as follows

$$\langle \Omega | \Omega \rangle = \sum_n c_n^* c_n = \frac{1}{2r_s} \sum_{n=1}^N (q_n^2 + p_n^2) = 1, \quad (53)$$

which properly enforces the total electronic diabatic population to be one for these MMST mapping variables

$$\sum_{n=1}^N \frac{1}{2}(q_n^2 + p_n^2 - \gamma) = 1. \quad (54)$$

Alternatively, one can obtain this condition from the basic property of the SW transform that preserves the trace of the electronic identity operator (Eq. 28) as follows

$$[\hat{\mathcal{I}}]_s = \sum_{n=1}^N [|n\rangle\langle n|]_s = 1 - r_s + \sum_n \frac{1}{2}(q_n^2 + p_n^2) = 1.$$

Comment: Such normalized "manifold" was firstly proposed in J. Chem. Phys. 151, 024105 (2019):

$$\sum_{n=1}^F P_n = \sum_{n=1}^F \frac{1}{2} \left(x^{(n)} x^{(n)} + p^{(n)} p^{(n)} \right) = 1 \quad (15)$$

Also in J. Phys. Chem. Lett. 12, 2496 (2021):

$P^T M^{-1} P / 2$ implies the constraint for the electronic DOFs¹⁵

$$S(\mathbf{x}, \mathbf{p}): \sum_{n=1}^F \left[\frac{1}{2} ((x^{(n)})^2 + (p^{(n)})^2) \right] = 1 + F\gamma \quad (4)$$

Using Eq. 50 and the Hamiltonian in Eq. 1, one can also directly obtain the mapping Hamiltonian expression

$$\begin{aligned} [\hat{H}(\hat{R})]_s = & \hat{T}_R + U_0(\hat{R}) + \sum_n \frac{1}{2} V_{nn}(\hat{R})(q_n^2 + p_n^2 - \gamma) \\ & + \sum_{n < m} V_{nm}(\hat{R})(q_n q_m + p_n p_m), \end{aligned} \quad (55)$$

which is indeed equivalent to Eq. 47 due to the constraint on the total population in Eq. 54.

The above transformation defined in Eq. 44 introduce an arbitrary global phase variable, such that there are $2N - 1$ independent variables among $\{q_n, p_n\}$ (with one constraint subject to Eq. 53), as opposed to only $2N - 2$ independent variables among $\{\theta_n, \varphi_n\}$. This is because c_n will also, in principle, contain $2N - 2$ independent real variables, with one arbitrary global phase compared to the $\{\theta_n, \varphi_n\}$ angles (see Eq. 17). This global phase will not influence the quantum dynamics.

Note that historically, the MMST mapping formalism (Eq. 47) is established through the Stock-Thoss mapping procedure^{8,10} by representing the N -level system with N harmonic oscillators' singly excited states, using the mapping relation of $|n\rangle \rightarrow |0_1, \dots, 1_n, \dots, 0_N\rangle = \hat{a}_n^\dagger |0_1, \dots, 0_n, \dots, 0_N\rangle$, where $\hat{a}_n^\dagger = \frac{1}{\sqrt{2\hbar}}(\hat{q}_n - i\hat{p}_n)$, $\hat{a}_n = \frac{1}{\sqrt{2\hbar}}(\hat{q}_n + i\hat{p}_n)$, and $[\hat{p}_n, \hat{q}_m] = i\delta_{nm}$. Using the mapping relation $\sum_{nm} V_{nm}(\hat{R})|n\rangle\langle m| \rightarrow \sum_{nm} V_{nm}(\hat{R})\hat{a}_n^\dagger \hat{a}_m$, the Stock-Thoss mapping Hamiltonian is

$$\begin{aligned} \hat{H} = & \hat{T}_R + U_0(\hat{R}) + \sum_n \frac{1}{2} V_{nn}(\hat{R})(\hat{q}_n^2 + \hat{p}_n^2 - 1) \\ & + \sum_{n < m} V_{nm}(\hat{R})(\hat{q}_n \hat{q}_m + \hat{p}_n \hat{p}_m). \end{aligned} \quad (56)$$

One can further down-grade these mapping operators into classical variables, for example, using the Wigner transform through the mixed quantum-classical approximation,⁵⁸ linearization approximation,^{11,59} or the Husimi representation (coherent state basis) for these mapping variables through the semi-classical approximation^{8,10,12,13,60,61} or the partial linearization approximation.¹⁶ This argument leads to the ZPE parameter $\gamma = 1$, and without the constraint provided in Eq. 54, even though $\sum_{n=1}^N \frac{1}{2}(q_n^2 + p_n^2 - \gamma)$ is a constant of motion. Most of the existing mapping approaches are based upon this mapping procedure.^{11,14}

As opposed to the Stock-Thoss mapping procedure which is a generalized Schwinger bosonization approach, the starting point of the $\mathfrak{su}(N)$ mapping formalism is completely different. The $\mathfrak{su}(N)$ mapping formalism uses the generators of the Lie group, which exactly preserves the symmetry and the dimensionality of the original electronic Hilbert subspace. It is interesting that despite a completely different mapping procedure, the same mapping Hamiltonian (Eq. 47) can be obtained upon a variable transformation (Eq. 46) of the mapping Hamiltonian $[\hat{H}(\hat{R})]_s(\Omega)$ in the $\mathfrak{su}(N)$ formalism. In the context of

Comment: Cartesian variables had been discussed in detail in Appendix B of J. Chem. Phys. 145, 204105 (2016).

$$c_n(t) = x^{(n)}(t) + i p^{(n)}(t), \quad (\text{B2})$$

the $\mathfrak{su}(N)$ mapping formalism, these conjugated mapping variables $\{q_n, p_n\}$ do not have the meaning of position and momentum of mapping oscillators as suggested in the Stock-Thoss mapping procedure;^{8,10} they are simply the real and imaginary components of the expansion coefficients⁵³ of the generalized spin coherent states in the diabatic basis as indicated in Eq. 44. Previous work by Runeson and Richardson²⁹ have also shown this connection using the transform expressed in Eq. 44.

IV. TIME-CORRELATION FUNCTION IN THE MIXED WIGNER/STRATONOVICH-WEYL REPRESENTATION

In this section, we derive the exact expression of the time correlation function (TCF) and the expression of estimators for different types of quantum operators. The exact and approximate forms of the Liouvillian will be discussed in Sec. V.

A. Time-correlation Functions

The quantum TCF is expressed as

$$C_{AB}(t) = \frac{1}{Z} \text{Tr}_e \text{Tr}_n [e^{-\beta \hat{H}} \hat{A}(0) \hat{B}(t)], \quad (57)$$

with the Hamiltonian defined in Eq. 1, and $\beta = 1/k_B T$. The density matrix under the canonical equilibrium condition is $\hat{\rho}_{\text{eq}} = e^{-\beta \hat{H}} / Z$ and the partition function is defined as $Z = \text{Tr}_e \text{Tr}_n [e^{-\beta \hat{H}}]$. In order to compute the nuclear trace Tr_n , we insert the identity $\hat{1}_{R'} = \int dR' |R'\rangle \langle R'|$. To compute the electronic trace we use the property of the SW transform in Eq. 31. This leads to

$$C_{AB}(t) = \frac{1}{Z} \int dR' \int d\Omega [\langle R' | e^{-\beta \hat{H}} \hat{A}(0) \hat{B}(t) | R' \rangle]_s(\Omega). \quad (58)$$

To proceed, we use the property given in Eq. 32 and identify $e^{-\beta \hat{H}} \hat{A}(0)$ and $\hat{B}(t)$ as two operators to compute the trace of $\int d\Omega$. By adding another nuclear identity $\hat{1}_{R''} = \int dR'' |R''\rangle \langle R''|$ between two operators, we can re-express Eq. 58 as

$$\begin{aligned} C_{AB}(t) &= \frac{1}{Z} \int dR' \int dR'' \int d\Omega \\ &\times [\langle R' | e^{-\beta \hat{H}} \hat{A}(0) | R'' \rangle]_{\bar{s}}(\Omega) [\langle R'' | \hat{B}(t) | R' \rangle]_s(\Omega). \end{aligned} \quad (59)$$

Introducing the nuclear mean path and path difference variables^{62–64}

$$R = \frac{1}{2}(R' + R''), \quad (60a)$$

$$\Delta = R' - R'', \quad (60b)$$

and inserting the following identity of the nuclear DOFs^{65,66}

$$\hat{\mathbb{1}}_R = \int d\Delta' \delta(\Delta + \Delta') = \frac{1}{2\pi\hbar} \int d\Delta' \int dP e^{\frac{i}{\hbar} P(\Delta + \Delta')} \quad (61)$$

into the TCF, Eq. 59 becomes

$$\begin{aligned} C_{AB}(t) &= \frac{1}{2\pi\hbar Z} \int dR \int d\Delta \int d\Delta' \int dP e^{\frac{i}{\hbar} P(\Delta + \Delta')} \int d\Omega \\ &\times [\langle R + \frac{\Delta}{2} | e^{-\beta\hat{H}} \hat{A}(0) | R - \frac{\Delta}{2} \rangle]_{\bar{s}}(\Omega) \\ &\times [\langle R - \frac{\Delta'}{2} | \hat{B}(t) | R + \frac{\Delta'}{2} \rangle]_s(\Omega). \end{aligned} \quad (62)$$

The above equation has an explicit Wigner transform^{47,67,68} over the nuclear DOFs, which is defined for an operator $\hat{O}(\hat{R})$ as follows

$$[\hat{O}(\hat{R})]_w = \int d\Delta e^{\frac{i}{\hbar} P\Delta} \langle R - \frac{\Delta}{2} | \hat{O}(\hat{R}) | R + \frac{\Delta}{2} \rangle. \quad (63)$$

Note that the lower case w used here represents the Wigner transform, whereas the capital case W represents a special choice of the SW transform through $r_w = \sqrt{N+1}$.

With the above definition, we can rewrite Eq. 62 as

$$\begin{aligned} C_{AB}(t) &= \frac{1}{2\pi\hbar Z} \int dR \int dP \int d\Omega [e^{-\beta\hat{H}} \hat{A}(0)]_{w\bar{s}} [\hat{B}(t)]_{ws}, \\ &= \frac{1}{2\pi\hbar Z} \int dR \int dP \int d\Omega [e^{-\beta\hat{H}} \hat{A}(0)]_{ws} e^{\hat{\mathcal{L}}t} [\hat{B}(t)]_{ws}, \end{aligned} \quad (64)$$

where $[\hat{A}(\hat{R})]_{ws}$ is a Wigner transform of the nuclear DOFs (defined in Eq. 63) and a SW transform of the electronic DOFs in the $\mathfrak{su}(N)$ representation (defined in Eq. 23 or Eq. 31). The time evolved expectation value $[\hat{B}(t)]_{ws}$ is written using the quantum Liouvillian $\hat{\mathcal{L}}$ to update $[\hat{B}(0)]_{ws}$. The exact expression of $\hat{\mathcal{L}}$ is derived in Sec. V. From now on, we will simply denote $\hat{A}(0)$ as \hat{A} and $\hat{B}(0)$ as \hat{B} .

Note that because the quantum Liouvillian is derived based on $[\hat{B}(t)]_s = e^{\hat{\mathcal{L}}(r_s)t} [\hat{B}]_s$, $\hat{\mathcal{L}}$ must have the same SW radius r_s as \hat{B} . This feature is different from the Spin-LSC approach^{24,29} which assumes that $\hat{\mathcal{L}}$ contains the same $r_{\bar{s}}$ as $[\hat{A}]_{\bar{s}}$, and operator \hat{B} has a different complementing radius r_s . Same choice is also made in a recent work on the extended Classical Mapping Method (eCMM).⁵⁵ Only under the special case where $r_s = r_{\bar{s}} = \sqrt{N+1}$ (for $s = W$ method), does our choice of r_s in $\hat{\mathcal{L}}$ agrees with spin-LSC.^{24,29} In practice we obtain numerically identical results when swapping the indices of the estimators, as long as the index of the Liouvillian coincides with the index used to define $\{q_n, p_n\}$ in Eq. 44 when using those mapping variables. This is necessary as it is required to get a dynamics equivalent to the dynamics using the $\{\theta_n, \varphi_n\}$ mapping variables, where no r_s appear in their definition.

B. Estimators of Different Types of Operators

To compute the transform of the operator $[e^{-\beta \hat{H}} \hat{A}(0)]_{ws}$, we need to perform the Wigner transform of the nuclear DOFs and SW transform of the electronic DOFs for a product of two operators. For the Wigner transform of two operators, one has^{47,48}

$$[\hat{A}\hat{B}]_w = [\hat{A}]_w e^{-i\hat{\Lambda}\hbar/2} [\hat{B}]_w, \quad (65)$$

where

$$\hat{\Lambda} = \frac{\overleftarrow{\partial}}{\partial P} \frac{\overrightarrow{\partial}}{\partial R} - \frac{\overleftarrow{\partial}}{\partial R} \frac{\overrightarrow{\partial}}{\partial P} \quad (66)$$

is the negative Poisson operator associated with the nuclear DOFs.^{67,69,70}

Combining Eq. 65 and Eq. 39, we can write down the general expression of the Wigner/Stratonovich-Weyl transform for a product of two operators $\hat{A}\hat{B}$ as follows

$$\begin{aligned} [\hat{A}\hat{B}]_{ws} &= [\mathcal{A}_0]_w e^{-i\frac{\hat{\Lambda}\hbar}{2}} [\mathcal{B}_0]_w + \frac{1}{2N} \sum_{k=1}^{N^2-1} [\mathcal{A}_k]_w e^{-i\frac{\hat{\Lambda}\hbar}{2}} [\mathcal{B}_k]_w \\ &\quad + r_{\bar{s}} \sum_{k=1}^{N^2-1} \Omega_k ([\mathcal{A}_k]_w e^{-i\frac{\hat{\Lambda}\hbar}{2}} [\mathcal{B}_0]_w + [\mathcal{A}_0]_w e^{-i\frac{\hat{\Lambda}\hbar}{2}} [\mathcal{B}_k]_w) \\ &\quad + \frac{r_{\bar{s}}}{2} \sum_{i,j,k=1}^{N^2-1} \Omega_i [\mathcal{A}_j]_w e^{-i\frac{\hat{\Lambda}\hbar}{2}} [\mathcal{B}_k]_w (d_{ijk} + i f_{ijk}), \end{aligned} \quad (67)$$

where $[\mathcal{A}_i]_w$ is the Wigner transform of $\mathcal{A}_i(\hat{R})$ (with the corresponding expression in Eq. 22). The above expression can be easily generalized into the symmetrized version of TCF with $\frac{1}{2} [e^{-\beta \hat{H}} \hat{A}(0) + A(0)e^{-\beta \hat{H}}]_{ws}$, and evaluating each term of the Wigner transform and SW transform.

For an operator \hat{A} that does not depend on the electronic DOFs (*e.g.* not an electronic operator $|n\rangle\langle m|$), we have $[\hat{A}]_{ws} = [\hat{A}_0]_w$, then

$$[e^{-\beta \hat{H}} \hat{A}]_{ws} = \mathcal{A}_0 \cdot \cos \frac{\hat{\Lambda}\hbar}{2} [e^{-\beta \hat{H}}]_{ws}.$$

Further, if \hat{A} is only linear in \hat{R} or \hat{P} , we have

$$[e^{-\beta \hat{H}} \hat{A}]_{ws} = \mathcal{A}_0 [e^{-\beta \hat{H}}]_{ws}.$$

The estimator $[\hat{B}]_{ws}$ in Eq. 64 is also a mixed Wigner/Stratonovich-Weyl transform of \hat{B} , but with a complementary index r_s . If \hat{B} is a position operator, then $\hat{B} = \hat{R}$, and $[\hat{B}]_{ws} = [\hat{R}]_w = R$. If \hat{B} is a pure electronic projection operator $\hat{B} = |n\rangle\langle n|$, the estimator is $[\hat{B}]_{ws} = [|n\rangle\langle n|]_s$, with the expression detailed in Eq. 41. In addition, the expression of $[|n\rangle\langle n|]_s$ in terms of the MMST variables can be found in Eq. 51.

C. Population Dynamics through Time Correlation Function

For a given photo-induced process, we are often interested in the reduced density matrix dynamics upon an initial excitation of the molecular system. In this case, the system is initially prepared in its ground state, with the ground state Hamiltonian

$$\hat{H}_g = (\hat{T}_R + U_g(\hat{R})), \quad (68)$$

and $U_g(\hat{R})$ is the ground state potential. Upon the initial photo-excitation of the system, the system is excited to state $|n\rangle$.

The reduced density matrix element can be expressed as

$$\rho_{ij}(t) = \text{Tr}_e \text{Tr}_n [\hat{\rho}(0) e^{\frac{i}{\hbar} \hat{H} t} |i\rangle \langle j| e^{-\frac{i}{\hbar} \hat{H} t}], \quad (69)$$

where the initial density operator $\hat{\rho}(0)$ is expressed as a tensor product of the electronic and nuclear DOFs as $\hat{\rho}(0) = |n\rangle \langle n| \otimes \frac{1}{Z} e^{-\beta \hat{H}_g}$, where $Z = \text{Tr}[e^{-\beta \hat{H}_g}]$, and \hat{H}_g is the ground state Hamiltonian in Eq. 68.

The reduced density matrix $\rho_{ij}(t)$ can also be equivalently expressed as a correlation function

$$\rho_{ij}(t) = C_{AB}(t) = \frac{1}{Z} \text{Tr}_e \text{Tr}_n [e^{-\beta \hat{H}_g} \hat{A} e^{\frac{i}{\hbar} \hat{H} t} \hat{B} e^{-\frac{i}{\hbar} \hat{H} t}], \quad (70)$$

where $\hat{A} = |n\rangle \langle n|$ is the initially occupied electronic state, and $\hat{B} = |i\rangle \langle j|$. Using the mixed Wigner/Stratonovich-Weyl representation for the TCF, we have

$$C_{AB}(t) = \frac{1}{2\pi\hbar Z} \int dR \int dP \int d\Omega \times [|n\rangle \langle n|]_{\bar{s}} [e^{-\beta \hat{H}_g}]_w e^{\hat{\mathcal{L}}t} [|i\rangle \langle j|]_s. \quad (71)$$

One can numerically perform the integrals over $d\Omega$ by sampling the initial conditions according to the differential phase space volume element expression in Eq. 19, and explicitly using the expression of $[|n\rangle \langle n|]_{\bar{s}}$ (Eq. 41 with $r_{\bar{s}}$, or Eq. 52 in terms of the MMST mapping variables).

Another numerically advantageous but *approximate* method is to focus the initial electronic state.^{24,29,61} The focused method requires to know what values to attribute to the mapping variables in order to enforce an initial projection onto state $|n\rangle$. As proposed in the previous work of spin-LSC, this requires to replace $[|n\rangle \langle n|]_{\bar{s}}$ in Eq. 71 by $[|n\rangle \langle n|]_s$ in order to achieve a properly normalized initial population.^{24,29} To this end, we first introduce the following variables

$$\Theta_n \equiv nr_s \sum_{k=n+1}^N \sqrt{\frac{2}{k(k-1)}} \Omega_{\gamma_k} = r_s \left(\frac{N-n}{N} - \prod_{k=1}^n \sin^2 \frac{\theta_k}{2} \right), \quad (72)$$

where $n \in [1, N-1]$. The derivation of the second equality in Eq. 72 is provided in the Supplemental Material. For $n = N$, we further introduce the proper boundaries

$\Theta_N = \Theta_0 = 0$. We then write the estimator in Eq. 41 with these new variables $\{\Theta_n\}$ as follows

$$\begin{aligned} [|\mathbf{n}\rangle\langle\mathbf{n}|]_s &= \frac{1}{N} + \frac{1}{n}\Theta_n - (n-1)\left(\frac{1}{n-1}\Theta_{n-1} - \frac{1}{n}\Theta_n\right) \\ &= \frac{1}{N} + \Theta_n - \Theta_{n-1} \\ &= \frac{1}{N} + r_s\left(-\frac{1}{N} + \cos^2\frac{\theta_n}{2} \prod_{k=1}^{n-1} \sin^2\frac{\theta_k}{2}\right), \quad (73) \end{aligned}$$

in the last line, $\cos^2\frac{\theta_n}{2}$ and $\prod_{k=1}^{n-1} \sin^2\frac{\theta_k}{2}$ are replaced by 1 when $n = N$ and $n = 1$, respectively.

To obtain the focused initial conditions for an initially populated state $|n\rangle$, one requires that²⁹

$$[|\mathbf{n}\rangle\langle\mathbf{n}|]_s = 1; \quad [|\mathbf{j}\rangle\langle\mathbf{j}|]_s = 0, \quad (j \neq n). \quad (74)$$

As Eq. 73 is recursive, we derive the expression starting from state 1 toward state N , and obtain the values of the $\{\Theta_j\}$ as

$$\Theta_{j < n} = -\frac{j}{N}; \quad \Theta_{j \geq n} = \frac{N-j}{N}. \quad (75)$$

More generally, when focusing on any combination of state with, for each state $|j\rangle$ an initial population P_j (such that $\sum_{j=1}^N P_j = 1$), we have the expression

$$\Theta_j = \sum_{k=1}^j P_k - \frac{j}{N}, \quad (76)$$

where the proof is provided in the Supplemental Material. The above focused initial conditions only affect angles $\{\theta_j\}$ for $j \in [1, N-1]$, whereas the $\{\varphi_j\}$ angles are sampled randomly in the range $[0, 2\pi]$. This effectively evaluates the integrals over $\{\theta_j\}$, but leaves the original integrals over $\{\varphi_j\}$.

From Eq. 72, we further derive the expression of the angles $\{\theta_n\}$ as follows

$$\cos\theta_n = 1 - 2\left(\frac{N-n}{N} - \frac{\Theta_n}{r_s}\right), \quad n = 1, \quad (77a)$$

$$\cos\theta_n = 1 - \frac{2\left(\frac{N-n}{N} - \frac{\Theta_n}{r_s}\right)}{\prod_{k=1}^{n-1} \sin^2\frac{\theta_k}{2}}, \quad 2 \leq n \leq N-1. \quad (77b)$$

The sines in the denominator of Eq. 77b can only be zero for $s = Q$, and in this case the equation for $\cos\theta_n$ is expressed in Eq. 77a. From the above equations, we note that any angle θ_n only depends on Θ_n and on the angles $\{\theta_j\}$ for $j < n$. Thus, the focused initial conditions in Eq. 75 (or more generally, Eq. 76) can be used to recursively generate values of θ_n based on Eq. 77.

In terms of the conjugate MMST mapping variables, the corresponding focused initial conditions in Eq. 74 are

$$q_n^2 + p_n^2 = 2 + \gamma; \quad q_j^2 + p_j^2 = \gamma, \quad (j \neq n), \quad (78)$$

based on the expression of the estimator in Eq. 51. This is the focused initial conditions proposed in the recently developed spin-LSC approach.²⁹ However, these focused conditions do not provide any specific choice of angles $\{\varphi_j\}$ in generalized spin variables (see Eq. 17). In principle, any algorithm that generates $\{q_n, p_n\}$ should guarantee a uniform distribution of $\{\varphi_j\}$ in the range $[0, 2\pi]$, required by the $\int d\Omega$ integral (see expression of $d\Omega$ in Eq. 19).

V. QUANTUM LIOUVILLIAN IN THE MIXED WIGNER/STRATONOVICH-WEYL REPRESENTATION

A. Exact Liouvillian Expression

In this section, we derive the exact expression of the quantum Liouvillian $\hat{\mathcal{L}}$ in Eq. 64. Using the Heisenberg EOMs in the Wigner/Stratonovich-Weyl representation, we have

$$\begin{aligned} \frac{d}{dt} [\hat{B}]_{ws} &= \frac{i}{\hbar} [\hat{H}, \hat{B}]_{ws} \equiv \hat{\mathcal{L}}[\hat{B}]_{ws} \quad (79) \\ &= \frac{2}{\hbar} [\mathcal{H}_0]_w \sin \frac{\hat{\Lambda}\hbar}{2} [\mathcal{B}_0]_w + \frac{1}{\hbar N} \sum_{k=1}^{N^2-1} [\mathcal{H}_k]_w \sin \frac{\hat{\Lambda}\hbar}{2} [\mathcal{B}_k]_w \\ &\quad + \frac{2r_s}{\hbar} \sum_{k=1}^{N^2-1} \Omega_k \left([\mathcal{H}_k]_w \sin \frac{\hat{\Lambda}\hbar}{2} [\mathcal{B}_0]_w + [\mathcal{H}_0]_w \sin \frac{\hat{\Lambda}\hbar}{2} [\mathcal{B}_k]_w \right) \\ &\quad + \frac{r_s}{\hbar} \sum_{i,j,k=1}^{N^2-1} d_{ijk} [\mathcal{H}_i]_w \Omega_j \sin \frac{\hat{\Lambda}\hbar}{2} [\mathcal{B}_k]_w \\ &\quad + \frac{r_s}{\hbar} \sum_{i,j,k=1}^{N^2-1} f_{ijk} [\mathcal{H}_i]_w \Omega_j \cos \frac{\hat{\Lambda}\hbar}{2} [\mathcal{B}_k]_w, \end{aligned}$$

where we have explicitly used the property in Eq. 39. One can in principle derive the Liouvillian expressed in terms of the MMST variables (defined in Eq. 44), using the kernel expressed in the MMST variables and diabatic basis (Eq. 49). However, this leads to a complicated expression of $[\hat{A}\hat{B}]_s$, as opposed to the simple expression in Eq. 39. We thus decide to use the $\mathfrak{su}(N)$ generators to derive the Liouvillian expression. One can then perform the transform (see Sec.VC-D) to obtain an expression with MMST variables.

Based on Eq. 79, we identify a state-independent part and a state-dependent part of the Liouvillian, acting respectively on the state-independent and state-dependent components of the operator \hat{B} . By rewriting the total

time-derivative of operator $[\hat{B}]_{ws}$ we have

$$\begin{aligned}\frac{d}{dt}[\hat{B}]_{ws} &= \frac{d}{dt}[\mathcal{B}_0\hat{\mathcal{I}}]_{ws} + \sum_{k=1}^{N^2-1} \frac{d}{dt}[\mathcal{B}_k \cdot \frac{1}{\hbar} \hat{\mathcal{S}}_k]_{ws} \quad (80) \\ &= \frac{d}{dt}[\mathcal{B}_0]_w + \sum_{k=1}^{N^2-1} \frac{d}{dt}([\mathcal{B}_k]_w \cdot r_s \Omega_k) \\ &= \hat{\mathcal{L}}_0[\mathcal{B}_0]_w + r_s \sum_{k=1}^{N^2-1} \hat{\mathcal{L}}_k(\Omega_k[\mathcal{B}_k]_w).\end{aligned}$$

By comparing Eq. 79 and Eq. 80, the state-independent Liouvillian is expressed as

$$\hat{\mathcal{L}}_0[\mathcal{B}_0]_w \equiv \frac{2}{\hbar} H_s \sin \frac{\hat{\Lambda}\hbar}{2} [\mathcal{B}_0]_w, \quad (81)$$

with H_s expressed as

$$\begin{aligned}H_s(R, P) &= [\hat{H}(\hat{R}, \hat{P})]_{ws} = [\mathcal{H}_0]_w + r_s \sum_{k=1}^{N^2-1} \Omega_k [\mathcal{H}_k]_w \\ &= \mathcal{H}_0(R, P) + r_s \sum_{k=1}^{N^2-1} \Omega_k \mathcal{H}_k(R). \quad (82)\end{aligned}$$

For the last line of the above equation, we have used the fact that $[\mathcal{H}_k(\hat{R})]_w = \mathcal{H}_k(R)$ (see Eq. 10b or Eq. 11 for its expression) and $[\mathcal{H}_0(\hat{R}, \hat{P})]_w = \mathcal{H}_0(R, P)$ because the Wigner transform of a function of position operator is the same function, and $\mathcal{H}_0(\hat{R}, \hat{P})$ only contains \hat{P} up to the quadratic order.⁶⁸

The state-dependent Liouvillian is expressed as

$$\begin{aligned}\hat{\mathcal{L}}_i(r_s \Omega_i [\mathcal{B}_i]_w) &\equiv \frac{1}{\hbar} \left[\left(\frac{1}{N} \mathcal{H}_i + 2r_s \Omega_i \mathcal{H}_0 \right) \sin \frac{\hat{\Lambda}\hbar}{2} \right. \\ &\quad + r_s d_{ijk} \mathcal{H}_j \Omega_k \sin \frac{\hat{\Lambda}\hbar}{2} \\ &\quad \left. + r_s f_{ijk} \mathcal{H}_j \Omega_k \cos \frac{\hat{\Lambda}\hbar}{2} \right] [\mathcal{B}_i]_w. \quad (83)\end{aligned}$$

Comment: Equations lack sum over index (jk)

We further identify two terms in $\hat{\mathcal{L}}_i$ as $\hat{\mathcal{L}}_i = \hat{\mathcal{L}}_i^e + \hat{\mathcal{L}}_i^n$. The first term evolves $\Omega_i [\mathcal{B}_i]_w$ as follows

$$\hat{\mathcal{L}}_i^e(r_s \Omega_i [\mathcal{B}_i]_w) \equiv \frac{1}{\hbar} r_s f_{ijk} \mathcal{H}_j \Omega_k \cos \frac{\hat{\Lambda}\hbar}{2} [\mathcal{B}_i]_w, \quad (84)$$

where the leading term $\cos \frac{\hat{\Lambda}\hbar}{2} \approx 1$ evolves only the spin mapping variables. The second term evolves the nuclear DOFs through the coupling between the spin mapping variables and the nuclear DOFs as follows

$$\hat{\mathcal{L}}_i^n(r_s \Omega_i [\mathcal{B}_i]_w) \equiv \frac{1}{\hbar} \left(\frac{1}{N} \mathcal{H}_i + 2r_s \Omega_i \mathcal{H}_0 + r_s d_{ijk} \mathcal{H}_j \Omega_k \right) \sin \frac{\hat{\Lambda}\hbar}{2} [\mathcal{B}_i]_w. \quad (85)$$

Naturally, if there is no state-dependent Hamiltonian ($H_s = [\mathcal{H}_0]_w$ and $\forall j, \mathcal{H}_j = 0$), the Liouvillian expression in Eq. 79 reduces back to the original Wigner-Moyal

series⁴⁸ as follows

$$\frac{d}{dt} [\hat{B}]_{ws} = \hat{\mathcal{L}} \left([\mathcal{B}_0]_w + r_s \sum_{i=1}^{N^2-1} \Omega_i [\mathcal{B}_i]_w \right) \quad (86a)$$

$$\hat{\mathcal{L}} = \frac{P}{m} \vec{\partial}_R - \frac{2}{\hbar} U_0(R) \sin \left(\frac{\hbar}{2} \vec{\partial}_R \vec{\partial}_P \right). \quad (86b)$$

Further, in the special case where there is no nuclear dependency, the only remaining term in the Liouvillian is

$$\hat{\mathcal{L}}_i^e(r_s \Omega_i) = \frac{1}{\hbar} r_s f_{ijk} \mathcal{H}_j \Omega_k, \quad (87)$$

which goes back, as expected, to the expression of the EOMs derived by Hioe and Eberly²⁵ given in Eq. 14.

To summarize, the TCF (Eq. 64) with the exact Liouvillian is expressed as

$$C_{AB}(t) = \frac{1}{2\pi\hbar Z} \int dR \int dP \int d\Omega [e^{-\beta \hat{H}} \hat{A}]_{ws} \quad (88)$$

$$\times [e^{\hat{\mathcal{L}}_0 t} [\mathcal{B}_0]_w + r_s \sum_{k=1}^{N^2-1} e^{\hat{\mathcal{L}}_k t} \Omega_k [\mathcal{B}_k]_w].$$

B. Linearization Approximation and the Equations of Motion

So far, we have not made any approximation to the TCF expression. Solving Eq. 88 will be as difficult as solving the exact quantum dynamics, if not more. To simplify the task, we use the linearized path-integral approximation,^{11,71} or equivalently, linearizing the sines and cosines⁷² of $\hat{\Lambda}$ in Eq. 79 as follows

$$\cos \frac{\hat{\Lambda}\hbar}{2} \approx 1, \quad \sin \frac{\hat{\Lambda}\hbar}{2} \approx \frac{\hat{\Lambda}\hbar}{2}. \quad (89)$$

This linearization approximation is equivalent to the approximation used in Linearized Semiclassical-Initial Value Representation (LSC-IVR),^{11,59,73} with the difference that the current approach uses the generalized spin mapping variables as opposed to the original MMST mapping variables.^{8,10}

Within the linearized approximation, we obtain for the state-independent component (in Eq. 81) the EOM as follows

$$\frac{d}{dt} [\mathcal{B}_0]_w = \left[\frac{P}{m} \vec{\partial}_R - (\partial_R \mathcal{H}_0 + r_s \sum_{k=1}^{N^2-1} \partial_R \mathcal{H}_k \Omega_k) \vec{\partial}_P \right] [\mathcal{B}_0]_w. \quad (90)$$

The state-dependent time-derivatives (in Eqs. 80 and 83) after the linearization approximation become

$$r_s \frac{d}{dt} (\Omega_i [\mathcal{B}_i]_w) = r_s \frac{d\Omega_i}{dt} \cdot [\mathcal{B}_i]_w + r_s \Omega_i \cdot \frac{d}{dt} [\mathcal{B}_i]_w \quad (91)$$

$$\approx \frac{1}{\hbar} \left[r_s f_{ijk} \mathcal{H}_j \Omega_k + \left(2r_s \Omega_i \mathcal{H}_0 + \frac{1}{N} \mathcal{H}_i \right) \frac{\hat{\Lambda}\hbar}{2} \right. \\ \left. + r_s d_{ijk} \mathcal{H}_j \Omega_k \frac{\hat{\Lambda}\hbar}{2} \right] [\mathcal{B}_i]_w, \quad \text{sum over index (jk)!}$$

which helps to identify the individual time derivatives for Ω_i as follows

$$\frac{d}{dt}\Omega_i = \frac{1}{\hbar} \sum_{j,k=1}^{N^2-1} f_{ijk} \mathcal{H}_j \Omega_k, \quad (92)$$

which is identical to Eq. 14, as well as time-derivative of $[\mathcal{B}_i]_w$ as follows

$$\begin{aligned} \frac{d}{dt}[\mathcal{B}_i]_w = & \left[\frac{P}{m} \vec{\partial}_R - \left(\partial_R \mathcal{H}_0 + \frac{1}{2Nr_s\Omega_i} \partial_R \mathcal{H}_i \right. \right. \\ & \left. \left. + d_{ijk} \frac{\Omega_j}{2\Omega_i} \partial_R \mathcal{H}_k \right) \vec{\partial}_P \right] [\mathcal{B}_i]_w. \end{aligned} \quad (93)$$

The Liouvillians acting on $[\mathcal{B}_0]_w$ (Eq. 90) and on $[\mathcal{B}_i]_w$ (Eq. 93) are different, which is the feature of the spin mapping formalism. In the practical implementations of this approximation, such as in the recently proposed spin-LSC,²⁴ the nuclear DOFs were proposed to be updated with the Liouvillian in Eq. 90. This should be viewed as an independent approximation, in addition to the linearized approximation expressed in Eq. 89. Future investigations will be carried to develop new propagation schemes taking into account the two Liouvillian components for a trajectory based method.

Thus, under the linearization approximation and using Eq. 90 to propagate the nuclear DOFs, we have the following classical EOMs

$$\dot{R} = \frac{P}{m}, \quad (94a)$$

$$\dot{P} = -\frac{\partial \mathcal{H}_0}{\partial R} - r_s \sum_{k=1}^{N^2-1} \frac{\partial \mathcal{H}_k}{\partial R} \Omega_k = -\frac{\partial H_s(R, P)}{\partial R}, \quad (94b)$$

$$\frac{d}{dt}\Omega_i = \frac{1}{\hbar} \sum_{j,k=1}^{N^2-1} f_{ijk} \mathcal{H}_j \Omega_k, \quad (94c)$$

where $H_s(R, P)$ is expressed in Eq. 82. The analytic expressions of the structure constants f_{ijk} are provided in Eq. A5.

The above equations were recently *proposed* as the EOMs for the Generalized Discrete Truncated Wigner Approximation (GDTWA) approach⁵² by choosing $r_s = \sqrt{N+1}$ (or $s = W$). The EOMs were argued as the classical limit of the Heisenberg EOMs⁵² for the corresponding operators \hat{R} , \hat{P} , and \hat{S}_k . Here, we present a rigorous derivation of these EOMs.

One can numerically propagate these EOMs in Eq. 94. However, the formal numerical scaling for solving Eq. 94c is $\mathcal{O}(N^4)$, due to the N^2 dimensionality of both \mathcal{H}_j and Ω_k . It is thus ideal to find alternative but equivalent EOMs that reduce this scaling. Below, we provide two possible choices of conjugate variables that fulfill this task.

Comment: The authors failed to understand that GDTWA whose EOMs can implicitly correspond to any specific r_s . Eq (94) provides nothing newer than Ref. 52 by Lang et. al..

C. Equations of Motion with the Angle Variables of $\mathfrak{su}(N)$ Generators

In order to obtain equivalent EOMs in terms of the $2N - 2$ underlying $\{\theta_n\}$ and $\{\varphi_n\}$ variables for $n \in [1, N - 1]$, we want to find a set of canonical variables. We recognize that in the two-state special case,^{38,74} the conjugate momentum of φ_1 is $r_s \cos \theta_1 \equiv r_s \Omega_{\gamma_2}$, where γ_2 is the index of the diagonal generator (see Eq. 5c). Hence, we expect a conjugate momentum of any φ_n being a combination of $\{\Omega_{\gamma_j}\}$ for $j \in [2, N]$. Based on this potential conjugate relationship, we postulate the following Hamilton's EOMs

$$r_s \sum_{j=1}^N C_n(j) \frac{d}{dt} \Omega_{\gamma_j} = -\frac{\partial H_s}{\partial \varphi_n} \quad (95a)$$

$$r_s \frac{d}{dt} \varphi_n = \frac{\partial H_s}{\partial \sum_{j=1}^N C_n(j) \Omega_{\gamma_j}}, \quad (95b)$$

which should be equivalent to Eq. 92. Here, $C_n(j)$ is the coefficient depending on the index of the generator γ_j , and the index of the *conjugate general coordinate* φ_n . Using Eq. 92 and the closed formulas of the structure constants (see Appendix A), we derive the expression of these coefficients as follows

$$C_n(j \leq n) = 0; \quad C_n(j > n) = n \sqrt{\frac{2}{j(j-1)}}, \quad (96)$$

where the derivation can be found in Appendix D.

The *conjugate variable* of φ_n for N -state systems, using the coefficients derived above, is

$$n \cdot r_s \sum_{j=n+1}^N \sqrt{\frac{2}{j(j-1)}} \Omega_{\gamma_j} \equiv \Theta_n, \quad (97)$$

which corresponds exactly to the variable Θ_n defined in Eq. 72. With the above finding, we can express Eq. 95 in its equivalent form as follows

$$\dot{\Theta}_n = -\frac{\partial H_s}{\partial \varphi_n} = -\sum_{j=1}^n r_s \dot{\theta}_j \frac{\sin \theta_j}{2} \prod_{\substack{k=1 \\ k \neq j}}^{n-1} \sin^2 \frac{\theta_k}{2} \quad (98a)$$

$$\dot{\varphi}_n = \frac{\partial H_s}{\partial \Theta_n}. \quad (98b)$$

We can further rewrite Eq. 98a with an equivalent but recursive expression as follows

$$-\frac{\partial H_s}{\partial \varphi_n} = -\frac{\partial H_s}{\partial \varphi_{n-1}} \sin^2 \frac{\theta_n}{2} - r_s \dot{\theta}_n \frac{\sin \theta_n}{2} \prod_{j=1}^{n-1} \sin^2 \frac{\theta_j}{2}. \quad (99)$$

The above equation gives a numerically efficient recursive expression of $\dot{\theta}_n$ as follows

$$\dot{\theta}_n = \left(\frac{\partial H_s}{\partial \varphi_n} \frac{2}{\sin \theta_n} - \frac{\partial H_s}{\partial \varphi_{n-1}} \tan \frac{\theta_n}{2} \right) / \left(r_s \prod_{j=1}^{n-1} \sin^2 \frac{\theta_j}{2} \right), \quad (100)$$

These equations of motion, eqs (98), (99), (101), (105), are all incorrect with the coherent states defined as eq (17)! The coherent states eq (17),

$$\langle n | \Omega \rangle = \begin{cases} \cos \frac{\theta_1}{2} e^{-i \frac{\varphi_1}{2}} & n = 1, \\ \cos \frac{\theta_n}{2} e^{-i \frac{\varphi_n}{2}} \prod_{l=1}^{n-1} \sin \frac{\theta_l}{2} e^{i \frac{\varphi_l}{2}} & 1 < n < N, \\ \prod_{l=1}^{N-1} \sin \frac{\theta_l}{2} e^{i \frac{\varphi_l}{2}} & n = N. \end{cases} \quad (17)$$

are completely incompatible with the following derivations eqs (B2) and (B3).

$$\begin{aligned} \hbar \Omega_{\alpha nm} &\equiv \langle \Omega | \hat{S}_{\alpha nm} | \Omega \rangle \\ &= \hbar \left(\cos \frac{\theta_m}{2} \prod_{j=1}^{m-1} e^{-i \varphi_j} \sin \frac{\theta_j}{2} \cos \frac{(1 - \delta_{nN}) \theta_n}{2} \prod_{k=1}^{n-1} e^{i \varphi_k} \right. \\ &\quad \times \sin \frac{\theta_k}{2} + \cos \frac{\theta_m}{2} \prod_{j=1}^{m-1} e^{i \varphi_j} \sin \frac{\theta_j}{2} \cos \frac{(1 - \delta_{nN}) \theta_n}{2} \\ &\quad \times \left. \prod_{k=1}^{n-1} e^{-i \varphi_k} \sin \frac{\theta_k}{2} \right) \\ &= \hbar \prod_{j=1}^{m-1} \sin^2 \frac{\theta_j}{2} \cos \frac{\theta_m}{2} \prod_{k=m}^{n-1} \sin \frac{\theta_k}{2} \cos \frac{(1 - \delta_{nN}) \theta_n}{2} \\ &\quad \times \cos \left(\sum_{l=m}^{n-1} \varphi_l \right), \end{aligned} \quad (B2)$$

$$\begin{aligned} \hbar \Omega_{\beta nm} &\equiv \langle \Omega | \hat{S}_{\beta nm} | \Omega \rangle \\ &= \hbar \prod_{j=1}^{m-1} \sin^2 \frac{\theta_j}{2} \cos \frac{\theta_m}{2} \prod_{k=m}^{n-1} \sin \frac{\theta_k}{2} \cos \frac{(1 - \delta_{nN}) \theta_n}{2} \\ &\quad \times \sin \left(\sum_{l=m}^{n-1} \varphi_l \right), \end{aligned} \quad (B3)$$

These equations of motion, eqs (98), (99), (101), (105), are all incorrect with the coherent states defined as eq (17)! The coherent states eq (17),

$$\langle n|\Omega\rangle = \begin{cases} \cos \frac{\theta_1}{2} e^{-i\frac{\varphi_1}{2}} & n=1, \\ \cos \frac{\theta_n}{2} e^{-i\frac{\varphi_n}{2}} \prod_{l=1}^{n-1} \sin \frac{\theta_l}{2} e^{i\frac{\varphi_l}{2}} & 1 < n < N, \\ \prod_{l=1}^{N-1} \sin \frac{\theta_l}{2} e^{i\frac{\varphi_l}{2}} & n=N. \end{cases} \quad (17)$$

are completely incompatible with the following derivations eqs(B2) and (B3).

$$\begin{aligned} \hbar\Omega_{\alpha nm} &\equiv \langle \Omega | \hat{S}_{\alpha nm} | \Omega \rangle \\ &= \frac{\hbar}{2} \left(\cos \frac{\theta_m}{2} \prod_{j=1}^{m-1} e^{-i\varphi_j} \sin \frac{\theta_j}{2} \cos \frac{(1-\delta_{nN})\theta_n}{2} \prod_{k=1}^{n-1} e^{i\varphi_k} \right. \\ &\quad \times \sin \frac{\theta_k}{2} + \cos \frac{\theta_m}{2} \prod_{j=1}^{m-1} e^{i\varphi_j} \sin \frac{\theta_j}{2} \cos \frac{(1-\delta_{nN})\theta_n}{2} \\ &\quad \times \left. \prod_{k=1}^{n-1} e^{-i\varphi_k} \sin \frac{\theta_k}{2} \right) \\ &= \hbar \prod_{j=1}^{m-1} \sin^2 \frac{\theta_j}{2} \cos \frac{\theta_m}{2} \prod_{k=m}^{n-1} \sin \frac{\theta_k}{2} \cos \frac{(1-\delta_{nN})\theta_n}{2} \\ &\quad \times \cos \left(\sum_{l=m}^{n-1} \varphi_l \right), \end{aligned} \quad (B2)$$

where for $n=1$ the denominator is replaced by r_s and the numerator only has the term that includes $\frac{\partial H_s}{\partial \varphi_n}$.

To use Eq. 100, one needs $\partial H_s / \partial \varphi_n$. To obtain such an expression, we use H_s in Eq. 82 and explicitly take the derivative with respect to φ_n . Note that only $\Omega_{\alpha_{jk}}$ and $\Omega_{\beta_{jk}}$ contain φ_n , whereas Ω_{γ_k} only contains $\{\theta_j\}$. Using the detailed expressions of $\Omega_{\alpha_{jk}}$ (Eq. B2) and $\Omega_{\beta_{jk}}$ (Eq. B3), we have

$$-\frac{\partial H_s}{\partial \varphi_n} = r_s \sum_{j=n+1}^N \sum_{k=1}^n (\mathcal{H}_{\alpha_{jk}} \Omega_{\beta_{jk}} - \mathcal{H}_{\beta_{jk}} \Omega_{\alpha_{jk}}). \quad (101)$$

To obtain the time derivative of φ_n , we can use the conjugate relationship between φ_n and Θ_n to get

$$\dot{\varphi}_n = \frac{\partial H_s}{\partial \Theta_n} = \sum_{j=1}^n \frac{\partial H_s}{\partial \theta_j} \frac{\partial \theta_j}{\partial \Theta_n} = \sum_{j=1}^n \frac{\partial H_s}{\partial \theta_j} \left(\frac{\partial \Theta_n}{\partial \theta_j} \right)^{-1},$$

but the detailed expression obtained from the above equation is long and tedious to use. Instead, we try to find an expression in terms of the generators that have a well-defined time-derivative in Eq. 92. From the expressions of $\Omega_{\alpha_{nm}}$ (Eq. B2) and $\Omega_{\beta_{nm}}$ (Eq. B3), we know that

$$\tan \varphi_n = \frac{\Omega_{\beta_{n+1,n}}}{\Omega_{\alpha_{n+1,n}}}, \quad (102)$$

leading to the expression of the time derivative of φ_n as

$$\begin{aligned} \dot{\varphi}_n &= \frac{d}{dt} \left(\arctan \frac{\Omega_{\beta_{n+1,n}}}{\Omega_{\alpha_{n+1,n}}} \right) \\ &= \frac{\dot{\Omega}_{\beta_{n+1,n}} \Omega_{\alpha_{n+1,n}} - \Omega_{\beta_{n+1,n}} \dot{\Omega}_{\alpha_{n+1,n}}}{\Omega_{\alpha_{n+1,n}}^2 + \Omega_{\beta_{n+1,n}}^2}. \end{aligned} \quad (103)$$

Using the analytical expressions of the $\mathfrak{su}(N)$ structure constants (Appendix A), we can obtain the closed analytic expression of $\dot{\Omega}_{\alpha_{n+1,n}}$ (Eq. D5) and $\dot{\Omega}_{\beta_{n+1,n}}$ (Eq. D6). For a two-level system, it is straightforward to show that Eqs. 100-103 reduce back to Eqs. E9a-E9b, which are the EOMs for the $\mathfrak{su}(2)$ mapping formalism derived in our previous work.³⁸

To summarize, using the transform between $\{\Omega\}$ and $\{\varphi_n, \Theta_n\}$ as follows

$$\Theta_n = n \cdot r_s \sum_{j=n+1}^N \sqrt{\frac{2}{j(j-1)}} \Omega_{\gamma_j}, \quad (104a)$$

$$\varphi_n = \tan^{-1} \frac{\Omega_{\beta_{n+1,n}}}{\Omega_{\alpha_{n+1,n}}}, \quad (104b)$$

the EOMs in Eq. 94 are expressed as

$$\dot{R} = \frac{P}{m}, \quad (105a)$$

$$\dot{P} = -\frac{\partial \mathcal{H}_0}{\partial R} - r_s \sum_{k=1}^{N^2-1} \frac{\partial \mathcal{H}_k}{\partial R} \Omega_k = -\frac{\partial H_s(R, P)}{\partial R}, \quad (105b)$$

$$\dot{\theta}_n = \left(\frac{\partial H_s}{\partial \varphi_n} \frac{2}{\sin \theta_n} - \frac{\partial H_s}{\partial \varphi_{n-1}} \tan \frac{\theta_n}{2} \right) / \left(r_s \prod_{j=1}^{n-1} \sin^2 \frac{\theta_j}{2} \right), \quad (105c)$$

$$\dot{\varphi}_n = \frac{\dot{\Omega}_{\beta_{n+1,n}} \Omega_{\alpha_{n+1,n}} - \Omega_{\beta_{n+1,n}} \dot{\Omega}_{\alpha_{n+1,n}}}{\Omega_{\alpha_{n+1,n}}^2 + \Omega_{\beta_{n+1,n}}^2}. \quad (105d)$$

To solve Eq. 105c, $\frac{\partial H_s}{\partial \varphi_n}$ is evaluated with Eq. 101, with the detailed expressions of $\Omega_{\alpha_{jk}}$ and $\Omega_{\beta_{jk}}$ in Eq. B2 and Eq. B3, respectively. To solve Eq. 105d, we use the expressions of $\dot{\Omega}_{\alpha_{n+1,n}}$ and $\dot{\Omega}_{\beta_{n+1,n}}$ in Eq. D5 and Eq. D6, respectively.

The advantage of using the conjugate variable relationship between Θ_n and φ_n in Eq. 105, instead of the EOMs expressed in Eq. 92 with $\{\Omega_j\}$ is that in the former case there are $2N - 2$ variables to explicitly propagate, as opposed to the $N^2 - 1$ variables of the latter. More importantly, one can evolve each Θ_n , or equivalently θ_n by using the chain rule, and φ_n using a velocity Verlet algorithm ($\{\Theta_n\}$ being the *generalized conjugate momenta* of $\{\varphi_n\}$), which does not require using the derivative of the potential, and guarantees symplecticity through the Verlet algorithm. To the best of our knowledge, we are not aware of any previous work reporting the EOMs outlined in Eq. 105.

D. Equations of Motion with the MMST mapping Variables

Instead of using conjugated variables $\{\varphi_n, \Theta_n\}$ (Eq. 98), one uses $\{q_n, p_n\}$ defined in Eq. 46, which are also conjugated variables.²⁹ Here, we explicitly show this using the EOMs. The electronic EOMs in Eq. 94c under the linearization approximation are equivalent to the following equation

$$i\hbar \frac{\partial}{\partial t} \hat{w}_s = [\hat{V}_e(R), \hat{w}_s], \quad (106)$$

where $\hat{V}_e(R)$ is defined as

$$\hat{V}_e(R) = \frac{1}{\hbar} \sum_{k=1}^{N^2-1} \mathcal{H}_k \cdot \hat{\mathcal{S}}_k, \quad (107)$$

and $\mathcal{H}_k(R) = \frac{2}{\hbar} \text{Tr}_e[\hat{H} \cdot \hat{\mathcal{S}}_k] = \frac{2}{\hbar} \text{Tr}_e[\hat{V}_e(R) \cdot \hat{\mathcal{S}}_k]$. Plugging the expression of $\hat{V}_e(R)$ (Eq. 107) as well as the expression of \hat{w}_s (Eq. 24) into Eq. 106, one can easily verify its equivalence with Eq. 94c.

These equations of motion, eqs (98), (99), (101), (105), are all incorrect with the coherent states defined as eq (17)! The coherent states eq (17),

$$\langle n | \Omega \rangle = \begin{cases} \cos \frac{\theta_1}{2} e^{-i \frac{\varphi_1}{2}} & n = 1, \\ \cos \frac{\theta_n}{2} e^{-i \frac{\varphi_n}{2}} \prod_{l=1}^{n-1} \sin \frac{\theta_l}{2} e^{i \frac{\varphi_l}{2}} & 1 < n < N, \\ \prod_{l=1}^{N-1} \sin \frac{\theta_l}{2} e^{i \frac{\varphi_l}{2}} & n = N. \end{cases} \quad (17)$$

are completely incompatible with the following derivations eqs (B2) and (B3).

$$\begin{aligned} \hbar \Omega_{\alpha_{nm}} &\equiv \langle \Omega | \hat{\mathcal{S}}_{\alpha_{nm}} | \Omega \rangle \\ &= \hbar \left(\cos \frac{\theta_m}{2} \prod_{j=1}^{m-1} e^{-i \varphi_j} \sin \frac{\theta_j}{2} \cos \frac{(1 - \delta_{nN}) \theta_n}{2} \prod_{k=1}^{n-1} e^{i \varphi_k} \right. \\ &\quad \times \sin \frac{\theta_k}{2} + \cos \frac{\theta_m}{2} \prod_{j=1}^{m-1} e^{i \varphi_j} \sin \frac{\theta_j}{2} \cos \frac{(1 - \delta_{nN}) \theta_n}{2} \\ &\quad \times \left. \prod_{k=1}^{n-1} e^{-i \varphi_k} \sin \frac{\theta_k}{2} \right) \\ &= \hbar \prod_{j=1}^{m-1} \sin^2 \frac{\theta_j}{2} \cos \frac{\theta_m}{2} \prod_{k=m}^{n-1} \sin \frac{\theta_k}{2} \cos \frac{(1 - \delta_{nN}) \theta_n}{2} \\ &\quad \times \cos \left(\sum_{l=m}^{n-1} \varphi_l \right), \end{aligned} \quad (B2)$$

$$\begin{aligned} \hbar \Omega_{\beta_{nm}} &\equiv \langle \Omega | \hat{\mathcal{S}}_{\beta_{nm}} | \Omega \rangle \\ &= \hbar \prod_{j=1}^{m-1} \sin^2 \frac{\theta_j}{2} \cos \frac{\theta_m}{2} \prod_{k=m}^{n-1} \sin \frac{\theta_k}{2} \cos \frac{(1 - \delta_{nN}) \theta_n}{2} \\ &\quad \times \sin \left(\sum_{l=m}^{n-1} \varphi_l \right), \end{aligned} \quad (B3)$$

The authors did not derive the self-consistent EOMs for 2F-2 Stratonovich angle variables defined in eq (17)!

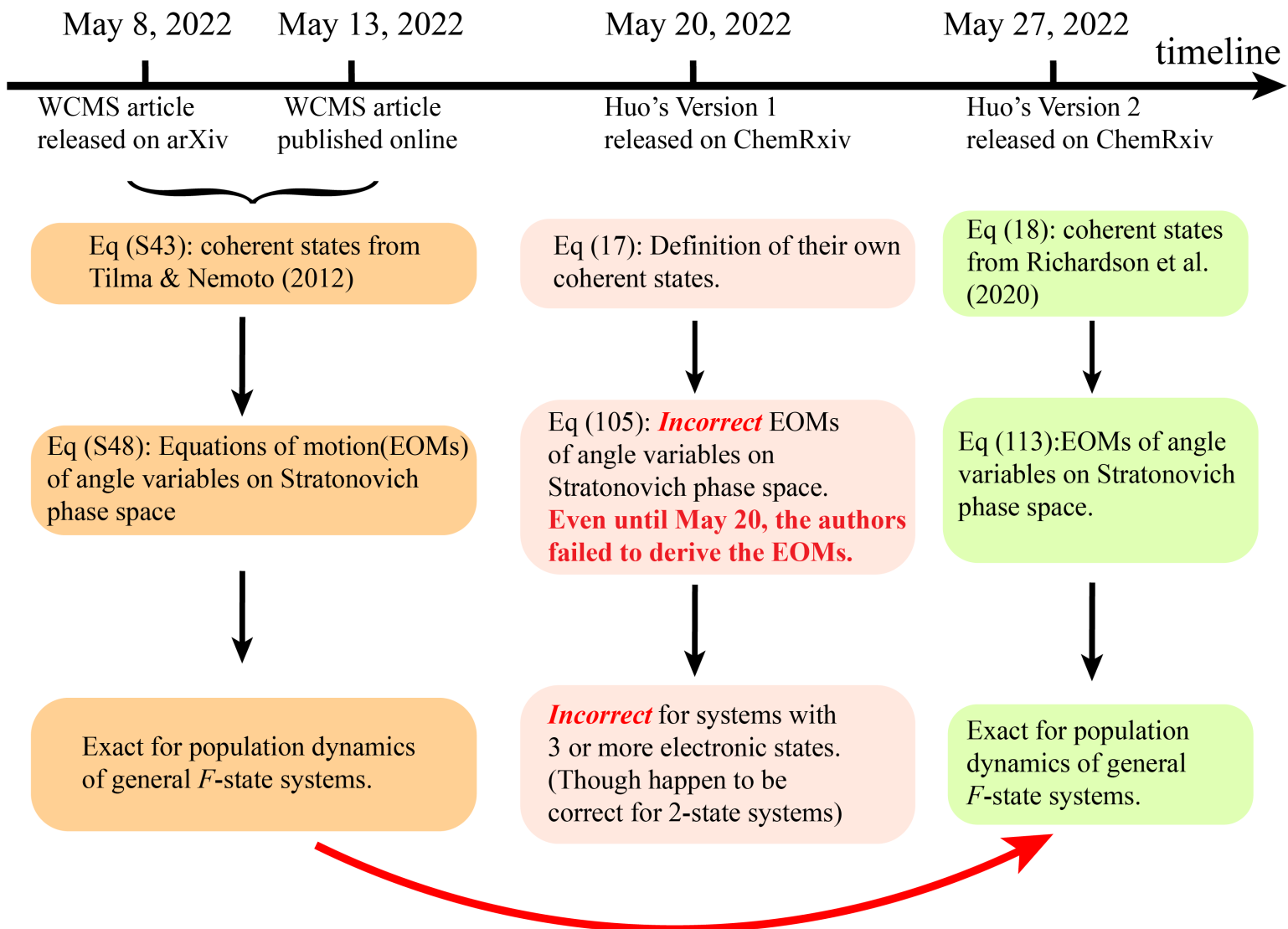
$$\dot{R} = \frac{P}{m}, \quad (105a)$$

$$\dot{P} = -\frac{\partial \mathcal{H}_0}{\partial R} - r_s \sum_{k=1}^{N^2-1} \frac{\partial \mathcal{H}_k}{\partial R} \Omega_k = -\frac{\partial H_s(R, P)}{\partial R}, \quad (105b)$$

$$\dot{\theta}_n = \left(\frac{\partial H_s}{\partial \varphi_n} \frac{2}{\sin \theta_n} - \frac{\partial H_s}{\partial \varphi_{n-1}} \tan \frac{\theta_n}{2} \right) / \left(r_s \prod_{j=1}^{n-1} \sin^2 \frac{\theta_j}{2} \right), \quad (105c)$$

$$\dot{\varphi}_n = \frac{\dot{\Omega}_{\beta_{n+1,n}} \Omega_{\alpha_{n+1,n}} - \Omega_{\beta_{n+1,n}} \dot{\Omega}_{\alpha_{n+1,n}}}{\Omega_{\alpha_{n+1,n}}^2 + \Omega_{\beta_{n+1,n}}^2}. \quad (105d)$$

Timeline of the Equations of Motion on SU(F) Stratonovich Phase Space



Plagiarized the ideas from the WCMS article after it was released nearly 3 weeks.

See details in Evidence #6 of evidence.pdf.

Comment: This is only a copy of EOMs which have been discussed in J. Chem. Phys. 145, 204105 (2016), with no citations.

$$i\dot{c}_n(t) = \sum_{m=1}^F H_{nm} c_m(t). \quad (\text{B1})$$

We then re-express Eq. 106 using Eq. 49, leading to

$$i\hbar \frac{\partial}{\partial t} \left(\sum_{na} c_n c_a^* |n\rangle \langle a| \right) = [\hat{V}_e(R), \sum_{mb} c_m c_b^* |m\rangle \langle b|],$$

which can be used to derive

$$i\hbar \dot{c}_n = \sum_m V_{nm}(R) \cdot c_m \quad (108)$$

and its complex conjugate equation. This means that Eq. 92 is equivalent to the Ehrenfest dynamics for the electronic DOFs. The nuclear force described in Eq. 94b, on the other hand, differs from the Ehrenfest dynamics if $r_s \neq 1$ ($s \neq Q$).

Using the transformation defined in Eq. 44, one can rewrite the EOM in Eq. 108 as the coupled equations for the conjugated variables $\{q_n, p_n\}$ as follows

$$\dot{q}_n = \sum_m V_{nm}(R) \cdot p_m = \frac{\partial \mathcal{H}}{\partial p_n}, \quad (109a)$$

$$\dot{p}_n = - \sum_m V_{nm}(R) \cdot q_m = - \frac{\partial \mathcal{H}}{\partial q_n}. \quad (109b)$$

Here, the MMST mapping Hamiltonian is

$$\begin{aligned} \mathcal{H} = & \frac{P^2}{2M} + U_0(R) + \sum_n \frac{1}{2} V_{nn}(R)(q_n^2 + p_n^2 - \gamma) \quad (110) \\ & + \sum_{n < m} V_{nm}(R)(q_n q_m + p_n p_m), \end{aligned}$$

where \mathcal{H} (Eq. 110) is equivalent to $H_s(R, P)$ (Eq. 82) through the transform defined in Eq. 46 (or equivalently in Eq. 44). The Hamiltonian \mathcal{H} in Eq. 110 can be viewed as Eq. 47 with the Wigner transform over only the nuclear DOFs. Further, using the transformation defined in Eq. 46, the nuclear EOMs in Eq. 94 can be expressed as

$$\dot{R} = \frac{\partial \mathcal{H}}{\partial P}, \quad \dot{P} = - \frac{\partial \mathcal{H}}{\partial R}. \quad (111)$$

Note that Eq. 109 are the classical Hamilton's EOMs of \mathcal{H} (Eq. 110), with the conjugated variables $\{q_n, p_n\}$. One can, in principle, directly derive Eq. 109 from Eq. 94c using the transformation in Eq. 46 and the expressions of the structure constant f_{ijk} in Eq. A5, through a rather tedious process.

Similarly, Eq. 98 are the Hamilton's EOMs of $H_s(R, P)$, with the conjugate variables $\{\varphi_n, \Theta_n\}$. Thus, the transformation in Eq. 46 (or equivalently in Eq. 44) is a canonical transform that preserves the form of Hamilton's EOMs. This transformation connects the generalized conjugate variables to the conjugate position and momentum of the harmonic oscillator as follows

$$\Theta_n = \left(\frac{1}{n} - \frac{1}{N} \right) \sum_{m=1}^n \frac{1}{2} (q_m^2 + p_m^2) - \frac{n}{N} \sum_{m=n+1}^N \frac{1}{2} (q_m^2 + p_m^2), \quad (112a)$$

$$\varphi_n = \tan^{-1} \left(\frac{p_{n+1} \cdot q_n - q_{n+1} \cdot p_n}{q_{n+1} \cdot q_n + p_{n+1} \cdot p_n} \right), \quad (112b)$$

Comment: This is merely repeating the canonical EOMs of MMST Hamiltonian dynamics without citing corresponding references.

Comment: The authors do not understand that there must exist an evolving global phase in connecting eq (105) [even if it is corrected] and eq (109).

where we have used the transform defined in Eq. 46 to convert Eq. 97 into Eq. 112a, and convert Eq. 102 into Eq. 112b. The inverse transform from $\{\varphi_n, \theta_n\}$ to the MMST mapping variables $\{q_n, p_n\}$ (based on Eq. 44) are

$$q_n = \sqrt{2r_s} \cdot \text{Re}[\langle n|\Omega \rangle] \quad (113a)$$

$$p_n = \sqrt{2r_s} \cdot \text{Im}[\langle n|\Omega \rangle], \quad (113b)$$

where the explicit expression of $\langle n|\Omega \rangle$ as a function of $\{\varphi_n, \theta_n\}$ can be found in Eq. 17.

Note that the EOMs in Eq. 109 and Eq. 111 are identical to the EOMs commonly used in the MMST mapping formalism.^{23,28} These EOMs are used in the spin-LSC approach,²⁹ by the argument that they are Hamilton's EOMs of \mathcal{H} (Eq. 110). Here, we rigorously prove that they are equivalent to the EOMs in Eq. 94. The $2N$ MMST mapping variables are subject to a constraint given in Eq. 53 (that comes originally from the $\{\Theta_n\}$ variables). Further, there is an overall phase factor among the $\{q_n, p_n\}$ variables which does not influence the dynamics. Thus, there are still $2N - 2$ truly independent variables, in agreement with the $2N - 2$ angle variables $\{\varphi_n, \theta_n\}$. The EOMs with $\{q_n, p_n\}$ in Eq. 109 are indeed analytically simpler than the EOMs with $\{\varphi_n, \theta_n\}$ in Eq. 105, making them more appealing for practical implementations.

For these MMST variables, one often define action-angle variables^{7,23,28} $\{\eta_n, \phi_n\}$ associated with the phase space mapping variables as follows

$$\eta_n = \frac{1}{2}(q_n^2 + p_n^2 - \gamma), \quad (114a)$$

$$\phi_n = -\tan^{-1}\left(\frac{p_n}{q_n}\right). \quad (114b)$$

Thus, Θ_n in Eq. 112a is a function of the action variables $\{\eta_n\}$, and the expression of φ_n in Eq. 112b suggests that the MMST angle variables $\{\phi_n\}$ are not independent from one another, as oppose to what has been originally hypothesized by Meyer and Miller. The correct correlation among them comes from Eq. 112b based upon the $\mathfrak{su}(N)$ representation. On the other hand, numerically sampling individual ϕ_n also results in a uniform distribution of individual φ_n .

E. Connections with Previous Methods

As we have discussed, the underlying EOMs for the generalized spin mapping approach (within the linearization approximation) are identical to Ehrenfest dynamics and the MMST-based approach under a specific choice of r_s . Nuclear initial conditions for all of these methods are also obtained from the Wigner transform of the initial nuclear density operator. Here, we connect these previous methods with the current method in the language of the $\mathfrak{su}(N)$ mapping formalism.

Comment: Comparing with what had been known in Ref. 29 [eqs (20) and (28)]. (without citation)

$$|\Omega\rangle = c_1|1\rangle + c_2|2\rangle + \cdots + c_N|N\rangle. \quad (20)$$

$$(N+1)^{1/4}c_n = \frac{X_n + iP_n}{\sqrt{2}}, \quad (28)$$

(1). Ehrenfest Dynamics is equivalent to use $r_s = 1$ ($s = Q$ method) for the EOMs (Eq. 110 and Eq. 111), and the focused initial conditions in Eq. 78 with $\gamma = 0$ (corresponding to $r_s = 1$). The original Ehrenfest dynamics also enforces all angles ϕ_n in Eq. 114 to be zero. However, having a random distribution in ϕ_n (Eq. 114) or in φ_n Eq. 112b does not influence the numerical results, based on the calculations of model systems we explored in this work.

(2). LSC-IVR^{11,59,73} uses $\gamma = 1$ (corresponding to $r_s = \frac{N}{2} + 1$) in the EOMs (Eq. 110 and Eq. 111). The estimator based on the Stock-Thoss mapping procedure^{8,10} is $|n\rangle\langle n| \rightarrow |1_n\rangle\langle 1_n|$ (mapped onto the singly excited oscillator state $|1_n\rangle \equiv |0_1, \dots, 1_n, \dots, 0_N\rangle$), and the Wigner transform (defined in the mapping oscillator phase space) of this operator is $\langle |1_n\rangle\langle 1_n| \rangle_w = G(\mathbf{q}, \mathbf{p})(q_n^2 + p_n^2 - \frac{1}{2})$, where the Gaussian function is $G(\mathbf{q}, \mathbf{p}) = 2^{N+1} \cdot \exp[-\sum_{l=1}^N (q_l^2 + p_l^2)]$. In LSC-IVR,^{11,59,73} both operator \hat{A} and \hat{B} in $C_{AB}(t)$ (Eq. 71) use the expression $\langle |1_n\rangle\langle 1_n| \rangle_w$. For the closely related Poisson Bracket Mapping Equation (PBME),^{14,21,75} method, the choice of the operator \hat{A} is the same, but the estimator \hat{B} is chosen to be $[\hat{a}_n^\dagger \hat{a}_n]_w = \frac{1}{2}(q_n^2 + \hat{p}_n^2 - 1)$, which is identical to Eq. 51 when using $\gamma = 1$. Both methods are more accurate than Ehrenfest,²⁴ but less accurate than Spin-LSC.²⁹ Using an identity trick^{22,49} which forces the identity operator's Wigner transform to be 1, the accuracy of the linearized MMST methods can be significantly improved.^{22,49} Note that with the spin mapping formalism, the identity is naturally forced to be one^{24,29} through the basic property of the SW transform (Eq. 28b).

(3). Spin-LSC^{24,29} is similar to the linearized method derived in this work (Eq. 109 and Eq. 111). The difference is the choice of r_s and $r_{\bar{s}}$ used in the operators \hat{A} , \hat{B} and inside the propagator $\hat{\mathcal{L}}$. In spin-LSC, $\langle |n\rangle\langle n| \rangle_s$ (Eq. 51) is used for operator \hat{A} and $\langle |n\rangle\langle n| \rangle_{\bar{s}}$ (Eq. 52) for operator \hat{B} in $C_{AB}(t)$ expression (Eq. 71). The EOMs are justified through the quantum-classical Liouville equation,²⁹ resulting in the EOMs in Eq. 109 and Eq. 111, with r_s (which is same as used in \hat{A}). Thus, spin-LSC uses the same r_s for operator \hat{A} and the propagator $\hat{\mathcal{L}}$. The approach we derive in this work, on the other hand, enforces the Liouvillian $\hat{\mathcal{L}}$ to have the same r_s parameter in operator \hat{B} (starting from Eq. 80). The other difference between spin-LSC and the current formalism is the initial conditions. In our current formalism, the sampling of the mapping variables is determined by the expression of $d\Omega$ in Eq. 19, whereas in spin-LSC, the mapping variables $\{q_n, p_n\}$ are randomly sampled from a Gaussian distribution, then universally scaled such that Eq. 54 (total population constraint) is satisfied.²⁹ For the focused initial condition, both the current formalism and spin-LSC use Eq. 78. The difference is that the current formalism randomly samples φ_n defined in Eq. 17, and spin-LSC randomly sample ϕ_n defined in Eq. 114b. These two angles are related to each other through Eq. 112b and Eq. 113. Numerically, we found that our current formal-

ism and spin-LSC produce similar initial conditions, for both the sampled and the focused procedures. Future investigations will focus on the rigorous mathematical connections between these two approaches.

(4). Generalized Discrete Truncated Wigner Approximation (GDTWA)⁵² is also based upon the $\mathfrak{su}(N)$ mapping formalism, and uses the *effective* value of $r_s = \sqrt{N+1}$ or $\gamma = \frac{2}{N}(\sqrt{N+1}-1)$ ($s=W$), although it is only possible to rigorously connect⁵² to Spin-LSC when $N=2$. The EOMs of GDTWA are *proposed* to be Eq. 94, which is the classical limit of the Heisenberg EOMs of \hat{S} , \hat{R} and \hat{P} . Thus, the EOMs are equivalent to the current linearized approach and Spin-LSC (Eq. 109 and Eq. 111). The initial conditions for the generalized coherent state variables Ω_i are chosen⁵² to be *eigenvalues* of \hat{S}_i (with the expressions in Eq. 2-4), which is in principle different than both the focused and the sampled procedure of the current linearized method or Spin-LSC.^{24,29} However, the detailed expressions of estimators in GDTWA require the quasi-phase point operator in Wootters's discrete phase space representation,^{76,77} and future work is needed to establish a formal connection between the current work/Spin-LSC and GDTWA.

(5). The extended Classical Mapping Model (eCMM) is based on the MMST formalism, and uses a γ parameter that can take values within the range $r_s \in (-\frac{2}{N}; \infty)$, which can in principle be negative,⁵⁵ as discussed under Eq. 48. The choice of the population estimator is $[\langle n \rangle \langle n \rangle]$ (Eq. 51) for operator \hat{A} and $[\langle n \rangle \langle n \rangle]_s$ (Eq. 52) for operator \hat{B} . The EOMs are proposed to be Eq. 109 and Eq. 111, with the same choice of r_s used in estimator for \hat{A} . The initial mapping variables are randomly sampled within the constraint given in Eq. 54. Even though eCMM and spin-LSC are seemingly derived from very different perspectives, where eCMM is formulated with the MMST

Hamiltonian with a total population constraint and spin-LSC is developed based on the $\mathfrak{su}(N)$ mapping formalism, the kernel of eCMM approach to evaluate the expectation value of the electronic operator turns out to be the Cartesian coordinates $\{\langle q_n, p_n \rangle\}$ expression of the SW kernel expressed in Eq. 49. In addition, the EOMs used in Spin-LSC and eCMM are identical as well. Considering all of the above, eCMM⁵⁶ is an *identical* approach compared to Spin-LSC.²⁹

(6). The Symmetric Quasi-Classical (SQC) method^{17,23} uses $\gamma = (\sqrt{3} - 1)/2$ for the square window²³, $\gamma = 1/3$ for the triangle window⁷⁸, or a state-and trajectory-specific γ to enforce initial electronic population⁷⁹ to be 1 or 0. The initial conditions for the action variable η_n (Eq. 114a) is uniformly sampled within a window function, and the angle variable ϕ_n (Eq. 114b) is randomly sampled. The EOMs are identical to Eq. 110 and Eq. 111 with the above mentioned specific choice of γ . Note that the SQC approach assumes the same γ parameter for both window estimators of \hat{A} and \hat{B} , as well as in the EOM.

Just repeating our contribution without any citation:

In J. Phys. Chem. A 125, 31, 6845-6863 (2021)

(submitted on May 19, 2021, released on arXiv on July 7, 2021 and officially published on August 2, 2021)

$$\sum_{n=1}^F \left[\frac{(x^{(n)})^2 + (p^{(n)})^2}{2} - \gamma \right] = 1 \quad (6)$$

the mapping Hamiltonian eq 4 is equal to the conventional Meyer–Miller Hamiltonian eq 3. This was first proposed in ref 41 for general F -state systems. The simplest way is to use the full constraint electronic space that eq 6 defines, i.e.,

$$S(\mathbf{x}, \mathbf{p}): \delta \left(\sum_{n=1}^F \left[\frac{(x^{(n)})^2 + (p^{(n)})^2}{2} \right] - (1 + F\gamma) \right) \quad (7)$$

for constructing the formulation for physical properties in the mapping approach. The possible value of parameter γ for eq 6 or eq 7 implies $\gamma \in (-\frac{1}{F}, \infty)$.

In J. Phys. Chem. Lett. 12, 2496 (2021)(submitted on January 22, 2021 and published online on March 5, 2021)

$$S(\mathbf{x}, \mathbf{p}): \sum_{n=1}^F \left[\frac{1}{2}((x^{(n)})^2 + (p^{(n)})^2) \right] = 1 + F\gamma \quad (4)$$

Although we use the diabatic representation to reach eq 4, the constraint holds in the adiabatic representation as well. The constraint (eq 4) has already been implied in eqs 43 and 44 of ref 17, and used in ref 15 where $\gamma = 0$ is considered. The physical meaning of eq 4 requires only $\gamma > -1/F$. This confirms that negative values for the ZPE parameter, γ , are possible!

In Acc. Chem. Res. 54, 23, 4215-4228 (2021)(submitted on August 14, 2021 and published online on November 10, 2021)

$$S(\mathbf{x}, \mathbf{p}): \delta \left(\sum_{n=1}^F \frac{(x^{(n)})^2 + (p^{(n)})^2}{2} - (1 + F\gamma) \right) \quad (34)$$

for developing the formulation for evaluation of physical observables. In eq 34, the possible value of parameter γ lies in $(-\frac{1}{F}, \infty)$. The trace of a product of two operators is expressed

The continuous parameter space was first proposed in J. Phys. Chem. Lett. 12, 2496 (2021), which was submitted on January 22, 2021 and published online on March 5, 2021. Huo and coworkers did not cite these contributions above at all!

VI. MODEL SYSTEMS AND SIMULATION DETAILS

Computational Method. Using the EOMs expressed in Eq. 105 and the out-of-equilibrium TCF expressions that we derived in Eq. 71, we use the spin mapping approach under the linearized approximation to study the non-adiabatic dynamics of model systems. Here, we briefly summarize the details of the propagation algorithm.

In this paper, we present numerical results with both sampled and focused initial conditions. The sampling of $\{\theta_n\}$ and $\{\varphi_n\}$ is done over the phase space volume element $\int d\Omega$ defined in Eqs. 19-20. The results are presented using $r_s = r_{\bar{s}} = r_W$. The focused initial condition are described in Eq. 77 and the procedure in Sec. IV. To propagate the dynamics, we use the simple Verlet algorithm because of the conjugate relation between Θ_n and φ_n (see Eq. 98), as well as the relation between $\dot{\Theta}_n$ and $\dot{\theta}_n$ in Eq. 98a.

First, the generalized angle variables $\{\varphi_n, \theta_n\}$ are propagated by a half time-step, which is done using the Verlet algorithm as follows

$$\theta_n(t + \frac{\Delta t}{4}) = \theta_n(t) + \dot{\theta}_n(t) \frac{\Delta t}{4}, \quad (115a)$$

$$\varphi_n(t + \frac{\Delta t}{2}) = \varphi_n(t) + \dot{\varphi}_n(t + \frac{\Delta t}{4}) \frac{\Delta t}{2}, \quad (115b)$$

$$\theta_n(t + \frac{\Delta t}{2}) = \theta_n(t + \frac{\Delta t}{4}) + \dot{\theta}_n(t + \frac{\Delta t}{2}) \frac{\Delta t}{4}, \quad (115c)$$

where $\dot{\theta}_n$ is expressed in Eq. 105c and $\dot{\varphi}_n$ is expressed in Eq. 105d. In theory it is possible to have a singular value for $\dot{\theta}_n$ (Eq. 105c) due to a zero value of the denominator $\sin^2 \frac{\theta_j}{2}$. In practice, for the calculations performed in this study, this situation rarely occurs for the sampled initial condition for $s = W$ approach, but may happen for the first time-steps for focused initial conditions of $s = Q$. Nevertheless, for the time-step where this situation occurs, one can switch back to Eq. 94c to avoid these rare numerical singularities in $\dot{\theta}_n$. In this case, one can switch to use a Verlet algorithm with $\dot{\Omega}_i$ and $\ddot{\Omega}_i = \frac{1}{\hbar} \sum_{j,k=1}^{N^2-1} f_{ijk} \mathcal{H}_j \dot{\Omega}_k$, or to the MMST variables by propagating Eq. 109.

The above half-propagation step for the electronic DOFs is followed by a propagation of the nuclear variables using the Verlet algorithm,

$$P(t + \frac{\Delta t}{2}) = P(t) + \dot{P}(t) \frac{\Delta t}{2}, \quad (116a)$$

$$R(t + \Delta t) = R(t) + \dot{R}(t + \frac{\Delta t}{2}) \Delta t, \quad (116b)$$

$$P(t + \Delta t) = P(t + \frac{\Delta t}{2}) + \dot{P}(t + \Delta t) \frac{\Delta t}{2}, \quad (116c)$$

and finally by the second half time-step of the mapping variables $\{\varphi_n, \theta_n\}$ with a similar Verlet scheme as outlined in Eq. 115. Thus, in principle, the non-adiabatic mapping dynamics in the $\mathfrak{su}(N)$ representation does not need the MMST mapping variables.

On the other hand, an alternative way to propagate the dynamics is to obtain the initial values of the angles for $\{\varphi_n, \theta_n\}$ through either the sampling or focusing approach described in Sec. IV, transform them into the MMST mapping variables $\{q_n, p_n\}$ through Eq. 113, and then directly propagate the EOMs with these MMST variables through Eq. 109 and Eq. 111. This is a much easier approach to implement into computer code, because these equations are much simpler than the corresponding EOMs in Eq. 105. In addition, there are several previously developed algorithms to propagate these EOMs, which can be directly borrowed. Our numerical tests suggest that identical numerical accuracy and results are generated from this approach and the approach in Eq. 115.

One dimensional spin-boson model. We use a one dimensional spin-boson model^{80,81} to investigate the accuracy of the non-adiabatic dynamics for various methods. The Hamiltonian is expressed as

$$\hat{H} = \left(\frac{\hat{P}^2}{2m} + \frac{1}{2}m\omega^2\hat{R}^2 \right) \hat{\mathcal{I}} + \sqrt{2}\zeta\hat{R}\hat{\sigma}_z + \Delta\hat{\sigma}_x, \quad (117)$$

where $\hat{\sigma}_x$ and $\hat{\sigma}_z$ are the Pauli matrices, $\hat{\mathcal{I}}$ is a 2×2 identity matrix, \hat{R} and \hat{P} are the position and momentum operators of the boson mode. The parameter ζ controls the electronic-nuclear coupling, and Δ is the electronic coupling between two electronic states. We choose $2\Delta = \omega = m = 1$ and increasing values of the coupling strength parameter, the temperature is chosen in order to have $\beta = 16$. The initial electronic state is prepared on state $|1\rangle$.

Spin-Boson model. The spin-boson model⁸² is a commonly used two-level benchmark model for non-adiabatic dynamics.^{23,24,83} It consists in two electronic states, coupled to a harmonic bath of F -nuclear modes. The Hamiltonian of the model system is

$$\hat{H} = \sum_{\nu=1}^F \left(\frac{\hat{P}_{\nu}^2}{2m_{\nu}} + \frac{1}{2}m_{\nu}\omega_{\nu}^2\hat{R}_{\nu}^2 \right) \hat{\mathcal{I}} + \left(\varepsilon + \sum_{\nu=1}^F c_{\nu}\hat{R}_{\nu} \right) \hat{\sigma}_z + \Delta\cdot\hat{\sigma}_x, \quad (118)$$

where m_{ν} is the nuclear mass set to be 1, Δ is the diabatic electronic coupling set to be 1, and ε is the energy bias between two electronic states. The F nuclear modes each have their frequency ω_{ν} and vibronic coupling coefficient c_{ν} , determined through the spectral density of the bath $J(\omega)$. Here, we use an Ohmic spectral density

$$J(\omega) = \frac{\pi}{2} \sum_{\nu=1}^F \frac{c_{\nu}^2}{\omega_{\nu}} \delta(\omega - \omega_{\nu}) = \frac{\pi\xi}{2} \omega e^{-\omega/\omega_c}, \quad (119)$$

where ξ is the Kondo parameter and ω_c the cut-off frequency for the bath. We perform simulations with three sets of model parameters, from a low to a high temperature and different system-bath coupling strengths (through the Kondo parameter), with parameters listed in Tab. I of Appendix F. The details of the bath discretization is also provided in Appendix F. The initial electronic state is prepared on state $|1\rangle$.

Two- and Three-States Linear Vibronic Coupling Models. The linear vibronic coupling (LVC) models describe conical intersections in molecules. The Hamiltonian is expressed as

$$\hat{H} = \frac{1}{2} \sum_{\nu} \omega_{\nu} \hat{P}_{\nu}^2 + \sum_{k,l} |k\rangle H_{kl}(\hat{\mathbf{R}}) \langle l|, \quad (120a)$$

$$H_{kk}(\hat{\mathbf{R}}) = E_k + \frac{1}{2} \sum_{\nu} \omega_{\nu} \hat{R}_{\nu}^2 + \sum_{\nu} \kappa_{\nu}^k \hat{R}_{\nu}, \quad (120b)$$

$$H_{kl}(\hat{\mathbf{R}}) = \sum_{\nu} \lambda_{\nu}^{kl} \hat{R}_{\nu}, \quad (120c)$$

where ω_{ν} is the frequency of the ν -th nuclear normal mode, E_k is the vertical transition energy of state k , and the electronic-nuclear coupling is λ_{ν}^{kl} . Here, we investigate two widely tested LVC models: the pyrazine model,⁸⁴ and the benzene cation radical model.^{85,86} The pyrazine model is a standard conical intersection model used to study non-adiabatic dynamics.^{52,87-89} It is a three-modes two-states model, with two tuning coordinates, \hat{R}_1 and \hat{R}_2 , and one coupling coordinate, \hat{R}_3 . The parameters are given in Tab. II of Appendix F. The initial electronic state is prepared on state $|2\rangle$. The benzene radical cation model is a five-modes three-states model with three tuning coordinates, \hat{R}_1 , \hat{R}_2 and \hat{R}_3 , and two coupling coordinates, \hat{R}_4 and \hat{R}_5 . The parameters are given in Tab. III of Appendix F. The initial electronic state⁵² is prepared on state $|3\rangle$.

Three-state Morse model. Finally, we consider an anharmonic model. We compute the population dynamics of a three-state Morse potential,¹² which is used to model photo-dissociation dynamics with three sets of parameters. The Hamiltonian is expressed as

$$\hat{H} = \frac{\hat{P}^2}{2m} \hat{\mathcal{I}} + \sum_{ij} V_{ij}(\hat{R}) |i\rangle \langle j|, \quad (121a)$$

$$V_{ii}(\hat{R}) = D_{ii}(1 - e^{-\alpha_{ii}(\hat{R}-R_{ii})^2} - c_{ii}), \quad (121b)$$

$$V_{ij}(\hat{R}) = A_{ij} e^{-\alpha_{ij}(\hat{R}-R_{ij})^2}, \quad i \neq j, \quad (121c)$$

where the mass is set to be $m = 20\,000$ a.u. and the rest of the parameters are specified in Tab. IV of Appendix F for the three models IA, IB and IC. The system is initially excited onto state $|1\rangle$.

Initial Conditions. The initial conditions for all of the model calculations are $\hat{\rho}(0) = |n\rangle \langle n| \otimes \hat{\rho}_{\mathbf{R}}$, where $|n\rangle$ indicates the initial electronic diabatic state (as described in each Model Hamiltonian section) and $\hat{\rho}_{\mathbf{R}}$ represents the initial nuclear density operator. For the spin-boson model calculations (presented in Figs. 1-2), we assume that each nuclear DOF has a canonical thermal density $\hat{\rho}_{\mathbf{R}} = \frac{1}{Z} e^{-\beta[\sum_{\nu} \hat{P}_{\nu}^2 / 2M_{\nu} + \frac{1}{2} M_{\nu} \omega_{\nu}^2 \hat{R}_{\nu}^2]} / Z$, where $\beta = 1/k_B T$, and Z is the partition function. The corresponding nuclear Wigner density is then

$$[\hat{\rho}_{\mathbf{R}}]_w = \prod_{\nu=1}^F \frac{1}{\pi} \tanh \frac{\beta \hbar \omega_{\nu}}{2} e^{-\tanh \frac{\beta \hbar \omega_{\nu}}{2} \left(\frac{1}{\hbar m_{\nu} \omega_{\nu}} P_{\nu}^2 + \frac{m_{\nu} \omega_{\nu}}{\hbar} R_{\nu}^2 \right)}. \quad (122)$$

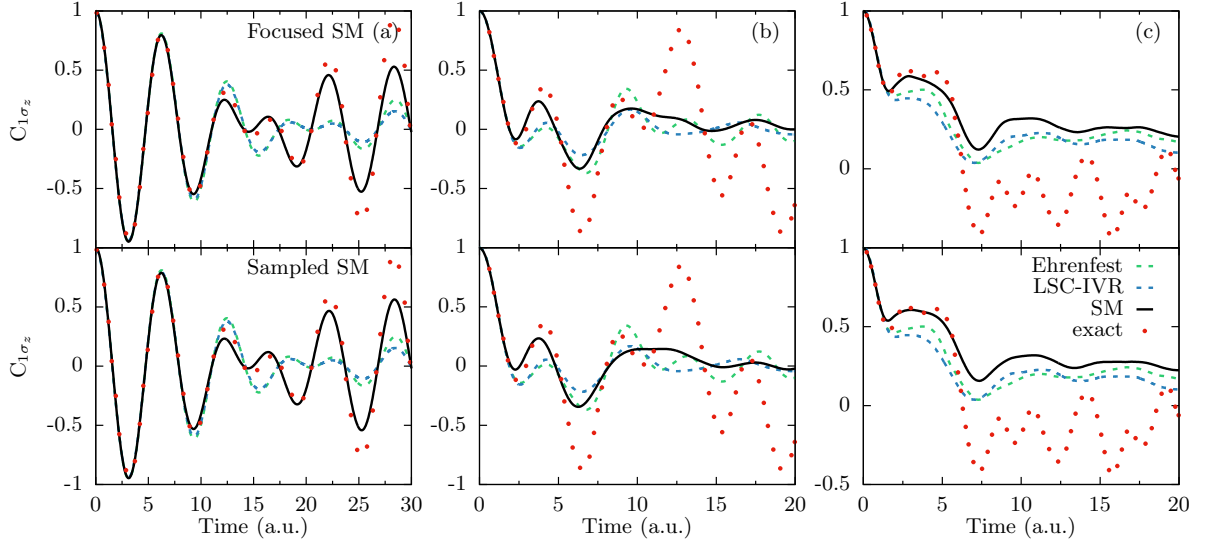


FIG. 1. Population dynamics of the 1-D spin boson models, obtained from focused initial conditions (top panels) and sampled initial conditions (bottom panels). The model parameters are (a) $\xi = 0.1$, (b) $\xi = 0.5$ and (c) $\xi = 1$, the rest of the parameters being provided in Tab. I of Appendix F. The Spin-Mapping results (black solid lines) are compared against the LSC-IVR (blue dashed lines), Ehrenfest (green dashed lines) and exact results (red dots).

For the LVC models and the photo-dissociation calculations of Morse Potential (presented in Fig. 3-5), we use $\hat{\rho}_{\mathbf{R}} = |\chi\rangle\langle\chi|$, where $\langle \mathbf{R}|\chi\rangle = (\frac{2\Gamma}{\pi})^{1/4} e^{-(\Gamma/2)(\mathbf{R}-\mathbf{R}_0)^2 + \frac{i}{\hbar}\mathbf{P}_0(\mathbf{R}-\mathbf{R}_0)}$ represents a Gaussian wavepacket centered around \mathbf{R}_0 and \mathbf{P}_0 . For the LVC models, $\mathbf{R}_0 = \mathbf{P}_0 = 0$ with a width $\Gamma = 2$. The corresponding nuclear Wigner density is

$$[\hat{\rho}_{\mathbf{R}}]_w = \prod_{\nu=1}^F \frac{1}{\pi} e^{-\Gamma(\mathbf{R}-\mathbf{R}_0)^2 - (\mathbf{P}-\mathbf{P}_0)^2/\Gamma}. \quad (123)$$

For the coupled Morse potential models, we use the same nuclear Wigner density in Eq. 123 with only one nuclear DOF, and $\Gamma = \frac{1}{m\omega}$ where the mass of the nuclear DOF is set to be $m = 20\ 000$ a.u., $\omega = 0.005$, and the values of R_0 are 2.1, 3.3 and 2.9 for models IA, IB and IC, respectively, and $P_0 = 0$ for all three models.

VII. RESULTS AND DISCUSSIONS

In this section, we refer to the linearized method in the $\mathfrak{su}(N)$ mapping formalism as the spin mapping (SM) approach, with the EOMs described in Eq. 94, or equivalently, in Eq. 105 or in Eq. 109. Here, we compare the numerical results obtained from the spin mapping formalism with other methods, including the LSC-IVR^{11,59,73} as well as the simple trajectory Ehrenfest method.^{90–92} The connection of these other method to the current formalism in the $\mathfrak{su}(N)$ mapping formalism is discussed in Sec. V E. Note that the current Spin Mapping approach is derived entirely based on the generators of the $\mathfrak{su}(N)$

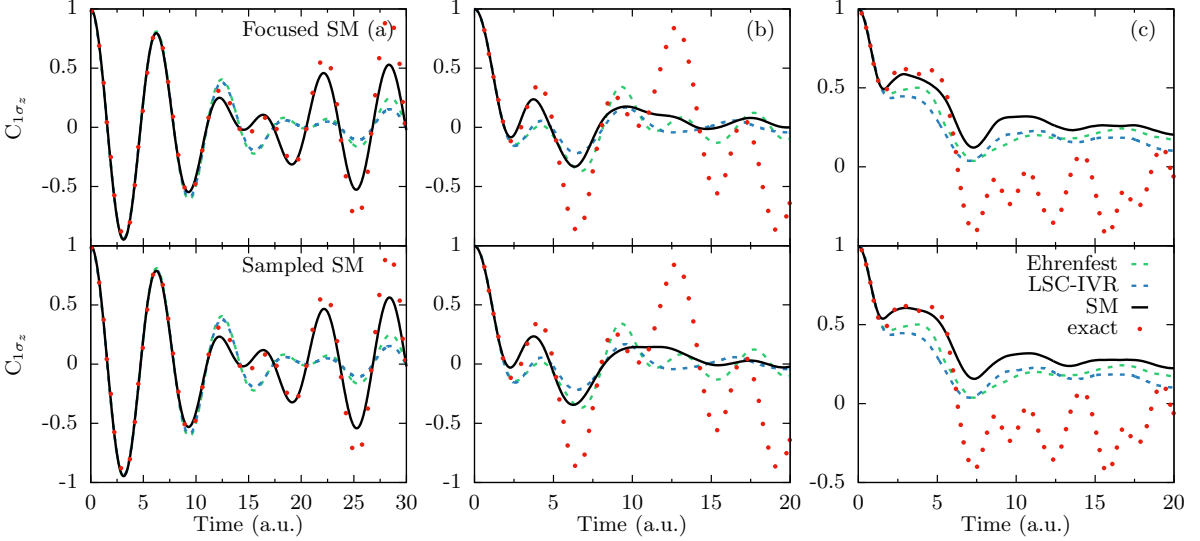


FIG. 1. Population dynamics of the 1-D spin boson models, obtained from focused initial conditions (top panels) and sampled initial conditions (bottom panels). The model parameters are (a) $\xi = 0.1$, (b) $\xi = 0.5$ and (c) $\xi = 1$, the rest of the parameters being provided in Tab. I of Appendix F. The Spin-Mapping results (black solid lines) are compared against the LSC-IVR (blue dashed lines), Ehrenfest (green dashed lines) and exact results (red dots).

Lie algebra, without the necessity to convert back to the Cartesian mapping variables of the MMST formalism that spin-LSC uses. Nevertheless, we found that the current formalism generates numerically similar results from spin-LSC.^{24,29}

Fig. 1 presents the population dynamics $\langle \sigma_z(t) \rangle = C_{1\sigma_z}(t)$ for a 1-D Spin-Boson model.⁸¹ For the spin mapping simulation, a time-step of $dt = 0.01$ a.u. is used, and the converged results are obtained with 10^4 trajectories for the focused initial conditions (upper panels) and 10^5 trajectories for the sampled initial conditions (lower panels). The population dynamics of the spin mapping approach are compared to the numerically exact calculations (red dots), LSC-IVR (blue) and Ehrenfest dynamics (green). The SM approach is in a very good agreement with the exact calculations for the model in panel (a), including all of the longer time recurrence of the electronic Rabi oscillations. It is important to note that the sampled and focused initial conditions yield almost exactly the same dynamics for this model. The LSC-IVR approach and the Ehrenfest dynamics, on the other hand, capture the initial electronic oscillations but fail to reproduce the longer time dynamics from LSC-IVR or Ehrenfest was thought⁸¹ causing by the zero point energy (ZPE) leakage problem associated with the classical Wigner dynamics of the nuclear DOF,^{93,94} which is typical for linearized path-integral approaches based on the classical Wigner dynamics.^{63,71,95} The ZPE leakage originates from the fact that classical dynamics does not preserve the ZPE incorporated in the nuclear initial Wigner distribution,^{93,94} causing an incorrect energy flow from the nuclear DOF to the electronic DOF,⁵⁴ equalizing the longer time popula-

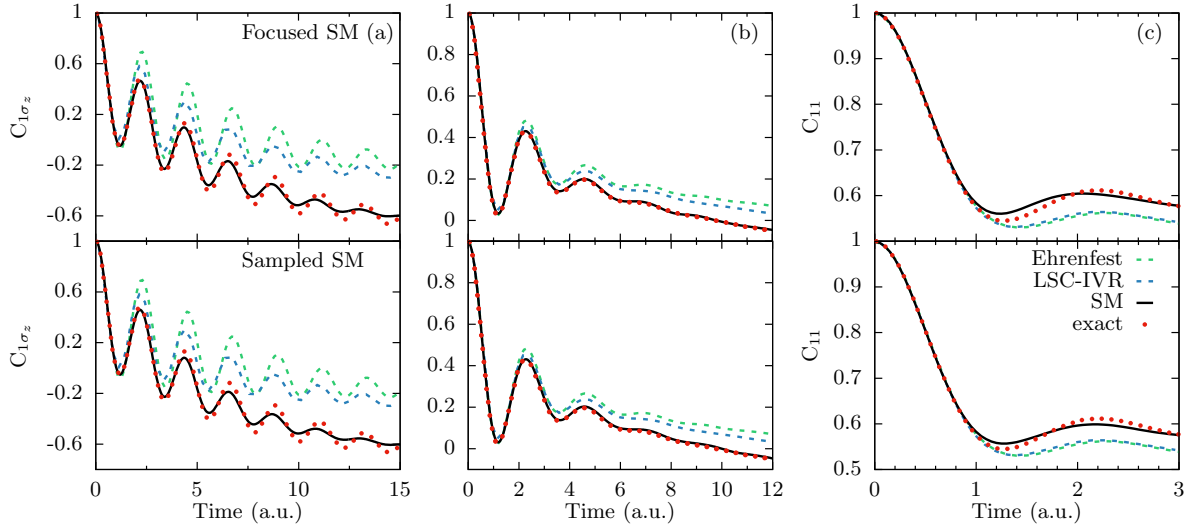


FIG. 2. Population dynamics $\langle \sigma_z(t) \rangle = C_{1\sigma_z}(t)$ (panels a-b) and time-correlation function $C_{11}(t)$ (panel c) from focused initial conditions (top panels) and sampled initial conditions (bottom panels) for the spin-boson models. The details of the parameters are described in Tab. I of Appendix F. The Spin Mapping results (black solid lines) are compared to LSC-IVR (blue dashed lines), Ehrenfest (green dashed lines) and exact results (red dots).

tions and giving $\langle \sigma_z(t) \rangle = 0$. In our previous work on non-adiabatic ring polymer molecular dynamics,⁸¹ we have shown that quantizing the nuclear DOF with a ring polymer can effectively incorporate nuclear quantum distribution and alleviate ZPE leaking problem, even when using the MMST mapping formalism. Here, our numerical results suggest that by using the $\mathfrak{su}(N)$ mapping formalism which exactly preserves the size of the electronic Hilbert space, this problem can be largely alleviated, compare to the traditional MMST mapping formalism which can get outside of the singly excited oscillator (SEO) mapping subspace, even though the classical Wigner type of dynamics is used for the nuclear DOF.

Fig. 1b-c presents the population dynamics for stronger electron-phonon couplings. We can see that the Spin Mapping method reproduces the exact result reasonably well up to $t=5$ a.u. At a longer time, however, this approach becomes less accurate compared to the exact results, missing the recurrence of the electronic Rabi oscillations. Nevertheless, as an independent trajectory-based approach, the Spin Mapping approach still outperforms both LSC-IVR and Ehrenfest for all model calculations presented here.

Fig. 2 presents the dynamics of three different spin-boson models, where LSC-IVR and Ehrenfest dynamics are known to provide less accurate results. This includes the electronic asymmetry in models presented in panels (a) and (b), as well as the strong system-bath coupling in the model presented in panel (c). The details of the parameters are provided in Tab. I of Appendix F. The Spin Mapping results (black solid lines) are compared to LSC-IVR (blue dashed lines), Ehrenfest (green dashed lines) and exact results (red dots). We used the same

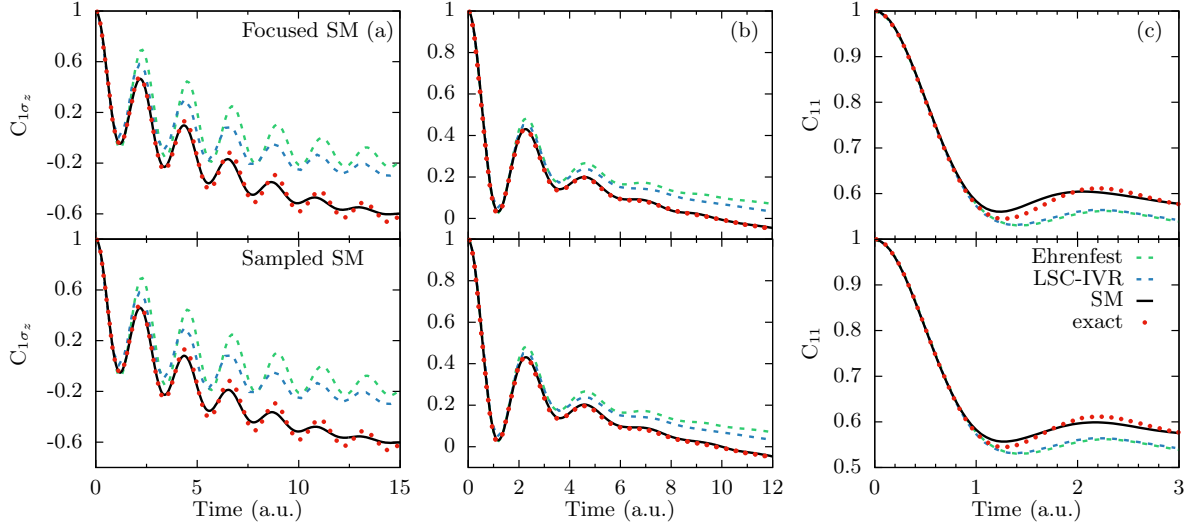


FIG. 2. Population dynamics $\langle \sigma_z(t) \rangle = C_{1\sigma_z}(t)$ (panels a-b) and time-correlation function $C_{11}(t)$ (panel c) from focused initial conditions (top panels) and sampled initial conditions (bottom panels) for the spin-boson models. The details of the parameters are described in Tab. I of Appendix F. The Spin Mapping results (black solid lines) are compared to LSC-IVR (blue dashed lines), Ehrenfest (green dashed lines) and exact results (red dots).

time-step and number of trajectories that has been used in the previous model. The $s = W$ choice of the spin mapping method slightly underestimates the oscillations in the population dynamics at low temperature, but gives more accurate results compared to the LSC-IVR method (blue dashed line) or Ehrenfest Dynamics (green dashed line). Both the sampled and the focused initial conditions provide almost identical results.

Fig. 3 presents the population dynamics of state $|2\rangle$ in the pyrazine model.⁸⁴ The results are obtained from the current Spin Mapping approach (red solid) with both focused and sampled initial conditions, and compared to Ehrenfest dynamics (green dash), as well as to the recently developed Generalized Discrete Truncated Wigner Approximation (GDTWA)⁵² approach (blue dashed line). The Spin Mapping approach generates very accurate population dynamics compared to the exact results, regardless of the initial conditions of the mapping variables, although the early dynamics is slightly more accurate when focusing the initial conditions, while the long-time dynamics seems closer to the exact result when using the sampled initial conditions. Interestingly, the current Spin Mapping approach almost coincides with the GDTWA approach. It was claimed⁵² that in the GDTWA approach, the discrete sampling of the phase space is the key to provide more accurate results compared to the spin mapping formalism, when comparing the population dynamics generated from GDTWA and spin-PLDM.^{96,97} However, it seems that this is because the spin-PLDM is less accurate than the current spin mapping approach or spin-LSC for the LVC model, even though the former is more accurate than the latter for spin-boson type problems.^{96,97} Future work is

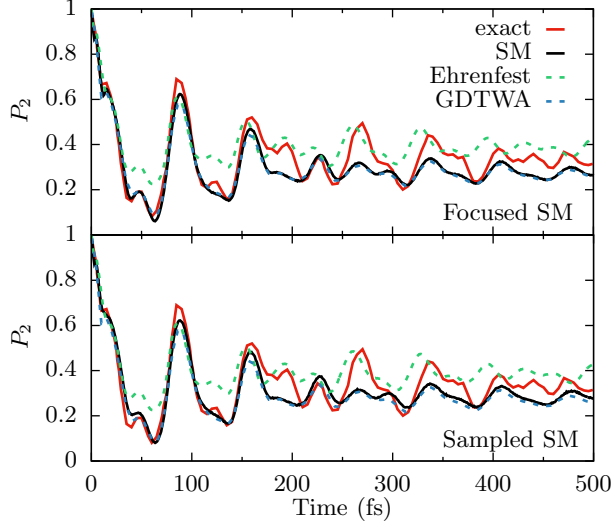


FIG. 3. Population dynamics of the pyrazine model with focused (upper panel) and sampled initial conditions (lower panel) for the Spin Mapping approach. The results obtained from Spin Mapping (black solid lines) are compared to the Ehrenfest method (green dashed line), the GDTWA approach⁵² (blue dashed line), and exact results (red solid line).

needed to further explore the numerical performance of these approaches.

Fig. 4 presents the numerical results of a three-state model for the benzene radical cation.^{85,86} This is a particularly challenging model due to the multi-state dynamics and the presence of conical intersection, especially for traditional mixed quantum-classical methods such as Ehrenfest (panel a) and Fewest Switches Surface Hopping³ (panel c), both of which generate less accurate population dynamics.⁹⁸ The spin mapping formalism, on the other hand, gives almost quantitatively accurate dynamics for this challenging system. For the Spin Mapping results presented here, we used 10^5 trajectories for the sampled initial condition and 10^4 for the focused initial condition, and a nuclear time-step of $dt = 0.5$ a.u. as well as a mapping time-step of $dt_{\text{map}} = dt_{\text{nuc}}/16$. While the focused initial conditions provide slightly more accurate short-time dynamics up to 150 fs (panel b), the sampled initial conditions seem to generate population closer to the exact result at a longer time.

Fig. 5 presents the results of population dynamics in the three-state coupled Morse potential.¹² Here, we present the Spin Mapping results only using focused initial conditions (solid lines). A time-step of 1 a.u., and 10^5 to 5×10^5 trajectories were used. The sampled initial conditions for spin mapping variables generates less accurate population as the initial nuclear force does not respect the physical occupancy of the electronic states.⁷⁹ This has been extensively discussed in the recent work on trajectory-adjusted electronic zero point energy in classi-

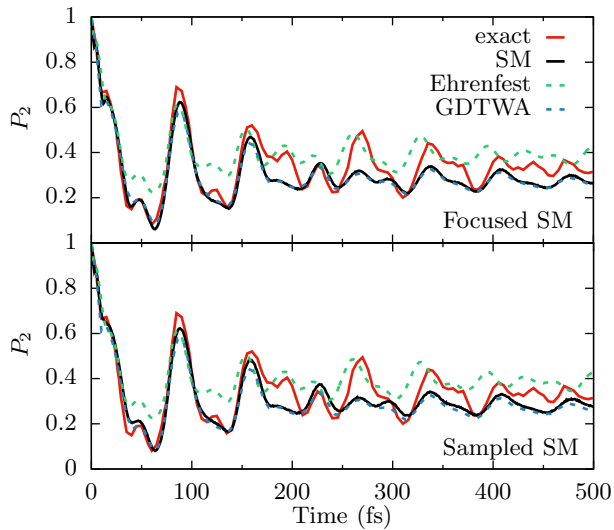


FIG. 3. Population dynamics of the pyrazine model with focused (upper panel) and sampled initial conditions (lower panel) for the Spin Mapping approach. The results obtained from Spin Mapping (black solid lines) are compared to the Ehrenfest method (green dashed line), the GDTWA approach⁵² (blue dashed line), and exact results (red solid line).

cal Meyer-Miller vibronic dynamics.⁷⁹ Nevertheless, the population dynamics of the Spin Mapping method with the focused initial conditions give almost exact results compared to the numerically exact calculations (dots), and outperform Ehrenfest dynamics (dashed lines). The Spin Mapping approach generates both accurate short time branching dynamics among three states as well as long time plateau value of the population, that is almost exact for models presented in panel (a) and (c). For the model presented in panel (b), the spin mapping formalism slightly outperforms the state-of-the-art γ -SQC approach,⁷⁹ as well as the non-adiabatic ring polymer molecular dynamics approach.⁸¹

VIII. CONCLUSION

We present the rigorous analytical derivation of the non-adiabatic dynamics using the generators (generalized spin matrices) of the $\mathfrak{su}(N)$ Lie algebra. Applying the Stratonovich-Weyl transform on the $\mathfrak{su}(N)$ -based mapping Hamiltonian provides the continuous variables (generalized spin coherence states) that can be viewed as the angle variables on a multi-dimensional Bloch sphere, hence establishing a mapping between discrete electronic states and continuous variables. The main advantage of the $\mathfrak{su}(N)$ representation is that the corresponding Stratonovich-Weyl transform exactly preserves the identity operator in the N dimensional Hilbert space,²⁹ as opposed to the MMST formalism where the identity is not preserved through the mapping and there is an ambiguity of how to evaluate it.²² This is because the MMST representation has a larger size of Hilbert space (that contains other states outside the single excitation manifold of the mapping oscillators) compared to the original electronic subspace, which then requires a projection back to the single excitation subspace of the mapping oscillators to obtain accurate results. The $\mathfrak{su}(N)$ representation, on the other hand, completely alleviates these problems and is the most natural way to map a N -level system into a classical phase space.

Using a mixed Wigner/Stratonovich-Weyl formalism, we derive a general expression of the time-correlation function, where the Wigner representation is used for the nuclear DOFs, and the Stratonovich-Weyl transform is applied to the generalized spin matrices associated to the electronic DOFs. We obtain the expression of the exact quantum Liouvillian in this formalism. Further making a linearization approximation, we obtain a set of EOMs that describe the coupled dynamics between the electronic and nuclear DOFs. We further connect EOMs with different mapping variables, including the spin coherence state variables, generalized Bloch spherical coordinates, as well as the MMST mapping variables. We formally establish the equivalence of these EOMs with different mapping variables. We also connect a variety of previously developed methods with the current formalism in the language of the $\mathfrak{su}(N)$ mapping formalism.

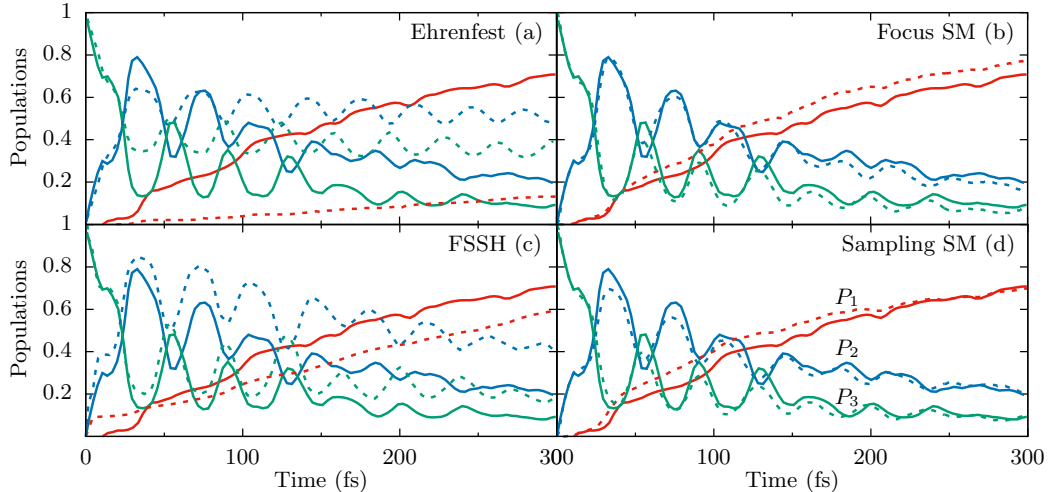


FIG. 4. Electronic populations of the benzene cation model, obtained from (a) Ehrenfest dynamics, (b) Spin Mapping formalism with focused initial condition, (c) fewest switches surface hopping (FSSH) as obtained from Ref. 98, and (d) Spin Mapping with sampled initial conditions. The population dynamics of state 1 (red), state 2 (blue) and state 3 (green) are presented (dashed lines) and compared to exact dynamics (solid lines).

Finally, we perform numerical simulations to assess the accuracy of the generalized spin mapping approach under the linearization approximation. We compute the population dynamics of systems with multiple electronic states coupled to the nuclear DOFs, including a condensed phase spin-boson model system, two conical intersection models, and an anharmonic three-state Morse model for photo-dissociation dynamics. The current formalism provides an excellent agreement compared to the numerically exact results, and a significant improvement compared to the Ehrenfest dynamics or LSC-IVR which is based on the MMST mapping formalism. Interestingly, the current formalism produces very similar numerical results compared to two recently developed approaches, Spin-LSC and GDTWA, both of which are based on the $\mathfrak{su}(N)$ mapping formalism.

The theoretical framework presented in this work provides a rigorous way to formally derive non-adiabatic quantum dynamics approaches with continuous mapping variables. Future work will use this framework to derive non-adiabatic spin-mapping Matsubara dynamics⁶⁶ and spin-mapping non-adiabatic ring polymer molecular dynamics^{38,66} based on the Kubo-transformed TCF.

ACKNOWLEDGMENTS

This work was supported by the National Science Foundation CAREER Award under Grant No. CHE-1845747. Computing resources were provided by the Center for Integrated Research Computing (CIRC) at the University of Rochester. D.B. would like to thank Wenxiang Ying and Braden M. Weight for valuable discussions.

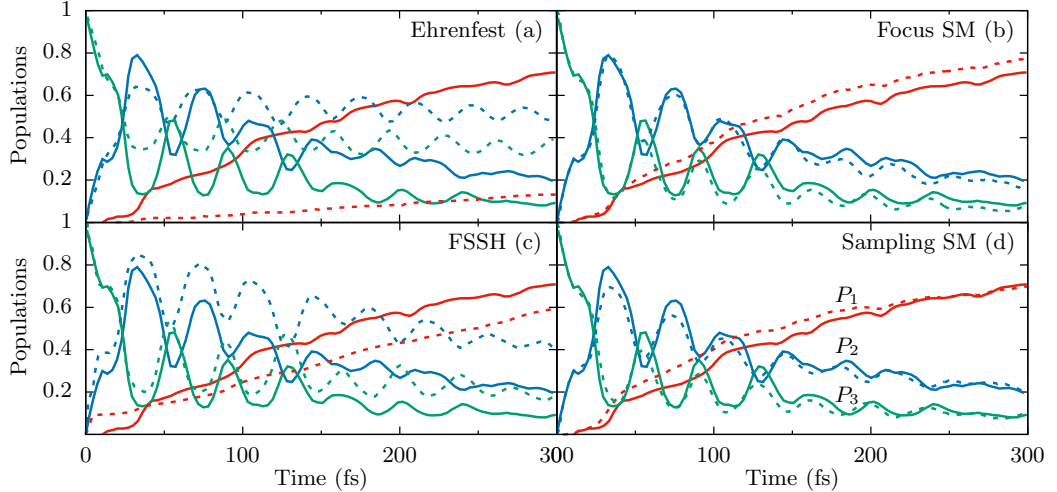


FIG. 4. Electronic populations of the benzene cation model, obtained from (a) Ehrenfest dynamics, (b) Spin Mapping formalism with focused initial condition, (c) fewest switches surface hopping (FSSH) as obtained from Ref. 98, and (d) Spin Mapping with sampled initial conditions. The population dynamics of state 1 (red), state 2 (blue) and state 3 (green) are presented (dashed lines) and compared to exact dynamics (solid lines).

CONFLICT OF INTEREST

The authors have no conflicts to disclose.

AVAILABILITY OF DATA

The data that support the findings of this study are available from the corresponding author upon a reasonable request.

Appendix A: Analytic expression of the structure constants

Despite the extensive usage and the crucial role these structure constants play in modern physics, to the best of our knowledge,⁹⁹ there is no analytic expression (closed formulas) of f_{ijk} and d_{ijk} . Here, we derive closed analytic formulas for these structure constants without requiring any matrix multiplication or involving the generator expressions. Their analytic expressions are listed in Eq. A5 (for f_{ijk}) and Eq. A14 (for d_{ijk}).

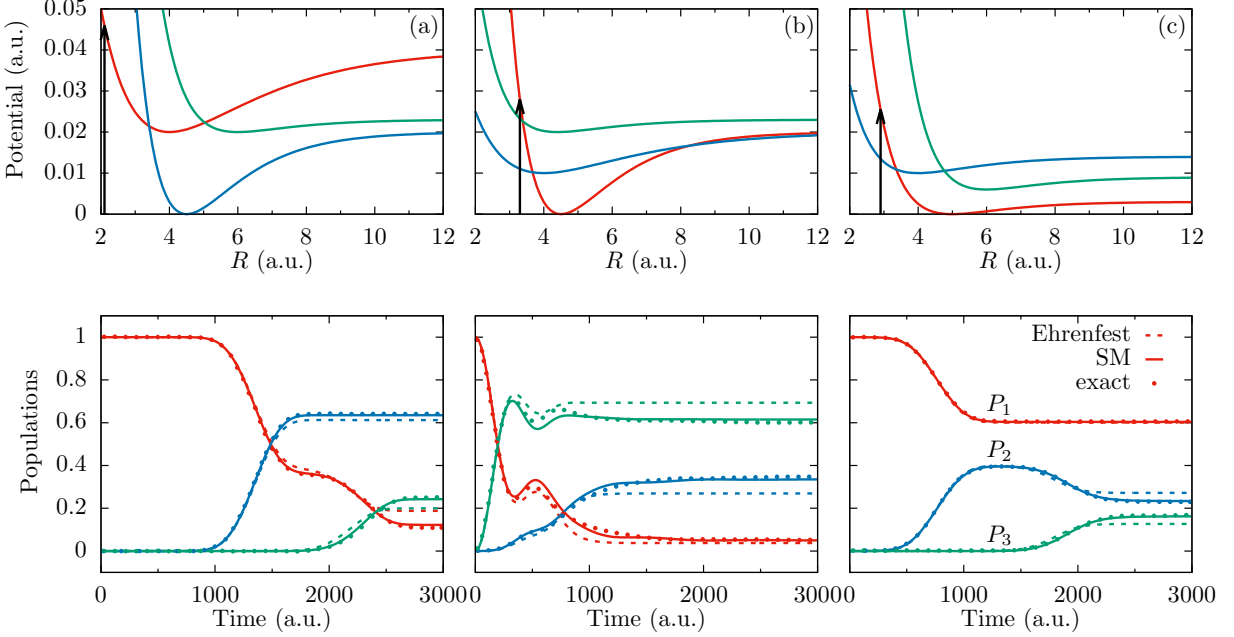


FIG. 5. Diabatic Potential Energy Surfaces (top panels) and the population dynamics (bottom panels) for the three-state coupled Morse models (a) IA, (b) IB and (c) IC, described in Tab. IV of Appendix F. The vertical black arrows in top panels indicate the Franck-Condon vertical photo-excitations. State 1 (red), state 2 (blue) and state 3 (green) populations are calculated with the focused spin-mapping approach (solid lines), and compared with the Ehrenfest dynamics (dashed lines) as well as the exact results (dots).

1. The Totally Anti-symmetric Structure Constants f_{ijk}

The commutation relation between two symmetric generators is

$$\begin{aligned}
 [\hat{\mathcal{S}}_{\alpha_{nm}}, \hat{\mathcal{S}}_{\alpha_{n'm'}}] &= i\hbar \sum_{k=1}^{N^2-1} f_{\alpha_{nm}\alpha_{n'm'}k} \hat{\mathcal{S}}_k \quad (\text{A1}) \\
 &= \frac{\hbar^2}{4} \left[\delta_{nm'} (|m\rangle\langle n'| - |n'\rangle\langle m|) + \delta_{nn'} (|m\rangle\langle m'| - |m'\rangle\langle m|) \right. \\
 &\quad \left. + \delta_{mm'} (|n\rangle\langle n'| - |n'\rangle\langle n|) + \delta_{mn'} (|n\rangle\langle m'| - |m'\rangle\langle n|) \right] \\
 &= i\frac{\hbar}{2} \left[\delta_{nm'} \hat{\mathcal{S}}_{\beta_{n'm}} + \delta_{nn'} (\hat{\mathcal{S}}_{\beta_{m'm}} - \hat{\mathcal{S}}_{\beta_{mm'}}) \right. \\
 &\quad \left. + \delta_{mm'} (\hat{\mathcal{S}}_{\beta_{n'n}} - \hat{\mathcal{S}}_{\beta_{nn'}}) - \delta_{mn'} \hat{\mathcal{S}}_{\beta_{nm'}} \right].
 \end{aligned}$$

With constraints from δ_{ij} , we can identify the indices of each generator, and hence obtain the analytic expressions of non-zero $f_{\alpha_{nm}\alpha_{n'm'}k}$, which are summarized in the first line of Eq. A1 of the main text.

For a symmetric and an anti-symmetric generator, the

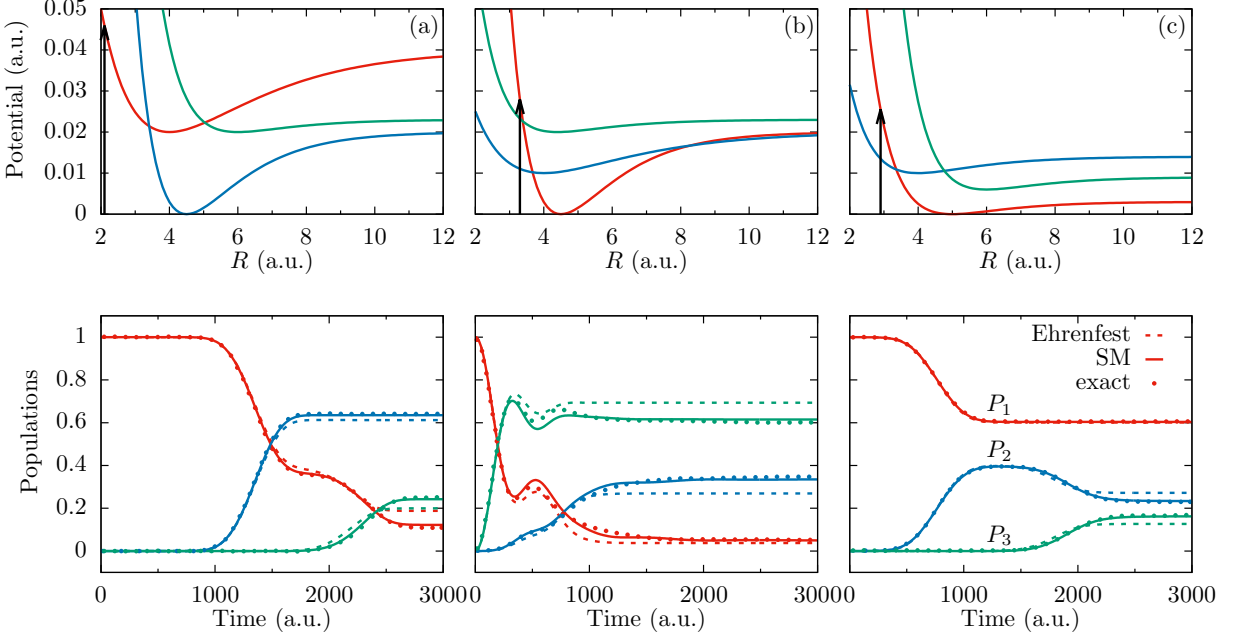


FIG. 5. Diabatic Potential Energy Surfaces (top panels) and the population dynamics (bottom panels) for the three-state coupled Morse models (a) IA, (b) IB and (c) IC, described in Tab. IV of Appendix F. The vertical black arrows in top panels indicate the Franck-Condon vertical photo-excitations. State 1 (red), state 2 (blue) and state 3 (green) populations are calculated with the focused spin-mapping approach (solid lines), and compared with the Ehrenfest dynamics (dashed lines) as well as the exact results (dots).

commutation relation is

$$\begin{aligned}
 [\hat{\mathcal{S}}_{\alpha_{nm}}, \hat{\mathcal{S}}_{\beta_{n'm'}}] &= i\hbar \sum_{k=1}^{N^2-1} f_{\alpha_{nm}\beta_{n'm'},k} \hat{\mathcal{S}}_k \\
 &= i\frac{\hbar^2}{4} \left[\delta_{nn'}(|m\rangle\langle m'| + |m'\rangle\langle m|) - \delta_{nm'}(|m\rangle\langle n'| + |n'\rangle\langle m|) \right. \\
 &\quad \left. + \delta_{mn'}(|n\rangle\langle m'| + |m'\rangle\langle n|) - \delta_{mm'}(|n\rangle\langle n'| + |n'\rangle\langle n|) \right] \\
 &= i\frac{\hbar}{2} \left[\delta_{nn'}(\hat{\mathcal{S}}_{\alpha_{m'm}} + \hat{\mathcal{S}}_{\alpha_{mm'}}) - \delta_{nm'}\hat{\mathcal{S}}_{\alpha_{n'm}} + \delta_{mn'}\hat{\mathcal{S}}_{\alpha_{nm'}} \right. \\
 &\quad \left. - \delta_{mm'}(\hat{\mathcal{S}}_{\alpha_{n'n}} + \hat{\mathcal{S}}_{\alpha_{nn'}}) + \frac{\hbar}{2}\delta_{mm'}\delta_{nn'}(2|m\rangle\langle m| - 2|n\rangle\langle n|) \right]. \tag{A2}
 \end{aligned}$$

The first two lines of the last equality in Eq. A2 directly give several structure constants. The last line of Eq. A2 contains diagonal elements, hence we know it will be a combination of diagonal generators. We can prove (see Supporting Information) that

$$\begin{aligned}
 i\frac{\hbar^2}{2}(|m\rangle\langle m| - |n\rangle\langle n|) &= i\hbar \left(\sqrt{\frac{n}{2(n-1)}}\hat{\mathcal{S}}_{\gamma_n} + \sum_{k>m}^{n-1} \frac{\hat{\mathcal{S}}_{\gamma_k}}{\sqrt{2k(k-1)}} - \sqrt{\frac{m-1}{2m}}\hat{\mathcal{S}}_{\gamma_m} \right). \tag{A3}
 \end{aligned}$$

This helps to determine the rest of the structure constants $f_{\alpha_{nm}\beta_{n'm'},k}$. The commutation relations between symmetric and diagonal generators are not required as

we have already obtained all the non-zero structure constants involving diagonal and symmetric generators (and we know that we cannot obtain a diagonal matrix through the commutator of a symmetric and a diagonal generator).

Between two anti-symmetric generators, the commutation relation is

$$\begin{aligned} [\hat{\mathcal{S}}_{\beta_{nm}}, \hat{\mathcal{S}}_{\beta_{n'm'}}] &= i\hbar \sum_{k=1}^{N^2-1} f_{\beta_{nm}\beta_{n'm'}, k} \hat{\mathcal{S}}_k & (\text{A4}) \\ &= \frac{\hbar^2}{4} \left[\delta_{nm'}(|n'\rangle\langle m| - |m\rangle\langle n'|) + \delta_{nn'}(|m\rangle\langle m'| - |m'\rangle\langle m|) \right. \\ &\quad \left. + \delta_{mm'}(|n\rangle\langle n'| - |n'\rangle\langle n|) + \delta_{mn'}(|m'\rangle\langle n| - |n\rangle\langle m'|) \right] \\ &= i\frac{\hbar}{2} \left[-\delta_{nm'}\hat{\mathcal{S}}_{\beta_{n'm}} + \delta_{nn'}(\hat{\mathcal{S}}_{\beta_{m'm}} - \hat{\mathcal{S}}_{\beta_{mm'}}) \right. \\ &\quad \left. + \delta_{mm'}(\hat{\mathcal{S}}_{\beta_{n'n}} - \hat{\mathcal{S}}_{\beta_{nn'}}) + \delta_{mn'}\hat{\mathcal{S}}_{\beta_{nm'}} \right], \end{aligned}$$

which helps to determine the structure constants involving all anti-symmetric generators (second line of Eq. A1 of the main text). The remaining totally anti-symmetric structure constants are computed through the commutator between two diagonal generators, which is $[\hat{\mathcal{S}}_{\gamma_n}, \hat{\mathcal{S}}_{\gamma_{n'}}] = i\hbar \sum_{k=1}^{N^2-1} f_{\gamma_n\gamma_{n'}, k} \hat{\mathcal{S}}_k = 0$, indicating a zero value for all $f_{\gamma_n\gamma_{n'}, k}$. This was a known fact, as the diagonal matrices are generators of the Cartan subalgebra of $\mathfrak{su}(N)$, and they commute by definition³⁴.

All of the non-zero totally anti-symmetric structure constants are expressed as follows

$$\begin{aligned} f_{\alpha_{nm}\alpha_{kn}\beta_{km}} &= f_{\alpha_{nm}\alpha_{nk}\beta_{km}} = f_{\alpha_{nm}\alpha_{km}\beta_{kn}} = \frac{1}{2}, & (\text{A5}) \\ f_{\beta_{nm}\beta_{km}\beta_{kn}} &= \frac{1}{2}, \\ f_{\alpha_{nm}\beta_{nm}\gamma_m} &= -\sqrt{\frac{m-1}{2m}}, \quad f_{\alpha_{nm}\beta_{nm}\gamma_n} = \sqrt{\frac{n}{2(n-1)}}, \\ f_{\alpha_{nm}\beta_{nm}\gamma_k} &= \sqrt{\frac{1}{2k(k-1)}}, \quad m < k < n. \end{aligned}$$

The structure constants derived here are within the basis of the GGM matrices $\hat{\mathcal{S}}$. Another choice of basis of $\hat{\mathcal{S}}'$ is also possible, which is related to the GGM basis through the following transformation

$$\hat{\mathcal{S}}_i = \sum_j [\mathcal{A}]_{ij} \hat{\mathcal{S}}'_j, & (\text{A6})$$

where \mathcal{A} is the transformation matrix, and $[\mathcal{A}]_{ij}$ is its ij th matrix element of \mathcal{A} . Within the new basis $\hat{\mathcal{S}}'$, one can always directly obtain the expressions of the structure constants through the following relation (see Chapter 4 of Ref. 100)

$$f'_{lmn} = \sum_{i,j,k} [\mathcal{A}^{-1}]_{li} [\mathcal{A}^{-1}]_{mj} f_{ijk} [\mathcal{A}]_{kn}, & (\text{A7})$$

where \mathcal{A}^{-1} is the inverse matrix of \mathcal{A} . With the analytic expressions of f_{ijk} in the GGM basis, this transformation becomes useful for obtaining structure constants in any basis of generators of $\mathfrak{su}(N)$.

2. The Totally Symmetric Structure Constants d_{ijk}

The anti-commutation relation between two symmetric generators is

$$\begin{aligned} \{\hat{\mathcal{S}}_{\alpha_{nm}}, \hat{\mathcal{S}}_{\alpha_{n'm'}}\} &= \frac{\hbar^2}{N} \delta_{\alpha_{nm}\alpha_{n'm'}} \hat{\mathcal{I}} + \hbar \sum_{k=1}^{N^2-1} d_{\alpha_{nm}\alpha_{n'm'}k} \hat{\mathcal{S}}_k \\ &= \frac{\hbar^2}{4} \left[\delta_{nm'} (|m\rangle\langle n'| + |n'\rangle\langle m|) + \delta_{nn'} (|m\rangle\langle m'| + |m'\rangle\langle m|) \right. \\ &\quad \left. + \delta_{mm'} (|n\rangle\langle n'| + |n'\rangle\langle n|) + \delta_{mn'} (|n\rangle\langle m'| + |m'\rangle\langle n|) \right] \\ &= \frac{\hbar}{2} \left[\delta_{nm'} \hat{\mathcal{S}}_{\alpha_{n'm}} + \delta_{nn'} (\hat{\mathcal{S}}_{\alpha_{m'm}} + \hat{\mathcal{S}}_{\alpha_{mm'}}) \right. \\ &\quad \left. + \delta_{mm'} (\hat{\mathcal{S}}_{\alpha_{n'n}} + \hat{\mathcal{S}}_{\alpha_{nn'}}) + \delta_{mn'} \hat{\mathcal{S}}_{\alpha_{nm'}} \right. \\ &\quad \left. + \delta_{nn'} \delta_{mm'} \frac{\hbar}{2} (2|m\rangle\langle m| + 2|n\rangle\langle n|) \right]. \end{aligned} \tag{A8}$$

We know that the last line of Eq. A8 only involves diagonal matrices. In fact we have (see proof in Supporting Information)

$$\begin{aligned} &\frac{\hbar^2}{2} (|m\rangle\langle m| + |n\rangle\langle n|) \\ &= \frac{\hbar^2}{N} \hat{\mathcal{I}} + \hbar \left(\sum_{k>n}^N \sqrt{\frac{2}{k(k-1)}} \hat{\mathcal{S}}_{\gamma_k} + \frac{2-n}{\sqrt{2n(n-1)}} \hat{\mathcal{S}}_{\gamma_n} \right. \\ &\quad \left. + \sum_{k>m}^{n-1} \frac{1}{\sqrt{2k(k-1)}} \hat{\mathcal{S}}_{\gamma_k} - \sqrt{\frac{m-1}{2m}} \hat{\mathcal{S}}_{\gamma_m} \right). \end{aligned} \tag{A9}$$

Thus, we can extract all the non-zero $d_{\alpha_{nm}\alpha_{n'm'}k}$.

Between a symmetric and an anti-symmetric generator, the anti-commutation relation reads

$$\begin{aligned} \{\hat{\mathcal{S}}_{\alpha_{nm}}, \hat{\mathcal{S}}_{\beta_{n'm'}}\} &= \hbar \sum_{k=1}^{N^2-1} d_{\alpha_{nm}\beta_{n'm'}k} \hat{\mathcal{S}}_k \\ &= i \frac{\hbar^2}{4} \left[\delta_{nm'} (|n'\rangle\langle m| - |m\rangle\langle n'|) + \delta_{nn'} (|m\rangle\langle m'| - |m'\rangle\langle m|) \right. \\ &\quad \left. + \delta_{mm'} (|n'\rangle\langle n| - |n\rangle\langle n'|) + \delta_{mn'} (|n\rangle\langle m'| - |m'\rangle\langle n|) \right] \\ &= \frac{\hbar}{2} \left[\delta_{nm'} \hat{\mathcal{S}}_{\beta_{n'm}} + \delta_{nn'} (\hat{\mathcal{S}}_{\beta_{m'm}} - \hat{\mathcal{S}}_{\beta_{m'm}}) \right. \\ &\quad \left. + \delta_{mm'} (\hat{\mathcal{S}}_{\beta_{n'n}} - \hat{\mathcal{S}}_{\beta_{nn'}}) + \delta_{mn'} \hat{\mathcal{S}}_{\beta_{nm'}} \right], \end{aligned} \tag{A10}$$

from which one can extract $d_{\alpha_{nm}\beta_{n'm'}k}$. Note that based on Eq. A10, there is no diagonal component $\hat{\mathcal{S}}_\gamma$, thus all $d_{\alpha\beta\gamma} = 0$. Computing the anti-commutator between symmetric and diagonal generators is not necessary as we

already obtained the structure constants involving those generators by permutation, because $d_{\alpha\gamma\gamma'}$ will be same as $d_{\gamma\gamma'\alpha}$, $d_{\alpha\gamma\alpha'}$ will be same as $d_{\alpha\alpha'\gamma}$, and $d_{\alpha\gamma\beta}$ will be same as $d_{\alpha\beta\gamma}$.

Computing the anti-commutators between two anti-symmetric generators gives

$$\begin{aligned} \{\hat{\mathcal{S}}_{\beta_{nm}}, \hat{\mathcal{S}}_{\beta_{n'm'}}\} &= \frac{\hbar^2}{N} \delta_{\beta_{nm}\beta_{n'm'}} \hat{\mathcal{I}} + \hbar \sum_{k=1}^{N^2-1} d_{\beta_{nm}\beta_{n'm'}k} \hat{\mathcal{S}}_k \\ &= \frac{\hbar^2}{4} \left[\delta_{nn'}(|m\rangle\langle m'| + |m'\rangle\langle m|) - \delta_{nm'}(|m\rangle\langle n'| + |n'\rangle\langle m|) \right. \\ &\quad \left. + \delta_{mm'}(|n\rangle\langle n'| + |n'\rangle\langle n|) - \delta_{mn'}(|n\rangle\langle m'| + |m'\rangle\langle n|) \right] \\ &= \frac{\hbar}{2} \left[\delta_{nn'}(\hat{\mathcal{S}}_{\alpha_{m'm}} + \hat{\mathcal{S}}_{\alpha_{m'm'}}) - \delta_{nm'}\hat{\mathcal{S}}_{\alpha_{n'm}} \right. \\ &\quad \left. + \delta_{mm'}(\hat{\mathcal{S}}_{\alpha_{n'n}} + \hat{\mathcal{S}}_{\alpha_{n'n'}}) - \delta_{mn'}\hat{\mathcal{S}}_{\alpha_{nm'}} \right. \\ &\quad \left. + \delta_{nn'}\delta_{mm'} \frac{\hbar}{2}(2|m\rangle\langle m| + 2|n\rangle\langle n|) \right], \end{aligned} \quad (\text{A11})$$

where we recognize that the last line of Eq. A11 is identical to the last line of Eq. A8, which can be expressed as generators in Eq. A9. We do not need to compute the anti-commutator between an asymmetric and a diagonal generator as we already have the result by permutation from Eq. A11 (and Eqs. A10 indicates $d_{\alpha\beta\gamma} = 0$).

The remaining d_{ijk} values are obtained through the anti-commutator between two diagonal generators

$$\begin{aligned} \{\hat{\mathcal{S}}_{\gamma_n}, \hat{\mathcal{S}}_{\gamma_{n'}}\} &= \frac{\hbar^2}{N} \delta_{\gamma_n\gamma_{n'}} \hat{\mathcal{I}} + \hbar \sum_{k=1}^{N^2-1} d_{\gamma_n\gamma_{n'}k} \hat{\mathcal{S}}_k \\ &= \frac{\hbar^2}{\sqrt{2n(n-1)2n'(n'-1)}} \left[\sum_{k=1}^{n-1} \sum_{k'=1}^{n'-1} \delta_{kk'}(|k\rangle\langle k'| + |k'\rangle\langle k|) \right. \\ &\quad \left. + \delta_{kn'}(1-n')(|k\rangle\langle n'| + |n'\rangle\langle k|) \right. \\ &\quad \left. + \delta_{nk'}(1-n)(|n\rangle\langle k'| + |k'\rangle\langle n|) \right. \\ &\quad \left. + \delta_{nn'}(1-n)(1-n')(|n\rangle\langle n'| + |n'\rangle\langle n|) \right] \\ &= \frac{\hbar}{\sqrt{2n(n-1)}} 2\delta_{kn'} \hat{\mathcal{S}}_{\gamma_{n'}} + \frac{\hbar}{\sqrt{2n'(n'-1)}} 2\delta_{nk'} \hat{\mathcal{S}}_{\gamma_n} \\ &\quad + \delta_{nn'} \frac{\hbar^2}{n(n-1)} \left(\sum_{k=1}^{n-1} |k\rangle\langle k| + (1-n)^2 |n\rangle\langle n| \right). \end{aligned} \quad (\text{A12})$$

One can see that only diagonal matrices are involved in the last line of Eq. A12 and there is no off-diagonal element. We show in Supporting Information that

$$\begin{aligned} \frac{\hbar^2}{n(n-1)} \left(\sum_{k=1}^{n-1} |k\rangle\langle k| + (1-n)^2 |n\rangle\langle n| \right) \\ = \frac{\hbar^2}{N} \hat{\mathcal{I}} + \hbar \left(\sum_{k>n}^N \sqrt{\frac{2}{k(k-1)}} \hat{\mathcal{S}}_{\gamma_k} + (2-n) \sqrt{\frac{2}{n(n-1)}} \hat{\mathcal{S}}_{\gamma_n} \right) \end{aligned} \quad (\text{A13})$$

which helps to determine all $d_{\gamma_n\gamma_{n'}k}$.

We summarize all the non-zero totally symmetric structure constants as follows

$$\begin{aligned}
d_{\alpha_{nm}\alpha_{kn}\alpha_{km}} &= d_{\alpha_{nm}\beta_{kn}\beta_{km}} = d_{\alpha_{nm}\beta_{mk}\beta_{nk}} = \frac{1}{2}, \quad (\text{A14}) \\
d_{\alpha_{nm}\beta_{nk}\beta_{km}} &= -\frac{1}{2}, \\
d_{\alpha_{nm}\alpha_{nm}\gamma_m} &= d_{\beta_{nm}\beta_{nm}\gamma_m} = -\sqrt{\frac{m-1}{2m}}, \\
d_{\alpha_{nm}\alpha_{nm}\gamma_k} &= d_{\beta_{nm}\beta_{nm}\gamma_k} = \sqrt{\frac{1}{2k(k-1)}}, \quad m < k < n, \\
d_{\alpha_{nm}\alpha_{nm}\gamma_n} &= d_{\beta_{nm}\beta_{nm}\gamma_n} = \frac{2-n}{\sqrt{2n(n-1)}}, \\
d_{\alpha_{nm}\gamma_{nm}\gamma_k} &= d_{\beta_{nm}\beta_{nm}\gamma_k} = \sqrt{\frac{2}{k(k-1)}}, \quad n < k, \\
d_{\gamma_n\gamma_k\gamma_k} &= \sqrt{\frac{2}{n(n-1)}}, \quad k < n, \\
d_{\gamma_n\gamma_n\gamma_n} &= (2-n)\sqrt{\frac{2}{n(n-1)}}.
\end{aligned}$$

Similarly to the totally anti-symmetric structure constants, the analytical expression of totally symmetric structure constants can be obtained in any basis of generators of $\mathfrak{su}(N)$ by mean of the transformation presented in Eq. A7.

Appendix B: Coherent state basis and expectation value of the spin operator

The expansion coefficients of the coherent state basis in the N -level diabatic basis are^{29,32}

$$\langle n|\Omega \rangle_N = \begin{cases} \langle n|\Omega \rangle_{N-1}, & 1 \leq n < N-1, \\ \langle N-1|\Omega \rangle_{N-1} e^{-i\frac{\varphi_{N-1}}{2}} \cos \frac{\theta_{N-1}}{2}, & n = N-1, \\ \langle N-1|\Omega \rangle_{N-1} e^{i\frac{\varphi_{N-1}}{2}} \sin \frac{\theta_{N-1}}{2}, & n = N, \end{cases} \quad (\text{B1})$$

where $\langle 1|\Omega \rangle_1 = 1$, and for $N > 1$ the spin coherent states are defined recursively. This is equivalent to the expression in Eq. 17.

Using the definition of the spin coherent states presented here (or defined in Eq. 17), and the definition of the generators of $\mathfrak{su}(N)$ in Eqs. 2-4, we can derive a general expression of the expectation value of the spin operators. The expression of the expectation value of the

symmetric spin operator is

$$\begin{aligned}
\hbar\Omega_{\alpha_{nm}} &\equiv \langle \Omega | \hat{\mathcal{S}}_{\alpha_{nm}} | \Omega \rangle \\
&= \frac{\hbar}{2} \left(\cos \frac{\theta_m}{2} \prod_{j=1}^{m-1} e^{-i\varphi_j} \sin \frac{\theta_j}{2} \cos \frac{(1-\delta_{nN})\theta_n}{2} \prod_{k=1}^{n-1} e^{i\varphi_k} \right. \\
&\quad \times \sin \frac{\theta_k}{2} + \cos \frac{\theta_m}{2} \prod_{j=1}^{m-1} e^{i\varphi_j} \sin \frac{\theta_j}{2} \cos \frac{(1-\delta_{nN})\theta_n}{2} \\
&\quad \times \left. \prod_{k=1}^{n-1} e^{-i\varphi_k} \sin \frac{\theta_k}{2} \right) \\
&= \hbar \prod_{j=1}^{m-1} \sin^2 \frac{\theta_j}{2} \cos \frac{\theta_m}{2} \prod_{k=m}^{n-1} \sin \frac{\theta_k}{2} \cos \frac{(1-\delta_{nN})\theta_n}{2} \\
&\quad \times \cos \left(\sum_{l=m}^{n-1} \varphi_l \right), \tag{B2}
\end{aligned}$$

where $1 \leq m < n \leq N$. When $m = 1$, $\prod_{j=1}^{m-1} \sin^2 \frac{\theta_j}{2}$ is replaced by 1.

Similarly, for the anti-symmetric spin operator, we have

$$\begin{aligned}
\hbar\Omega_{\beta_{nm}} &\equiv \langle \Omega | \hat{\mathcal{S}}_{\beta_{nm}} | \Omega \rangle \\
&= \hbar \prod_{j=1}^{m-1} \sin^2 \frac{\theta_j}{2} \cos \frac{\theta_m}{2} \prod_{k=m}^{n-1} \sin \frac{\theta_k}{2} \cos \frac{(1-\delta_{nN})\theta_n}{2} \\
&\quad \times \sin \left(\sum_{l=m}^{n-1} \varphi_l \right), \tag{B3}
\end{aligned}$$

and the term $\prod_{j=1}^{m-1} \sin^2 \frac{\theta_j}{2}$ is replaced by 1 when $m = 1$.

For the diagonal spin operator there is only one index $1 < n \leq N$ and the expression is

$$\begin{aligned}
\hbar\Omega_{\gamma_n} &\equiv \langle \Omega | \hat{\mathcal{S}}_{\gamma_n} | \Omega \rangle \\
&= \frac{\hbar}{\sqrt{2n(n-1)}} \left(\sum_{j=1}^{n-1} \cos^2 \frac{\theta_j}{2} \prod_{k=1}^{j-1} \sin^2 \frac{\theta_k}{2} \right. \\
&\quad \left. + (1-n) \cos^2 \frac{(1-\delta_{nN})\theta_n}{2} \prod_{j=1}^{n-1} \sin^2 \frac{\theta_j}{2} \right), \tag{B4}
\end{aligned}$$

where $\prod_{k=1}^{j-1} \sin^2 \frac{\theta_k}{2}$ is replaced by 1 when $n = 2$ (or $j = 1$).

Appendix C: Differential Phase-Space Volume Element of $\mathfrak{su}(N)$

The volume element defined in Eq. 19, which is expressed as

$$d\Omega = \frac{N!}{(2\pi)^{N-1}} \prod_{n=1}^{N-1} \cos \frac{\theta_n}{2} \left(\sin \frac{\theta_n}{2} \right)^{2(N-n)-1} d\theta_n d\varphi_n. \tag{C1}$$

These derivations, eqs (B2) and (B3), are incompatible with the coherent states eq (17):

$$\langle n | \Omega \rangle = \begin{cases} \cos \frac{\theta_1}{2} e^{-i\frac{\varphi_1}{2}} & n = 1, \\ \cos \frac{\theta_n}{2} e^{-i\frac{\varphi_n}{2}} \prod_{l=1}^{n-1} \sin \frac{\theta_l}{2} e^{i\frac{\varphi_l}{2}} & 1 < n < N, \\ \prod_{l=1}^{N-1} \sin \frac{\theta_l}{2} e^{i\frac{\varphi_l}{2}} & n = N. \end{cases} \tag{17}$$

It is easy to verify that to derive eqs (B2) and (B3), the correct coherent states are shown directly below, not eq (17)!

Correct coherent states should be:

$$\langle n | \Omega \rangle = \begin{cases} \cos \frac{\theta_1}{2} & n = 1, \\ \cos \frac{\theta_n}{2} \prod_{l=1}^{n-1} \sin \frac{\theta_l}{2} e^{i\varphi_l} & 1 < n < N, \\ \prod_{l=1}^{N-1} \sin \frac{\theta_l}{2} e^{i\varphi_l} & n = N. \end{cases}$$

is different than the expression defined in Ref. 29. Here, we justify our choice.

The differential phase-space volume element must respect the normalization condition

$$\int d\Omega = N. \quad (C2)$$

To compute the integral over a given θ_n we express it as

$$\begin{aligned} & \int_0^\pi \cos \frac{\theta_n}{2} \left(\sin \frac{\theta_n}{2} \right)^{2(N-n)-1} d\theta_n \\ &= 2 \int_0^{\frac{\pi}{2}} \cos \theta'_n \left(\sin \theta'_n \right)^{2(N-n)-1} d\theta'_n, \quad \theta'_n = \frac{\theta_n}{2} \\ &= 2 \int_0^1 y_n (1 - y_n^2)^{N-n-1} dy_n, \quad y_n = \cos \theta'_n \\ &= \int_0^1 (1 - t_n)^{N-n-1} dt_n, \quad t_n = y_n^2. \end{aligned} \quad (C3)$$

We recognize the expression of the beta function, $B(x, y) = \int_0^1 t^{x-1} (1-t)^{y-1} dt = \frac{\Gamma(x)\Gamma(y)}{\Gamma(x+y)}$, with $\Gamma(x)$ as the gamma function, and when x is a positive integer, $\Gamma(x) = (x-1)!$. We identify x and y leading to

$$\begin{aligned} & \int_0^\pi \cos \frac{\theta_n}{2} \left(\sin \frac{\theta_n}{2} \right)^{2(N-n)-1} d\theta_n = B(1, N-n) \\ &= \frac{1}{N-n}. \end{aligned} \quad (C4)$$

Considering the product over all the angles we have

$$\prod_{n=1}^{N-1} \int_0^\pi \cos \frac{\theta_n}{2} \left(\sin \frac{\theta_n}{2} \right)^{2(N-n)-1} d\theta_n = \frac{1}{(N-1)!}, \quad (C5)$$

hence

$$\int d\Omega = \frac{N!}{(2\pi)^{N-1}} \frac{1}{(N-1)!} (2\pi)^{N-1} = N. \quad (C6)$$

By definition we should also have

$$\int |\Omega\rangle\langle\Omega| d\Omega = \hat{I}, \quad (C7)$$

and we provide a concise proof below. The starting point is to prove that

$$\int \langle n|\Omega\rangle\langle\Omega|m\rangle d\Omega = \int c_n c_m^* d\Omega = \delta_{nm}. \quad (C8)$$

where $\langle n|\Omega\rangle$ is expressed in Eq. 16. For all the non-diagonal elements in Eq. C8, c_n and c_m^* include at least one angle φ_l (see Eq. 17), such that

$$\int_0^{2\pi} e^{\pm i\varphi_l} d\varphi_l = 0, \quad (C9)$$

hence $\int c_n c_m^* d\Omega = 0$ for $n \neq m$.

Next, we consider the diagonal components of the integral, and separate them in three cases, $\int c_1 c_1^* d\Omega$, $\int c_n c_n^* d\Omega$ with $1 < n < N$, and $\int c_N c_N^* d\Omega$, due to the separate expressions of c_n in Eq. 17. For the θ_1 integral of the $\int c_1 c_1^* d\Omega$, we have

$$\begin{aligned} \int_0^\pi \left(\cos \frac{\theta_1}{2} \right)^3 \left(\sin \frac{\theta_1}{2} \right)^{2N-3} d\theta_1 &= B(2, N-1) \\ &= \frac{1}{N(N-1)}, \quad (\text{C10}) \end{aligned}$$

whereas for the integral related to θ_n , $n > 1$ we have

$$\prod_{n=2}^{N-1} \int_0^\pi K(\theta_n) d\theta_n = \frac{1}{(N-2)!}. \quad (\text{C11})$$

Combining these results, we have

$$\frac{N!}{(2\pi)^{N-1}} \frac{1}{N(N-1)} \prod_{n=2}^{N-1} \int_0^\pi K(\theta_n) d\theta_n \int_0^{2\pi} d\varphi_n = 1. \quad (\text{C12})$$

For the $\int c_N c_N^* d\Omega$ integral, each angle is integrated as

$$\begin{aligned} \int_0^\pi \cos \frac{\theta_l}{2} \left(\sin \frac{\theta_l}{2} \right)^{2(N-l)+1} d\theta_l &= B(1, N-l+1) \\ &= \frac{1}{N-l+1}, \quad (\text{C13}) \end{aligned}$$

leading to

$$\prod_{l=1}^{N-1} \int_0^\pi \cos \frac{\theta_l}{2} \left(\sin \frac{\theta_l}{2} \right)^{2(N-l)+1} d\theta_l = \frac{1}{N!}. \quad (\text{C14})$$

Finally for the remaining components $\int c_n c_n^* d\Omega$, with $1 < n < N$, the θ_n dependent integral is

$$\int \cos^2 \frac{\theta_n}{2} \prod_{l=1}^{n-1} \sin^2 \frac{\theta_l}{2} d\Omega. \quad (\text{C15})$$

For the angles with indices l lower than n , the integral along θ_l is evaluated as

$$\int_0^\pi \cos \frac{\theta_l}{2} \left(\sin \frac{\theta_l}{2} \right)^{2(N-l)+1} d\theta_l = \frac{1}{N-l+1}, \quad (\text{C16})$$

which is equivalent to Eq. C13, while for indices l higher than n , the integral with θ_l is evaluate as

$$\int_0^\pi \cos \frac{\theta_l}{2} \left(\sin \frac{\theta_l}{2} \right)^{2(N-l)-1} d\theta_l = \frac{1}{N-l}, \quad (\text{C17})$$

equivalent to Eq. C4. For the index $l = n$, the integral related to θ_l is

$$\begin{aligned} \int_0^\pi \left(\cos \frac{\theta_n}{2} \right)^3 \left(\sin \frac{\theta_n}{2} \right)^{2(N-n)-1} d\theta_n &= B(2, N-n) \\ &= \frac{1}{(N-n+1)(N-n)}, \quad (\text{C18}) \end{aligned}$$

which leads for any $|n\rangle\langle n|$ component to be

$$\int \cos^2 \frac{\theta_n}{2} \prod_{l=1}^{n-1} \sin^2 \frac{\theta_l}{2} d\Omega = \frac{1}{N!}. \quad (\text{C19})$$

Combining all of the above results, we have

$$\frac{N!}{(2\pi)^{N-1}} \prod_{n=1}^{N-1} \int_0^\pi K(\theta_n) d\theta_n \int_0^{2\pi} d\varphi_n \langle l|\Omega\rangle\langle\Omega|l\rangle = 1, \quad (\text{C20})$$

for $1 \leq l \leq N$. Combining with the result in Eq. C9, we have

$$\frac{N!}{(2\pi)^{N-1}} \prod_{n=1}^{N-1} \int_0^\pi K(\theta_n) d\theta_n \int_0^{2\pi} d\varphi_n |\Omega\rangle\langle\Omega| = \hat{\mathcal{I}}. \quad (\text{C21})$$

Using those derivations, it is trivial to demonstrate the identity of the Stratonovich-Weyl kernel $\int \hat{w}_s d\Omega = \hat{\mathcal{I}}$. Starting from

$$\begin{aligned} \int d\Omega \Omega_i &= \int d\Omega \langle \Omega | \hat{S}_i | \Omega \rangle = \text{Tr}_e \left[\hat{S}_i \int d\Omega | \Omega \rangle \langle \Omega | \right] \\ &= \text{Tr}_e [\hat{S}_i \hat{\mathcal{I}}] = 0, \end{aligned} \quad (\text{C22})$$

we have

$$\begin{aligned} \int \hat{w}_s d\Omega &= \int \left(\frac{1}{N} \hat{\mathcal{I}} + r_s \frac{2}{\hbar} \sum_i^{N^2-1} \Omega_i \hat{S}_i \right) d\Omega \\ &= \int d\Omega \frac{1}{N} \hat{\mathcal{I}} = \hat{\mathcal{I}}. \end{aligned} \quad (\text{C23})$$

Fig. 6 presents a system with $N = 5$ electronic states on the four Bloch spheres (for the $s = W$ case), and the distribution of θ_i with the solid curves. As a comparison, the distribution used in Ref. 29 is shown with dashed curves. For a general N states system, we can see that the last Bloch sphere (here $n = 4$ in Fig. 6) always contains only the last two electronic states, hence requiring a distribution of the last angle, θ_{N-1} , to be symmetric around $\frac{\pi}{2}$ (for any choice of s index). On the contrary, the first Bloch sphere ($n = 1$ in Fig. 6) always puts the first electronic state on the north hemisphere, and all the other electronic states on the south hemisphere, requiring a distribution centered on the south hemisphere. As the index of the Bloch sphere increases (here, for example, $n = 2$ and $n = 3$ in Fig. 6), less states are present on the south hemisphere, and the distribution slowly shifts toward the center. This means that the previously used distribution^{29,40} (dashed curves in Fig. 6) could potentially have an inconsistent labeling of the angles (the θ_1 distribution belongs to θ_{N-1} and inversely), as well as an inconsistent distributions for $1 < \theta_n < N - 1$ which does not have the right peak on the hemisphere of the Bloch spheres. This demonstrates that the differential phase-space volume element in Eq. 19 is the proper one to consider for the spin coherent state representation of $\mathfrak{su}(N)$, as opposed to the one presented in Ref. 29, which gives incorrect distribution of the θ_n variables.

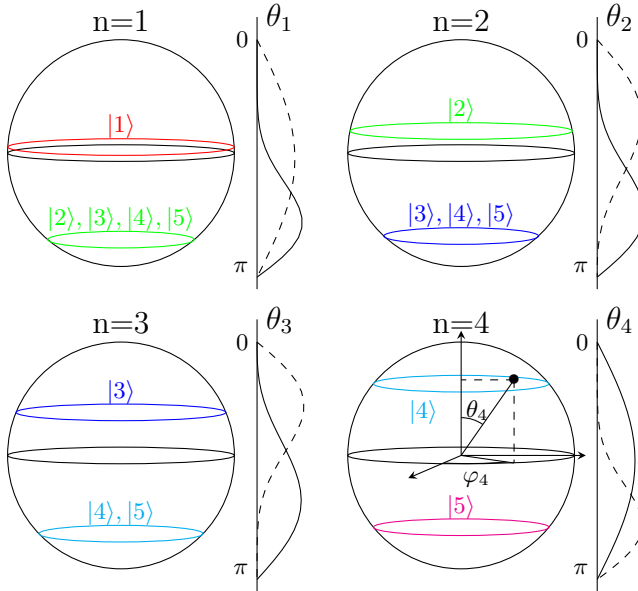


FIG. 6. Schematic representation of the Bloch spheres for a $N = 5$ system (with $s = \bar{s} = W$). On the $n = 4$ sphere are represented θ_4 and φ_4 . On the right of each sphere, the θ_n distribution is sketched from the differential phase space volume element in Eq. 19 (solid lines), and the distribution from the volume element previously derived in the literature^{29,39,40} (dashed lines).

Appendix D: Derivation of the conjugate relationship between φ and θ

We begin with the proposed conjugate relation

$$r_{\bar{s}} \sum_{j=1}^N C_n(j) \frac{d}{dt} \Omega_{\gamma_j} = -\frac{\partial H_{\bar{s}}}{\partial \varphi_n} \quad (\text{D1a})$$

$$r_{\bar{s}} \frac{d}{dt} \varphi_n = \frac{\partial H_{\bar{s}}}{\partial \sum_{j=1}^N C_n(j) \Omega_{\gamma_j}}, \quad (\text{D1b})$$

and compute $-\frac{\partial H_{\bar{s}}}{\partial \varphi_n}$ (using Eq. B2 and Eq. B3) as follows

$$-\frac{\partial H_{\bar{s}}}{\partial \varphi_n} = r_{\bar{s}} \sum_{j=n+1}^N \sum_{k=1}^n (\mathcal{H}_{\alpha_{jk}} \Omega_{\beta_{jk}} - \mathcal{H}_{\beta_{jk}} \Omega_{\alpha_{jk}}), \quad (\text{D2})$$

and compare it to $r_{\bar{s}} \sum_{j=1}^N C_n(j) \frac{d}{dt} \Omega_{\gamma_j}$ (using Eq. 92) to determine the coefficients $C_n(j)$. We derived in Appendix A the closed formulas for the structure constants of $\mathfrak{su}(N)$ and hence can explicitly express the derivatives

of Eq. 92 as

$$\begin{aligned} \frac{d}{dt}\Omega_{\gamma_j} = & \frac{1}{\hbar} \left[\sqrt{\frac{j}{2(j-1)}} \sum_{k=1}^j (\mathcal{H}_{\alpha_{jk}}\Omega_{\beta_{jk}} - \mathcal{H}_{\beta_{jk}}\Omega_{\alpha_{jk}}) \right. \\ & - \sqrt{\frac{j-1}{2j}} \sum_{k=j+1}^N (\mathcal{H}_{\alpha_{kj}}\Omega_{\beta_{kj}} - \mathcal{H}_{\beta_{kj}}\Omega_{\alpha_{kj}}) \\ & \left. + \sqrt{\frac{1}{2j(j-1)}} \sum_{k=j+1}^N \sum_{l=1}^{j-1} (\mathcal{H}_{\alpha_{kl}}\Omega_{\beta_{kl}} - \mathcal{H}_{\beta_{kl}}\Omega_{\alpha_{kl}}) \right]. \end{aligned} \quad (D3)$$

Starting from φ_n , $n = 1$, and solving iteratively Eq. D1a for every element $\mathcal{H}_{\alpha_{kl}}\Omega_{\beta_{kl}} - \mathcal{H}_{\beta_{kl}}\Omega_{\alpha_{kl}}$ (from $k = 2$, $l = 1$ and ascending) until deducing the expression of the coefficients $C_1(j)$, then using the same approach for $n > 1$, we obtain a formula that can be generalized, hence an expression for any coefficient

$$C_n(j \leq n) = 0; \quad C_n(j > n) = n \sqrt{\frac{2}{j(j-1)}}. \quad (D4)$$

Further, the analytical expression of the time derivative of the symmetric generators is (we write $n+1 \equiv k$ for convenience)

$$\begin{aligned} \frac{d}{dt}\Omega_{\alpha_{k,n}} = & \frac{1}{\hbar} \left[\sqrt{\frac{n-1}{2n}} (\mathcal{H}_{\gamma_n}\Omega_{\beta_{kn}} - \mathcal{H}_{\beta_{kn}}\Omega_{\gamma_n}) \right. \\ & - \sqrt{\frac{n+1}{2n}} (\mathcal{H}_{\gamma_k}\Omega_{\beta_{kn}} - \mathcal{H}_{\beta_{kn}}\Omega_{\gamma_k}) \\ & + \frac{1}{2} \sum_{j=1}^{n-1} (\mathcal{H}_{\beta_{nj}}\Omega_{\alpha_{kj}} - \mathcal{H}_{\alpha_{kj}}\Omega_{\beta_{nj}} - \mathcal{H}_{\alpha_{nj}}\Omega_{\beta_{kj}} + \mathcal{H}_{\beta_{kj}}\Omega_{\alpha_{nj}}) \\ & \left. + \frac{1}{2} \sum_{l=n+2}^N (\mathcal{H}_{\alpha_{ln}}\Omega_{\beta_{lk}} - \mathcal{H}_{\beta_{lk}}\Omega_{\alpha_{ln}} - \mathcal{H}_{\beta_{ln}}\Omega_{\alpha_{lk}} + \mathcal{H}_{\alpha_{lk}}\Omega_{\beta_{ln}}) \right]. \end{aligned} \quad (D5)$$

and the time derivative of anti-symmetric generators are

$$\begin{aligned} \frac{d}{dt}\Omega_{\beta_{kn}} = & \frac{1}{\hbar} \left[\sqrt{\frac{n+1}{2n}} (\mathcal{H}_{\gamma_k}\Omega_{\alpha_{kn}} - \mathcal{H}_{\alpha_{kn}}\Omega_{\gamma_k}) \right. \\ & - \sqrt{\frac{n-1}{2n}} (\mathcal{H}_{\gamma_n}\Omega_{\alpha_{kn}} - \mathcal{H}_{\alpha_{kn}}\Omega_{\gamma_n}) \\ & + \frac{1}{2} \sum_{j=1}^{n-1} (\mathcal{H}_{\alpha_{nj}}\Omega_{\alpha_{kj}} - \mathcal{H}_{\alpha_{kj}}\Omega_{\alpha_{nj}} + \mathcal{H}_{\beta_{nj}}\Omega_{\beta_{kj}} - \mathcal{H}_{\beta_{kj}}\Omega_{\beta_{nj}}) \\ & \left. + \frac{1}{2} \sum_{l=n+2}^N (\mathcal{H}_{\alpha_{ln}}\Omega_{\alpha_{lk}} - \mathcal{H}_{\alpha_{lk}}\Omega_{\alpha_{ln}} + \mathcal{H}_{\beta_{ln}}\Omega_{\beta_{lk}} - \mathcal{H}_{\beta_{lk}}\Omega_{\beta_{ln}}) \right], \end{aligned} \quad (D6)$$

where the elements of the sum are null when the conditions cannot be satisfied.

Appendix E: Mapping of Two-Level Systems under the $\mathfrak{su}(2)$ representation

For a two-level system $\hat{H} = \frac{\hat{P}^2}{2M}\hat{\mathcal{I}} + U_0(\hat{R})\hat{\mathcal{I}} + \hat{V}_e(\hat{R})$ where $\hat{\mathcal{I}}$ is the 2×2 identity matrix, and

$$\hat{V}_e(\hat{R}) = \begin{pmatrix} V_{11}(\hat{R}) & V_{12}(\hat{R}) \\ V_{21}(\hat{R}) & V_{22}(\hat{R}) \end{pmatrix}. \quad (\text{E1})$$

For this special case, $f_{ijk} = \varepsilon_{ijk}$ and $d_{ijk} = 0$, all of the equations in the main text remain general. Nevertheless, it will be beneficial to explicitly give several key equations under this special limit, whereas more detailed discussion of the $\mathfrak{su}(2)$ can be found in the previous work of Spin-LSC²⁴ and spin-mapping non-adiabatic RPMD (SM-NRPMD).³⁸

Using the $\mathfrak{su}(2)$ representation, one can express the original two-states Hamiltonian as follows

$$\hat{H} = \mathcal{H}_0\hat{\mathcal{I}} + \frac{1}{\hbar}\mathbf{H}\cdot\hat{\mathbf{S}} = H_0\hat{\mathcal{I}} + \frac{1}{\hbar}(\mathcal{H}_x\cdot\hat{\mathcal{S}}_x + \mathcal{H}_y\cdot\hat{\mathcal{S}}_y + \mathcal{H}_z\cdot\hat{\mathcal{S}}_z), \quad (\text{E2})$$

where $\hat{S}_i = \frac{\hbar}{2}\hat{\sigma}_i$ (for $i \in \{x, y, z\}$) is the quantum spin operator, with $\hat{\sigma}_i$ as the Pauli matrices expressed in Eq. 2, and $\mathcal{H}_0 = \frac{\hat{P}^2}{2m} + U_0(\hat{R}) + \frac{1}{2}(V_{11}(\hat{R}) + V_{22}(\hat{R}))$, $\mathcal{H}_x = 2\text{Re}(V_{12}(\hat{R}))$, $\mathcal{H}_y = 2\text{Im}(V_{12}(\hat{R}))$, $\mathcal{H}_z = V_{11}(\hat{R}) - V_{22}(\hat{R})$, which are the $N = 2$ limit of Eq. 11.

Using the spin coherent state for $N = 2$ (Eq. 15), the expectation value of the spin operator is

$$\hbar\Omega_i(\mathbf{u}) = \langle \mathbf{u} | \hat{S}_i | \mathbf{u} \rangle = \frac{\hbar}{2}u_i, \quad i \in \{x, y, z\}, \quad (\text{E3})$$

where $u_x = \sin\theta\cos\varphi$, $u_y = \sin\theta\sin\varphi$, $u_z = \cos\theta$ as the special case of Eqs. B2-B4. The identity in Eq. 18 becomes $\hat{\mathcal{I}} = \int d\mathbf{u}|\mathbf{u}\rangle\langle\mathbf{u}|$, where $\int d\mathbf{u} = \frac{1}{2\pi}\int_0^\pi d\theta \sin\theta \int_0^{2\pi} d\varphi$ is the $N = 2$ limit of Eq. 19.

Under the $\mathfrak{su}(2)$ Lie Algebra, the Stratonovich-Weyl kernel in Eq. 24 becomes

$$\hat{w}_s = \frac{1}{2}\hat{\mathcal{I}} + r_s\boldsymbol{\Omega}\cdot\hat{\boldsymbol{\sigma}}, \quad (\text{E4})$$

where $\boldsymbol{\Omega}\cdot\hat{\boldsymbol{\sigma}} = \Omega_x\cdot\hat{\sigma}_x + \Omega_y\cdot\hat{\sigma}_y + \Omega_z\cdot\hat{\sigma}_z$. Note that the r_s used in this paper is twice the one defined in the previous work,^{24,38} (see the factor between $\boldsymbol{\Omega}$ and \mathbf{u} in Eq. E3).

The Stratonovich-Weyl transform of the Hamiltonian becomes

$$\begin{aligned} [\hat{H}]_s(\boldsymbol{\Omega}) &= \mathcal{H}_0 + r_s\mathcal{H}\cdot\boldsymbol{\Omega} \\ &= \frac{P^2}{2m} + U_0 + \left(\frac{1}{2} + \frac{r_s}{2}\cos\theta\right)\cdot V_{11}(\hat{R}) \\ &\quad + \left(\frac{1}{2} - \frac{r_s}{2}\cos\theta\right)\cdot V_{22}(\hat{R}) + r_s\sin\theta\cos\varphi\cdot\text{Re}[V_{12}(\hat{R}) \\ &\quad + ir_s\sin\theta\sin\varphi\cdot\text{Im}[V_{12}(\hat{R})], \end{aligned} \quad (\text{E5})$$

and the projection operators are transformed as

$$\begin{aligned} [|1\rangle\langle 1|]_s &= [\frac{1}{2}\hat{\mathcal{I}} + \frac{1}{\hbar}\hat{S}_z]_s = \frac{1}{2} + \frac{r_s}{2}\cos\theta, \\ [|2\rangle\langle 2|]_s &= [\frac{1}{2}\hat{\mathcal{I}} - \frac{1}{\hbar}\hat{S}_z]_s = \frac{1}{2} - \frac{r_s}{2}\cos\theta, \\ [|1\rangle\langle 2| + |2\rangle\langle 1|]_s &= 2[\frac{1}{\hbar}\hat{S}_x]_s = r_s\sin\theta\cos\varphi, \\ [|1\rangle\langle 2| - |2\rangle\langle 1|]_s &= 2i[\frac{1}{\hbar}\hat{S}_y]_s = ir_s\sin\theta\sin\varphi. \end{aligned}$$

The derivation procedure of the TCF and exact Liouvillian are same as outlined in the main text. The electronic EOM under the linearization approximation is

$$\frac{d}{dt}\Omega_i = \frac{1}{\hbar}\sum_{j,k=1}^3\varepsilon_{ijk}H_j(R)\Omega_k, \quad (\text{E7})$$

which is the $N = 2$ limit of Eq. 94c. This is commonly written as

$$\frac{d}{dt}\boldsymbol{\Omega} = \frac{1}{\hbar}\mathbf{H}(\hat{R}) \times \boldsymbol{\Omega}. \quad (\text{E8})$$

For a two-level system, Eqs. 100 and 103 reduce back to

$$\dot{\theta} = \frac{1}{\hbar}(-\mathcal{H}_x\sin\varphi + \mathcal{H}_y\cos\varphi), \quad (\text{E9a})$$

$$\dot{\varphi} = \frac{1}{\hbar}\left(\mathcal{H}_z - \mathcal{H}_x\frac{\cos\varphi}{\tan\theta} - \mathcal{H}_y\frac{\sin\varphi}{\tan\theta}\right), \quad (\text{E9b})$$

Appendix F: Parameters of the models

Here we provides all parameters used in the numerical simulations.

TABLE I. Parameters for the spin-boson models presented in Fig. 2, in a.u.

Model	ϵ	ξ	β	ω_c
(a)	1.0	0.1	5.0	2.5
(b)	1.0	0.1	0.25	1.0
(c)	0.0	2.0	1.0	1.0

TABLE II. Parameters for the pyrazine model presented in top panels of Fig. 3, given in eV.

ν/k	E_k	ω_ν	$\kappa_\nu^{(1)}$	$\kappa_\nu^{(2)}$	λ_ν^{12}
1	3.94	0.126	0.037	-0.254	0.0
2	4.84	0.074	-0.105	0.149	0.0
3		0.118	0.0	0.0	0.262

We discretize the Ohmic spectral density with F discrete nuclear modes Ref. 101 as follows

$$\omega_\nu = -\omega_c \ln\left(\frac{\nu - 1/2}{F}\right), \quad (\text{F1a})$$

$$c_\nu = \omega_\nu \sqrt{\frac{\xi\omega_c m_\nu}{F}}. \quad (\text{F1b})$$

TABLE III. Parameters for the benzene radical cation model presented in bottom panels of Fig. 4, given in eV.

ν/k	E_k	ω_ν	$\kappa_\nu^{(1)}$	$\kappa_\nu^{(2)}$	$\kappa_\nu^{(3)}$	λ_ν^{12}	λ_ν^{23}
1	9.75	0.123	-0.042	-0.042	-0.301	0.0	0.0
2	11.84	0.198	-0.246	0.242	0.0	0.0	0.0
3	12.44	0.075	-0.125	0.1	0.0	0.0	0.0
4		0.088	0.0	0.0	0.0	0.164	0.0
5		0.12	0.0	0.0	0.0	0.0	0.154

TABLE IV. Parameters for the three-state Morse potential presented in Fig. 5, in a.u.

i	IA			IB			IC		
	1	2	3	1	2	3	1	2	3
D_{ii}	0.02	0.02	0.003	0.02	0.01	0.003	0.003	0.004	0.003
α_{ii}	0.4	0.65	0.65	0.65	0.4	0.65	0.65	0.6	0.65
R_{ii}	4.0	4.5	6.0	4.5	4.0	4.4	5.0	4.0	6.0
c_{ii}	0.02	0.0	0.02	0.0	0.01	0.02	0.0	0.0	0.006
ij	12	13	23	12	13	23	12	13	23
A_{ij}	0.005	0.005	0.0	0.005	0.005	0.0	0.002	0.0	0.002
α_{ij}	32.0	32.0	0.0	0.005	0.005	0.0	0.002	0.0	0.002
R_{ij}	3.4	4.97	0.0	3.66	3.34	0.0	3.4	0.0	4.8

- ¹J. C. Tully, J. Chem. Phys. **137**, 22A301 (2012).
- ²J. C. Tully and R. K. Preston, J. Chem. Phys. **55**, 562 (1971).
- ³J. C. Tully, J. Chem. Phys. **93**, 1061 (1990).
- ⁴J. E. Subotnik, A. Jain, B. Landry, A. Petit, W. Ouyang, and N. Bellonzi, Annu. Rev. Phys. Chem. **67**, 387 (2016).
- ⁵L. Wang, A. Akimov, and O. V. Prezhdo, J. Phys. Chem. Lett. **7**, 2100 (2016).
- ⁶R. Crespo-Otero and M. Barbatti, Chem. Rev. **118**, 7026 (2018).
- ⁷H.-D. Meyer and W. H. Miller, J. Chem. Phys. **71**, 2156 (1979).
- ⁸G. Stock and M. Thoss, Phys. Rev. Lett. **78**, 578 (1997).
- ⁹H.-D. Meyer and W. H. Miller, J. Chem. Phys. **70**, 3214 (1979).
- ¹⁰M. Thoss and G. Stock, Phys. Rev. A **59**, 64 (1999).
- ¹¹X. Sun and W. H. Miller, J. Chem. Phys. **106**, 916 (1997).
- ¹²E. A. Coronado, J. Xing, and W. H. Miller, Chem. Phys. Lett. **349**, 521 (2001).
- ¹³S. Bonella and D. F. Coker, J. Chem. Phys. **114**, 7778 (2001).
- ¹⁴H. Kim, A. Nassimi, and R. Kapral, J. Chem. Phys. **129**, 084102 (2008).
- ¹⁵P. Huo and D. F. Coker, J. Chem. Phys. **135**, 201101 (2011).
- ¹⁶P. Huo and D. F. Coker, J. Chem. Phys. **137**, 22A535 (2012).
- ¹⁷W. H. Miller and S. J. Cotton, Faraday Discuss. **195**, 9 (2016).
- ¹⁸J. O. Richardson, P. Meyer, M.-O. Pleinert, and M. Thoss, Chem. Phys. **482**, 124 (2017), electrons and nuclei in motion - correlation and dynamics in molecules (on the occasion of the 70th birthday of Lorenz S. Cederbaum).
- ¹⁹J. O. Richardson and M. Thoss, J. Chem. Phys. **139**, 031102 (2013).
- ²⁰N. Ananth and T. F. Miller, J. Chem. Phys. **133**, 234103 (2010).
- ²¹A. Kelly, R. van Zon, J. Schofield, and R. Kapral, J. Chem. Phys. **136**, 084101 (2012).
- ²²M. A. C. Saller, A. Kelly, and J. O. Richardson, J. Chem. Phys. **150**, 071101 (2019).
- ²³S. J. Cotton and W. H. Miller, J. Chem. Phys. **139**, 234112 (2013).
- ²⁴J. E. Runeson and J. O. Richardson, J. Chem. Phys. **151**, 044119 (2019).
- ²⁵F. T. Hioe and J. H. Eberly, Phys. Rev. Lett. **47**, 838 (1981).
- ²⁶C. W. McCurdy, H. D. Meyer, and W. H. Miller, J. Chem. Phys. **70**, 3177 (1979).
- ²⁷H. Meyer and W. H. Miller, J. Chem. Phys. **72**, 2272 (1980).
- ²⁸S. J. Cotton and W. H. Miller, J. Phys. Chem. A **119**, 12138 (2015).
- ²⁹J. E. Runeson and J. O. Richardson, J. Chem. Phys. **152**, 084110 (2020).
- ³⁰R. L. Stratovich, Sov. Phys. JETP **4** (1957).
- ³¹J. M. Radcliffe, J. Phys. A: Gen. Phys. **4**, 313 (1971).
- ³²K. Nemoto, J. Phys. A: Math. Gen. **33**, 3493 (2000).
- ³³F. Halzen and A. Martin, *Quarks and Leptons: An Introductory Course in Modern Particle Physics* (Wiley, 1984).
- ³⁴H. Georgi, *Lie Algebras In Particle Physics: from Isospin To Unified Theories* (CRC Press, 2000).
- ³⁵W. Pfeifer, *The Lie Algebras SU(N): An Introduction* (Springer, 2003).
- ³⁶M. Gell-Mann, Phys. Rev. **125**, 1067 (1962).
- ³⁷R. A. Bertlmann and P. Krammer, J. Phys. A: Math. Theor. **41**, 235303 (2008).
- ³⁸D. Bossion, S. N. Chowdhury, and P. Huo, J. Chem. Phys. **154**, 184106 (2021).
- ³⁹T. Tilma and E. C. G. Sudarshan, J. Phys. A: Math. Gen. **35**, 10467 (2002).
- ⁴⁰T. Tilma and E. Sudarshan, J. Geom. Phys. **52**, 263 (2004).
- ⁴¹C. Brif and A. Mann, J. Phys. A: Math. Gen. **31**, L9 (1998).
- ⁴²C. Brif and A. Mann, Phys. Rev. A **59**, 971 (1999).
- ⁴³T. Tilma and K. Nemoto, J. Phys. A: Math. Theor. **45**, 015302 (2011).
- ⁴⁴F. Bloch, Phys. Rev. **70**, 460 (1946).
- ⁴⁵R. K. Wangsness and F. Bloch, Phys. Rev. **89**, 728 (1953).
- ⁴⁶I. I. Rabi, N. F. Ramsey, and J. Schwinger, Rev. Mod. Phys. **26**, 167 (1954).
- ⁴⁷E. Wigner, Phys. Rev. **40**, 749 (1932).
- ⁴⁸J. E. Moyal, Math. Proc. Camb. Philos. Soc. **45**, 99–124 (1949).
- ⁴⁹M. A. C. Saller, A. Kelly, and J. O. Richardson, Faraday Discuss. **221**, 150 (2020).
- ⁵⁰M. A. C. Saller, J. E. Runeson, and J. O. Richardson, Path-integral approaches to non-adiabatic dynamics, in *Quantum Chemistry and Dynamics of Excited States* (John Wiley & Sons, 2020) Chap. 20, pp. 629–653.
- ⁵¹J. C. Várilly and J. M. Gracia-Bondía, Ann. Phys. **190**, 107 (1989).
- ⁵²H. Lang, O. Vendrell, and P. Hauke, J. Chem. Phys. **155**, 024111 (2021).
- ⁵³A. Heslot, Phys. Rev. D **31**, 1341 (1985).
- ⁵⁴U. Müller and G. Stock, J. Chem. Phys. **111**, 77 (1999).
- ⁵⁵X. He, Z. Gong, B. Wu, and J. Liu, J. Phys. Chem. Lett. **12**, 2496 (2021).
- ⁵⁶X. He, B. Wu, Z. Gong, and J. Liu, J. Phys. Chem. A **125**, 6845 (2021).
- ⁵⁷W.-M. Zhang and D. H. Feng, Phys. Rep. **252**, 1 (1995).
- ⁵⁸H. Kim, Chem. Phys. Lett. **436**, 111 (2007).
- ⁵⁹X. Sun, H. Wang, and W. H. Miller, J. Chem. Phys. **109**, 7064 (1998).
- ⁶⁰S. Bonella and D. F. Coker, Chem. Phys. **268**, 189 (2001).
- ⁶¹S. Bonella and D. Coker, J. Chem. Phys. **118**, 4370 (2003).
- ⁶²X. Sun, H. Wang, and W. H. Miller, J. Chem. Phys. **109**, 7064 (1998).
- ⁶³J. A. Poulsen, G. Nyman, and P. J. Rossky, J. Chem. Phys. **119**, 12179 (2003).
- ⁶⁴Q. Shi and E. Geva, J. Chem. Phys. **118**, 8173 (2003).
- ⁶⁵T. J. H. Hele, M. J. Willatt, A. Muolo, and S. C. Althorpe, J. Chem. Phys. **142**, 134103 (2015).
- ⁶⁶S. N. Chowdhury and P. Huo, J. Chem. Phys. **154**, 124124 (2021).
- ⁶⁷M. Hillery, R. O'Connell, M. Scully, and E. Wigner, Phys. Rep. **106**, 121 (1984).
- ⁶⁸W. B. Case, American Journal of Physics **76**, 937 (2008).
- ⁶⁹H. Groenewold, Physica **12**, 405 (1946).
- ⁷⁰K. Imre, E. Özizmir, M. Rosenbaum, and P. F. Zweifel, J. Math. Phys. **8**, 1097 (1967).
- ⁷¹Q. Shi and E. Geva, J. Phys. Chem. A **108**, 6109 (2004).
- ⁷²T. J. H. Hele and N. Ananth, Faraday Discuss. **195**, 269 (2016).

- ⁷³H. Wang, X. Sun, and W. H. Miller, *J. Chem. Phys.* **108**, 9726 (1998).
- ⁷⁴J. R. Klauder, *Phys. Rev. D* **19**, 2349 (1979).
- ⁷⁵A. Nassimi, S. Bonella, and R. Kapral, *J. Chem. Phys.* **133**, 134115 (2010).
- ⁷⁶W. K. Wootters, *Ann. Phys.* **176**, 1 (1987).
- ⁷⁷K. S. Gibbons, M. J. Hoffman, and W. K. Wootters, *Phys. Rev. A* **70**, 062101 (2004).
- ⁷⁸S. J. Cotton and W. H. Miller, *J. Chem. Phys.* **145**, 144108 (2016).
- ⁷⁹S. J. Cotton and W. H. Miller, *J. Chem. Phys.* **150**, 194110 (2019).
- ⁸⁰S. A. Sato, A. Kelly, and A. Rubio, *Phys. Rev. B* **97**, 134308 (2018).
- ⁸¹S. N. Chowdhury and P. Huo, *J. Chem. Phys.* **150**, 244102 (2019).
- ⁸²A. Garg, J. N. Onuchic, and V. Ambegaokar, *J. Chem. Phys.* **83**, 4491 (1985).
- ⁸³A. Kelly, N. Brackbill, and T. E. Markland, *J. Chem. Phys.* **142**, 094110 (2015).
- ⁸⁴R. Schneider and W. Domcke, *Chem. Phys. Lett.* **150**, 235 (1988).
- ⁸⁵H. Köppel, L. S. Cederbaum, and W. Domcke, *J. Chem. Phys.* **89**, 2023 (1988).
- ⁸⁶H. Köppel, *Chem. Phys. Lett.* **205**, 361 (1993).
- ⁸⁷R. Schneider and W. Domcke, *Chem. Phys. Lett.* **159**, 61 (1989).
- ⁸⁸G. Stock, *J. Chem. Phys.* **103**, 2888 (1995).
- ⁸⁹A. Mandal, S. S. Yamjala, and P. Huo, *J. Chem. Theory Comput.* **14**, 1828 (2018).
- ⁹⁰P. Ehrenfest, *Z. Phys.* **45**, 455 (1927).
- ⁹¹A. D. McLachlan, *Mol. Phys.* **8**, 39 (1964).
- ⁹²R. Grunwald, A. Kelly, and R. Kapral, Quantum dynamics in almost classical environments, in *Energy Transfer Dynamics in Biomaterial Systems*, edited by I. Burghardt, V. May, D. A. Micha, and E. R. Bittner (Springer Berlin Heidelberg, Berlin, Heidelberg, 2009) pp. 383–413.
- ⁹³J. Liu and W. H. Miller, *J. Chem. Phys.* **134**, 104101 (2011).
- ⁹⁴S. Habershon and D. E. Manolopoulos, *J. Chem. Phys.* **131**, 244518 (2009).
- ⁹⁵W. H. Miller, *J. Phys. Chem. A* **113**, 1405 (2009).
- ⁹⁶J. R. Mannouch and J. O. Richardson, *J. Chem. Phys.* **153**, 194109 (2020).
- ⁹⁷J. R. Mannouch and J. O. Richardson, *J. Chem. Phys.* **153**, 194110 (2020).
- ⁹⁸G. Stock and M. Thoss, Mixed quantum-classical description of the dynamics at conical intersections, in *Conical Intersections* (World Scientific Publishing, 2004) pp. 619–695.
- ⁹⁹On page 106 of Ref.³⁵ (Chapter 6), the author suggested that “In order to determine the structure constants of $\mathfrak{su}(N)$, no closed formulas are known, they have to be calculated by means of performing matrix multiplications [Eq. 8 in the current note].”.
- ¹⁰⁰R. Gilmore, *Lie Groups, Physics, and Geometry: An Introduction for Physicists, Engineers and Chemists* (Cambridge University Press, 2008).
- ¹⁰¹I. R. Craig and D. E. Manolopoulos, *J. Chem. Phys.* **122**, 084106 (2005).